

OFFICE OF CIVILIAN RADIOACTIVE WASTE MANAGEMENT
ANALYSIS/MODEL COVER SHEET

1. QA: QA
Page: 1 of 80

Complete Only Applicable Items

2. <input type="checkbox"/> Analysis	<input type="checkbox"/> Engineering	3. <input checked="" type="checkbox"/> Model	<input checked="" type="checkbox"/> Conceptual Model Documentation
	<input type="checkbox"/> Performance Assessment		<input checked="" type="checkbox"/> Model Documentation
	<input type="checkbox"/> Scientific		<input checked="" type="checkbox"/> Model Validation Documentation

4. Title:
Mineralogical Model (MM3.0)

5. Document Identifier (including Rev. No. and Change No., if applicable):
MDL-NBS-GS-000003 REV 00 ICN 01

6. Total Attachments: 2	7. Attachment Numbers - No. of Pages in Each: I - # II = 16
--------------------------------	--

	Printed Name	Signature	Date
8. Originator	T. William Carey	<i>for Clinton Lum</i>	1/27/00
9. Checker	G. H. Nieder-Westermann	<i>G. H. Nieder-Westermann</i>	01/27/00
10. Lead/Supervisor	Clinton Lum	<i>Clinton Lum</i>	1/27/00
11. Responsible Manager	Dwight Hoxie	<i>Dwight Hoxie</i>	1/27/00

12. Remarks:

NM 5307
WM-11

OFFICE OF CIVILIAN RADIOACTIVE WASTE MANAGEMENT
ANALYSIS/MODEL COVER SHEET

1. QA: QA
Page: 1 of 80

Complete Only Applicable Items

2. <input type="checkbox"/> Analysis <input type="checkbox"/> Engineering <input type="checkbox"/> Performance Assessment <input type="checkbox"/> Scientific	3. <input checked="" type="checkbox"/> Model <input checked="" type="checkbox"/> Conceptual Model Documentation <input checked="" type="checkbox"/> Model Documentation <input checked="" type="checkbox"/> Model Validation Documentation
---	--

4. Title:
Mineralogical Model (MM3.0)

5. Document Identifier (including Rev. No. and Change No., if applicable):
MDL-NBS-GS-000003 REV 00 ICN 01

6. Total Attachments: 2	7. Attachment Numbers - No. of Pages in Each: I - # II = 16
--------------------------------	--

	Printed Name	Signature	Date
8. Originator	T. William Carey	<i>for Clinton Lum</i>	1/27/00
9. Checker	G. H. Nieder-Westermann	<i>[Handwritten Signature]</i>	01/27/00
10. Lead/Supervisor	Clinton Lum	<i>Clinton Lum</i>	1/27/00
11. Responsible Manager	Dwight Hoxie	<i>[Handwritten Signature]</i>	1/27/00

12. Remarks:

INFORMATION COPY
 LAS VEGAS DOCUMENT CONTROL

OFFICE OF CIVILIAN RADIOACTIVE WASTE MANAGEMENT
ANALYSIS/MODEL REVISION RECORD

1. Page 2 of 80

Complete Only Applicable Items

2. Analysis or Model Title:

Mineralogical Model (MM3.0)

3. Document Identifier (including Rev. No. and Change No., if applicable):

MDL-NBS-GS-000003 REV 00 ICN 01

4. Revision/Change No.

5. Description of Revision/Change

00

Initial issue.

00/01

ICN 01 incorporates DOE comments and editorial changes. Changes are designated by a change bar in the right margin.

FOR RECORD DOCUMENT CONTROL
INFORMATION ONLY

CONTENTS

	Page
ACRONYMS	9
1. PURPOSE	11
1.1 MINERALOGY AND HYDROLOGIC PROPERTIES	11
1.2 MINERALOGY AND RADIONUCLIDE TRANSPORT	18
1.3 MINERAL DISTRIBUTIONS AND HEALTH HAZARDS	18
1.4 MINERAL DISTRIBUTIONS AND REPOSITORY PERFORMANCE	18
1.5 PREDICTION OF MINERAL DISTRIBUTIONS AND REPOSITORY DESIGN ...	18
2. QUALITY ASSURANCE	21
3. COMPUTER SOFTWARE AND MODEL USAGE	23
4. INPUTS	25
4.1 DATA AND PARAMETERS	25
4.1.1 Mineralogic Data	25
4.1.2 Stratigraphic Surfaces	25
4.2 CRITERIA	25
4.3 CODES AND STANDARDS	28
5. ASSUMPTIONS	29
5.1 SPATIAL CORRELATION OF MINERALOGY	29
5.2 USE OF DRILL CUTTINGS DATA	29
6. MINERALOGIC MODEL	31
6.1 CHANGES FROM PREVIOUS VERSIONS TO MM3.0	31
6.2 METHODOLOGY	32
6.2.1 Modification of GFM3.1 Files	32
6.2.2 Creation of Stratigraphic Framework	33
6.2.3 Incorporation of Mineralogic Data from Boreholes	39
6.2.4 Calculation of Mineral Distributions	41
6.3 RESULTS AND DISCUSSION	42
6.3.1 Model Limits and Illustration of Results	42
6.3.2 Sorptive Zeolite Distribution	42
6.3.3 Smectite + Illite Distribution	57
6.3.4 Volcanic Glass Distribution	57
6.3.5 Silica Polymorph Distribution	58
6.4 UNCERTAINTIES AND LIMITATIONS IN MINERALOGIC MODEL	63
6.4.1 Model Limitations	63
6.4.2 Magnitude of Increased Uncertainty with Exclusion of TBV Data	70
6.5 MODEL VALIDATION	71
7. CONCLUSIONS	75

CONTENTS (Continued)

	Page
8. INPUTS AND REFERENCES	77
8.1. DOCUMENTS CITED.....	77
8.2. CODES, STANDARDS, REGULATIONS, AND PROCEDURES.....	79
8.3. SOURCE DATA, LISTED BY DATA TRACKING NUMBER.....	79
8.4. SOFTWARE.....	80

ATTACHMENTS

I. DOCUMENT INPUT REFERENCE SHEETS (DIRS) REMOVED	I-1
II. GENERAL OBSERVATIONS AND SUMMARY OF MINERALOGY	II-1

FIGURES

	Page
1. Interrelationships Between Component Models, Integrated Site Model, and Downstream Uses.....	16
2. Location Map of Yucca Mountain, Nevada, Showing Location of Exploratory Studies Facility, Cross-Block Drift, and Area of Integrated Site Model with Boundaries of Component Models.....	17
3. Locations of Boreholes Used in MM3.0.....	27
4. Shaded Relief View of Tpcpv1, Nonwelded Subzone of Vitric Zone of Tiva Canyon Tuff.....	34
5. North-South Cross Section Through Potential Repository, Illustrating Sequences Used in MM3.0, Excluding Paleozoic.....	35
6. East-West Cross Section Through Potential Repository, Illustrating Sequences Used in MM3.0, Excluding Paleozoic.....	36
7. Schematic Stratigraphic Column Showing Approximate Thicknesses of Units Listed in Table 1 (excluding units between Qal or Qc and Tpc, and Paleozoic units).....	37
8. Map View of Volcanic Glass Distribution in "PTn" Unit, Tpcpv1-Tptrv2 (Sequence 20) for Entire MM3.0.....	43
9. Zeolite Distribution in North-South and East-West Cross Sections Through Center of Potential Repository Block.....	45
10. Zeolite Distribution in North-South Cross Section Through Potential Repository Block.....	46
11. Zeolite Distribution in East-West Cross Section Through Potential Repository Block.....	47
12. Zeolite Distribution in North-South Cross Section Through Potential Repository Block and Above the Water Table.....	48
13. Zeolite Distribution in East-West Cross Section Through Potential Repository Block and Above Water Table.....	49
14. Zeolite Distribution in Map View of Upper Layer (Layer 14) of Calico Hills Formation (Tac, Sequence 11).....	51

FIGURES (Continued)

	Page
15. Zeolite Distribution in Map View of Middle-Upper Layer (Layer 13) of Calico Hills Formation (Tac, Sequence 11)	52
16. Zeolite Distribution in Map View of Middle-Lower Layer (Layer 12) of Calico Hills Formation (Tac, Sequence 11)	53
17. Zeolite Distribution in Map View of Lower Layer (Layer 11) of Calico Hills Formation (Tac, Sequence 11)	54
18. Zeolite Distribution in Map View of Bedded Tuff of Calico Hills Formation (Tactb, Sequence 10).....	55
19. Zeolite Distribution in Map View of Upper Vitric Zone of Prow Pass Tuff (Tcupv, Sequence 9).....	56
20. Smectite + Illite Distribution in North-South Cross Section Through Potential Repository	59
21. Smectite + Illite Distribution in East-West Cross Section Through Potential Repository	60
22. Volcanic Glass Distribution in North-South Cross Section Through Potential Repository	61
23. Volcanic Glass Distribution in East-West Cross Section Through Potential Repository	62
24. Tridymite Distribution in North-South Cross Section Through Potential Repository	64
25. Tridymite Distribution in East-West Cross Section Through Potential Repository	65
26. Cristobalite + Opal-CT Distribution in North-South Cross Section Through Potential Repository	66
27. Cristobalite + Opal-CT Distribution in East-West Cross Section Through Potential Repository	67
28. Quartz Distribution in North-South Cross Section Through Potential Repository	68
29. Quartz Distribution in East-West Cross Section Through Potential Repository.....	69

TABLES

	Page
1. Correlation Chart for Model Stratigraphy.....	12
2. Model-Development Documentation for Mineralogic Model	21
3. Quality Assurance Information for Model Software.....	23
4. Data Input.....	26
5. Mineralogy of the Topopah Spring Tuff and Upper Calico Hills Formation	73
II-1 Adjustments to Borehole Sample Elevations.....	II-9

~~INTENTIONALLY LEFT BLANK~~

ACRONYMS

AMR	Analysis/Model Report
CRWMS M&O	Civilian Radioactive Waste Management System Management and Operating Contractor
DIRS	Document Input Reference System
DTN	data tracking number
ESF	Exploratory Studies Facility
GFM	Geologic Framework Model
ISM	Integrated Site Model
LA	License Application
MM	Mineralogic Model
QA	quality assurance
QARD	Quality Assurance and Requirements Description
RHH	Repository Host Horizon
RPM	Rock Properties Model
STN	software tracking number
TBV	to be verified
TDMS	technical data management system
3-D	three-dimensional
TSPA	Total System Performance Assessment
XRD	x-ray diffraction

INTENTIONALLY LEFT BLANK

1. PURPOSE

The purpose of this report is to document the Mineralogic Model (MM), Version 3.0 (MM3.0) with regard to data input, modeling methods, assumptions, uncertainties, limitations and validation of the model results, qualification status of the model, and the differences between Version 3.0 and previous versions.

A three-dimensional (3-D) Mineralogic Model was developed for Yucca Mountain to support the analyses of hydrologic properties, radionuclide transport, mineral health hazards, repository performance, and repository design. Version 3.0 of the MM was developed from mineralogic data obtained from borehole samples. It consists of matrix mineral abundances as a function of x (easting), y (northing), and z (elevation), referenced to the stratigraphic framework defined in Version 3.1 of the Geologic Framework Model (GFM). The MM was developed specifically for incorporation into the 3-D Integrated Site Model (ISM). The MM enables project personnel to obtain calculated mineral abundances at any position, within any region, or within any stratigraphic unit in the model area. The significance of the MM for key aspects of site characterization and performance assessment is explained in the following subsections.

This work was conducted in accordance with the Development Plan for the MM (CRWMS M&O 1999a). Constraints and limitations of the MM are discussed in the appropriate sections that follow.

The MM is one component of the ISM, which has been developed to provide a consistent volumetric portrayal of the rock layers, rock properties, and mineralogy of the Yucca Mountain site. The ISM consists of three components:

- Geologic Framework Model (GFM)
- Rock Properties Model (RPM)
- Mineralogic Model (MM).

The ISM merges the detailed stratigraphy (described in Table 1) and structural features of the site into a 3-D model that will be useful in primary downstream models and repository design. These downstream models include the hydrologic flow models and the radionuclide transport models. All the models and the repository design, in turn, will be incorporated into the Total System Performance Assessment (TSPA) of the potential nuclear waste repository block and vicinity to determine the suitability of Yucca Mountain as a host for a repository. The interrelationship of the three components of the ISM and their interface with downstream uses are illustrated in Figure 1. The lateral boundaries of the ISM and its three component models are shown in Figure 2.

1.1 MINERALOGY AND HYDROLOGIC PROPERTIES

The hydrologic properties and behavior of rock units are correlated with mineralogy. For example, nonwelded vitric tuffs and zeolitized tuffs can have very different hydraulic conductivities (Loeven 1993, pp. 15-20). The use of the observed correlation between mineralogic and hydrologic data provides a means of improving the

Table 1. Correlation Chart for Model Stratigraphy

Stratigraphic Unit ^{a, d}					Abbreviation ^a	RHH ^b	Geologic Framework Model Unit ^h	Mineralogic Model Unit
Group	Formation	Member	Zone	Subzone				
				Alluvium and Colluvium	Qal, Qc		Alluvium (only)	
				Timber Mountain Group	Tm			
				Rainier Mesa Tuff	Tmr			
				Paintbrush Group	Tp			
				Post-tuff unit "x" bedded tuff	Tpbt6			
				Tuff unit "x" ^c	Tpki (informal)			
				Pre-tuff unit "x" bedded tuff	Tpbt5			
				Tiva Canyon Tuff	Tpc			
				Crystal-Rich Member	Tpcr			
				Vitric zone	Tpcrv			
				Nonwelded subzone	Tpcrv3			
				Moderately welded subzone	Tpcrv2			
				Densely welded subzone	Tpcrv1			
				Nonlithophysal subzone	Tpcm			
				Subvitrophyre transition subzone	Tpcrn4			
				Pumice-poor subzone	Tpcrn3			
				Mixed pumice subzone	Tpcrn2			
				Crystal transition subzone	Tpcrn1			
				Lithophysal zone	Tpcl			
				Crystal transition subzone	Tpcl1		Post-Tiva	
				Crystal-Poor Member	Tpcp			
				Upper lithophysal zone	Tpcpul			
				Spherulite-rich subzone	Tpcpul1			
				Middle nonlithophysal zone	Tpcpmn			
				Upper subzone	Tpcpmn3			
				Lithophysal subzone	Tpcpmn2			
				Lower subzone	Tpcpmn1			
				Lower lithophysal zone	Tpcpl			
				Hackly-fractured subzone	Tpcpllh			
				Lower nonlithophysal zone	Tpcpln			
				Hackly subzone	Tpcplnh			
				Columnar subzone	Tpcplnc			
				Vitric zone	Tpcpv			
				Densely welded subzone	Tpcpv3			
				Moderately welded subzone	Tpcpv2			
				Nonwelded subzone	Tpcpv1			
				Pre-Tiva Canyon bedded tuff	Tpbt4			
				Yucca Mountain Tuff	Tpy			
								Sequence 22 (Layer 26) Alluvium- Tpc_un
							Tpcp	
							TpcLD	
							Tpcpv3	Sequence 21 (Layer 25) Tpcpv3-Tpcpv2
							Tpcpv2	
							Tpcpv1	Sequence 20 (Layer 24) Tpcpv1- Tptrv2
							Tpbt4	
							Yucca	

Table 1. Correlation Chart for Model Stratigraphy (Continued)

Stratigraphic Unit ^{a,d}				Abbreviation ^a	RHH ^b	Geologic Framework Model Unit ^h	Mineralogic Model Unit	
Group	Formation	Member	Zone	Subzone				
				Pre-Yucca Mountain bedded tuff	Tpbt3		Tpbt3_dc	
				Pah Canyon Tuff	Tpp		Pah	
				Pre-Pah Canyon bedded tuff	Tpbt2		Tpbt2	
				Topopah Spring Tuff	Tpt			
				Crystal-Rich Member	Tptr			
				Vitric zone	Tptrv			Sequence 20 (Layer 24)
				Nonwelded subzone	Tptrv3		Tptrv3	Tpcpv1-Tptrv2
				Moderately welded subzone	Tptrv2		Tptrv2	
				Densely welded subzone	Tptrv1		Tptrv1	Sequence 19 (Layer 23) Tptrv1
				Nonlithophysal zone	Tptm			
				Dense subzone	Tptm3			
				Vapor-phase corroded subzone	Tptm2			
				Crystal transition subzone	Tptm1		Tptrn	
				Lithophysal zone	Tptrl			
				Crystal transition subzone	Tptrl1		Tptrl	Sequence 18 (Layer 22)
				Crystal-Poor Member	Tptp			
				Lithic-rich zone	Tptpf or Tptrf		Tptf	Tptm-Tptf
				Upper lithophysal zone	Tptpul		Tptpul	Sequence 17 (Layer 21)
							RHHtop	Tptpul
				Middle nonlithophysal zone	Ttptmn			
				Nonlithophysal subzone	Ttptmn3			Sequence 16 (Layer 20)
				Lithophysal bearing subzone	Ttptmn2		Ttptmn	Ttptmn
				Nonlithophysal subzone	Ttptmn1			
				Lower lithophysal zone	Ttptll		Ttptll	Sequence 15 (Layer 19) Ttptll
				Lower nonlithophysal zone	Ttptln		Ttptln	Sequence 14 (Layer 18) Ttptln
				Vitric zone	Ttptv			
				Densely welded subzone	Ttptv3		Ttptv3	Sequence 13* (Layers 16 & 17)
				Moderately welded subzone	Ttptv2		Ttptv2	Ttptv3-Ttptv2
				Nonwelded subzone	Ttptv1		Ttptv1	Sequence 12 (Layer 15) Ttptv1 - Tpbt1
				Pre-Topopah Spring bedded tuff	Tpbt1		Tpbt1	

Table 1. Correlation Chart for Model Stratigraphy (Continued)

Stratigraphic Unit ^{a, d}					Abbreviation ^a	RHH ^b	Geologic Framework Model Unit ^h	Mineralogic Model Unit
Group	Formation	Member	Zone	Subzone				
	Calico Hills Formation				Ta		Calico	Sequence 11 ⁱ (Layers 11, 12, 13, 14) Tac
	Bedded tuff				Tacbt		Calicobt	Sequence 10 (Layer 10) Tacbt
	Crater Flat Group				Tc			
	Prow Pass Tuff				Tcp			
		Prow Pass Tuff upper vitric nonwelded zone			(Tcupv) ^d		Prowuv	Sequence 9 (Layer 9) Tcupv
		Prow Pass Tuff upper crystalline nonwelded zone			(Tcupc) ^d		Prowuc	Sequence 8 (Layer 8) Tcupc-Tcplc
		Prow Pass Tuff moderately-densely welded zone			(Tcprd) ^d		Prowmd	
		Prow Pass Tuff lower crystalline nonwelded zone			(Tcplc) ^d		Prowlc	
		Prow Pass Tuff lower vitric nonwelded zone			(Tcplv) ^d		Prowlv	Sequence 7 (Layer 7) Tcplv-Tcbuv
		Pre-Prow Pass Tuff bedded tuff			(Tcprt) ^d		Prowbt	
	Bullfrog Tuff				Tcb			
		Bullfrog Tuff upper vitric nonwelded zone			(Tcbuv) ^d		Bullfroguv	Sequence 6 (Layer 6) Tcbuc-Tcblc
		Bullfrog Tuff upper crystalline nonwelded zone			(Tcbuc) ^d		Bullfroguc	
		Bullfrog Tuff welded zone			(Tcbmd) ^d		Bullfrogmd	Sequence 5 (Layer 5) Tcblv-Tctuv
		Bullfrog Tuff lower crystalline nonwelded zone			(Tcblc) ^d		Bullfroglc	
		Bullfrog Tuff lower vitric nonwelded zone			(Tcblv) ^d		Bullfroglv	Sequence 4 (Layer 4) Tctuc-Tctlc
		Pre-Bullfrog Tuff bedded tuff			(Tcprt) ^d		Bullfrogbt	
	Tram Tuff				Tct			
		Tram Tuff upper vitric nonwelded zone			(Tctuv) ^d		Tramuv	Sequence 3 (Layer 3) Tctlv-Tctbt
		Tram Tuff upper crystalline nonwelded zone			(Tctuc) ^d		Tramuc	
		Tram Tuff moderately-densely welded zone			(Tctmd) ^d		Trammd	Sequence 4 (Layer 4) Tctuc-Tctlc
		Tram Tuff lower crystalline nonwelded zone			(Tctlc) ^d		Tramlc	
		Tram Tuff lower vitric nonwelded zone			(Tctlv) ^d		Tramlv	

Table 1. Correlation Chart for Model Stratigraphy (Continued)

Stratigraphic Unit ^{a,d}					Abbreviation ^a	RHH ^b	Geologic Framework Model Unit ^h	Mineralogic Model Unit
Group	Formation	Member	Zone	Subzone				
	Pre-Tram Tuff bedded tuff				(Tctbt) ^d		Trambt	
	Lava and flow breccia (informal)				TII			
	Bedded tuff				TIIbt			
	Lithic Ridge Tuff				Tr			
	Bedded tuff				Trbt			
	Lava and flow breccia (informal)				TII2			
	Bedded tuff				TIIbt			
	Lava and flow breccia (informal)				TII3			
	Bedded tuff				TII3bt			
	Older tuffs (informal)				Tt			
	Unit a (informal)				Tta			
	Unit b (informal)				Ttb			
	Unit c (informal)				Ttc			
	Sedimentary rocks and calcified tuff (informal)				Tca			
	Tuff of Yucca Flat (informal)				Tyf			
	Pre-Tertiary sedimentary rock						Tund	Sequence 2 (Layer 2) Tund
	Lone Mountain Dolomite				Slm			
	Roberts Mountain Formation				Srm			
							Paleozoic	Sequence 1 (Layer 1) Paleozoic ^g

^aSource: DTN: MO9510RIB00002.004.

^bSource: CRWMS M&O 1997a, pp. 43-50.

^cCorrelated with the rhyolite of Comb Peak (Buesch et al. 1996, Table 2).

^dFor the purposes of GFM3.1, each formation in the Crater Flat Group was subdivided into six zones based on the requirements of the users of the GFM. The subdivisions are upper vitric (uv), upper crystalline (uc), moderately to densely welded (md), lower crystalline (lc), lower vitric (lv), and bedded tuff (bt) (Buesch and Spengler 1999, pp. 62-63).

^eSequence 13 (Ttpv3-Ttpv2) is subdivided into 2 layers of equal thickness.

^fSequence 11 (Tac) is subdivided into 4 layers of equal thickness.

^gSequence 1 (Paleozoic) represents a lower bounding surface.

^hSource: DTN: MO9901MWDGFM31.000

NOTE: RHH = Repository Host Horizon
 Shaded rows indicate header lines for subdivided units.

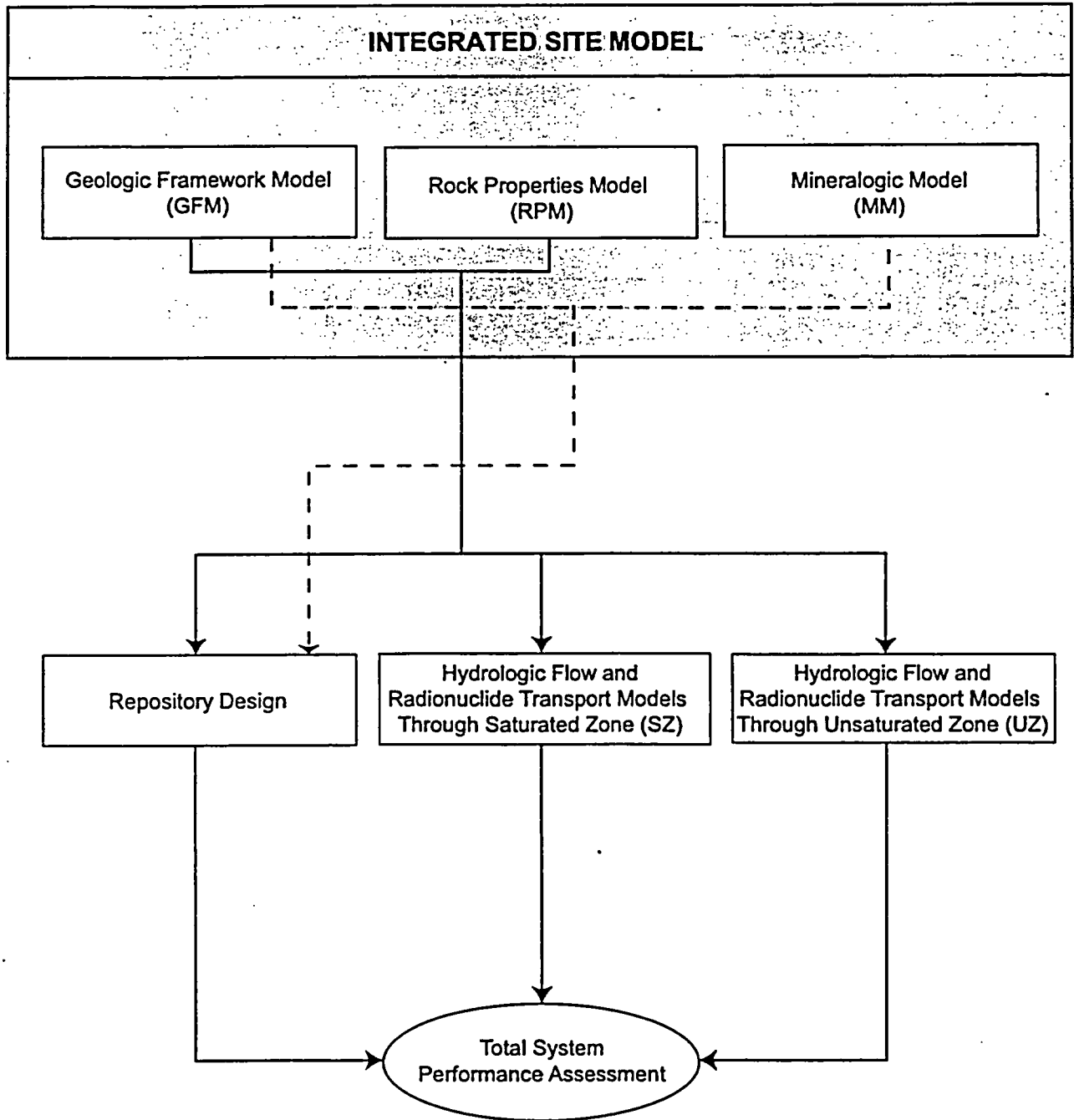


Figure 1. Interrelationships Between Component Models, Integrated Site Model, and Downstream Uses

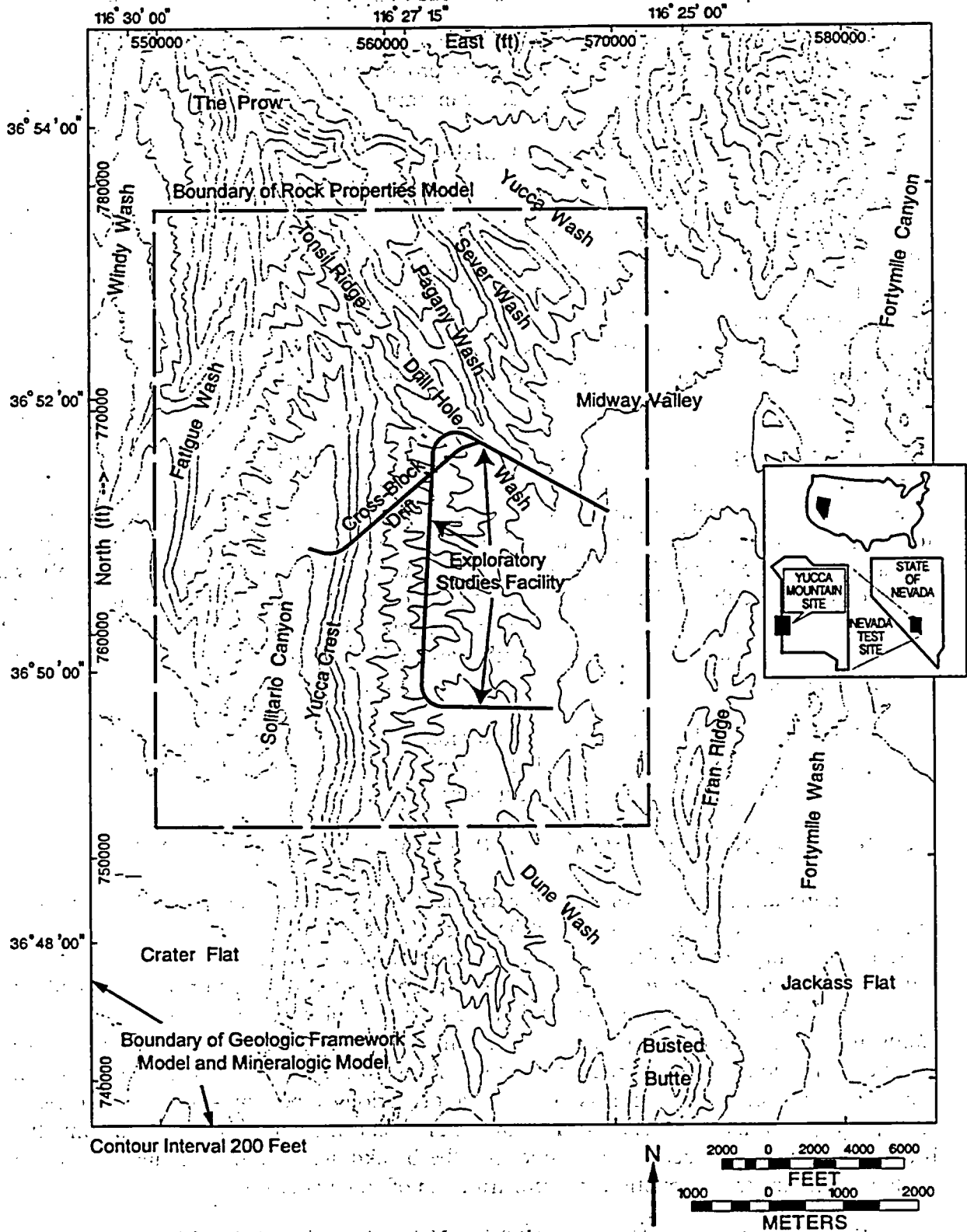


Figure 2. Location Map of Yucca Mountain, Nevada, Showing Location of Exploratory Studies Facility, Cross-Block Drift, and Area of Integrated Site Model With Boundaries of Component Models

accuracy and confidence of both hydrologic and mineralogic models. For example, in some areas, high-confidence mineralogic data can improve estimates of hydrologic properties; and in other areas, high-confidence hydrologic data can improve estimates of mineral abundance.

1.2 MINERALOGY AND RADIONUCLIDE TRANSPORT

Zeolitic horizons have long been an important factor in models of radionuclide transport at Yucca Mountain. Zeolites are capable of sorbing many cationic radionuclides (Johnstone and Wolfsberg 1980, pp. 112–117, Tables A1, A2, A3). The MM incorporates zeolite and other mineral weight percentages as the basic distributed property, allowing the volumes of minerals present, represented as weight percentages of rock mass, to be defined explicitly in a spatial-manner for specific performance assessment studies. The data in MM3.0 provide the basis for geostatistical calculations and simulations of zeolite abundance should such calculations be required.

1.3 MINERAL DISTRIBUTIONS AND HEALTH HAZARDS

The presence of crystalline silica polymorphs led to requirements for dust abatement measures for those working in the Exploratory Studies Facility (ESF) and has significantly affected operations (CRWMS M&O 1997b, pp. 3–17). The Topopah Spring Tuff has highly variable ratios of the crystalline silica polymorphs and knowing the distributions of these minerals in three dimensions may help in planning the mitigation of hazards due to dust inhalation. MM3.0 includes quartz, tridymite, and cristobalite + opal-CT, so that all of the silica polymorphs are now considered.

The 3-D model also allows prediction of possible locations of the carcinogenic zeolite erionite. Such predictions can be used as a basis for planning work in suspect zones and eliminating the need to follow stringent safety requirements when working in safe areas.

1.4 MINERAL DISTRIBUTIONS AND REPOSITORY PERFORMANCE

Hydrous minerals, such as zeolites and clays, and volcanic glass are particularly susceptible to reactions caused by repository-induced heating. These reactions can produce or absorb water; yield changes in porosity, permeability, and retardation characteristics; and moderate heat flux within the rock mass (Vaniman and Bish 1995, pp. 533–546). Other minerals, particularly silica polymorphs, may undergo phase transitions or may control the aqueous silica concentrations of fluids migrating under thermal loads, resulting in silica dissolution or precipitation, redistribution of silica, and modification of rock properties. All of these effects must be considered in three dimensions to adequately address the impact of various repository-loading strategies on the repository performance. The MM allows numerical modeling of reactions involving the breakdown of glass to zeolites and smectite, the breakdown of clinoptilolite and mordenite to analcime, and the transformation and redistribution of silica polymorphs.

1.5 PREDICTION OF MINERAL DISTRIBUTIONS AND REPOSITORY DESIGN

Guidelines for repository performance address concerns over mineral stability in systems exposed to repository conditions (see Section 4.2). Previous studies of thermal effects (Buscheck and Nitao 1993, pp. 847–867) relevant to assessment of mineral stability have not

been able to assess solid phase transformations (e.g., transitions between silica polymorphs) or hydrous-mineral dehydration/rehydration because of a lack of 3-D mineralogic data. MM3.0 allows the formulation of thermal models to indicate much more precisely the maximum possible thermal loads that are consistent with maintaining relatively low temperatures for zeolite-rich zones, and it provides the abundances of silica polymorphs that are susceptible to phase transformations adjacent to the repository. Once models that couple the 3-D MM with mineral-reaction and heat-flow data are developed, it will be possible to model thermal limits with fewer assumptions.

INTENTIONALLY LEFT BLANK

2. QUALITY ASSURANCE

This analysis activity was evaluated in accordance with QAP-2-0, *Conduct of Activities* (CRWMS M&O 1999b, 1999c), and determined to be quality affecting and subject to the requirements of the QARD, *Quality Assurance Requirements and Description* (DOE 1998). Accordingly, efforts to conduct the analysis have been conducted in accordance with approved quality assurance (QA) procedures under the auspices of the QA program of the Civilian Radioactive Waste Management System Management and Operating Contractor (CRWMS M&O), using procedures identified in the MM Development Plan (CRWMS M&O 1999a).

This analysis/model report (AMR) has been developed in accordance with procedure AP-3.10Q, *Analyses and Models*, and modeling work was performed in accordance with QA procedure LANL-YMP-QP-03.5, *Scientific Notebooks*, and AP-SIII.1Q, *Scientific Notebooks*. The Development Plan (CRWMS M&O 1999a) describes the scope, objectives, tasks, methodology, and implementing procedures for model construction. The planning document for this AMR, implementation procedure, and scientific notebook for the MM are provided in Table 2.

Table 2. Model-Development Documentation for Mineralogic Model

Model	Planning Document	Scientific Notebook Procedure	Scientific Notebook
MM3.0	CRMWS M&O 1999a	LANL-YMP-QP-03.5 AP-SIII.1Q	LA-EES-1-NBK-99-001 (CRWMS M&O registry no. SN-LANL-SCI-190-V1) (Carey 1999)

INTENTIONALLY LEFT BLANK

3. COMPUTER SOFTWARE AND MODEL USAGE

The MM was constructed using STRATAMODEL modeling software, Version 4.1.1 (an industry-standard software), produced by Landmark Graphics Corporation, Houston, Texas. The software has been determined to be appropriate for its intended use in 3-D mineralogic modeling, and is under Configuration Management control (Table 3). The qualification status of the software is provided in the DIRS database.

Table 3. Quality Assurance Information for Model Software

Computer Type	Software Name	Version	Qualification Procedure	Software Tracking Number (STN)
Silicon Graphics Octane	STRATAMODEL	4.1.1	AP-SI.1Q	10121-4.1.1-00

During the construction and use of the MM, it is stored on internal computer disks, backup tapes, and compact disks. The electronic files for MM3.0 were submitted to the Technical Data Management System (TDMS) in ASCII format. All files necessary to reconstruct the MM are available in the TDMS in DTN: LA9908JC831321.001, including data, interpretive data, parameter files, and instructions. Reconstruction of MM3.0 requires STRATAMODEL software Version 4.1.1 or higher. ASCII format files containing all model results are also provided in the TDMS for use in the other software used in downstream modeling.

STRATAMODEL was used to maximize the potential for multiple uses of the MM. Transport codes such as FEHM, which incorporate thermal and geochemical effects, are compatible with STRATAMODEL. STRATAMODEL also embodies the preferred methods for interpolation of mineral abundances between drill holes and in stratigraphic coordinates. In addition, the data in STRATAMODEL can be directly analyzed using geostatistical software.

Information from the Geologic Framework Model, versions 3.1 (DTN: MO9901MWDGFM31.000) and 3.0 (DTN: MO9804MWDGFM03.001), was used in construction of MM3.0 (Section 4.1.2). The qualification status of these models is provided in the DIRS database.

INTENTIONALLY LEFT BLANK

4. INPUTS

Inputs for the MM 3.0 consist of stratigraphic surfaces from GFM3.1 and *quantitative* x-ray diffraction (XRD) analyses of mineral abundances.

4.1 DATA AND PARAMETERS

A list of inputs is provided in Table 4 and their qualification status is provided in the DIRS database. Figure 3 shows the location of the boreholes from which derived mineralogic data was used in the construction of the MM. A brief discussion of the data is provided in the following subsections.

4.1.1 Mineralogic Data

The MM depends directly on quantitative XRD analyses. XRD offers the most direct and accurate analytical method for determining mineral abundance because the data are fundamentally linked to crystal structure. Other methods based on down-hole logs or chemical or spectral properties from which mineral identities can be inferred are subject to much greater uncertainty. The development of quantitative XRD for application to core and cuttings analysis at Yucca Mountain (Bish and Chipera 1988, pp. 295-306; Chipera and Bish 1995, pp. 47-55) resulted in the development of an input data file of mineral abundances (in DTN: LA9908JC831321.001) as a function of map position and depth at Yucca Mountain.

The primary mineralogic data listed in Table 4 are quantitative XRD data used for constructing the MM. All data are mineral abundances in weight percent and are used as reported in these files, with the following exceptions. Where a mineral was detected but in only trace abundance (i.e., much less than 1 percent) the result is reported in the tables as "Trc." or "Tr." In these cases, a uniform numeric value of 0.1 percent was assigned to each trace occurrence in order to have real (but appropriately small) numeric values in the MM. In some instances, depending on the mineralogic makeup of the sample, approximate or upper-limit values, such as "~1 percent" or "< 2 percent," are reported in the data package. In these cases, the ~ or < symbol was dropped, and the numeric value was used in the MM.

4.1.2 Stratigraphic Surfaces

The stratigraphic framework for MM3.0 was constructed from stratigraphic surfaces obtained as ASCII-format export files from GFM3.1 (DTN: MO9901MWDGFM31.000). The water table surface was extracted from GFM3.0 (DTN: MO9804MWDGFM03.001), as this information is not included in the GFM3.1 output files. The creation of the stratigraphic framework required modification of the ASCII-format export files as described in Section 6.2.1.

4.2 CRITERIA

This AMR complies with the DOE interim guidance (Dyer 1999). Subparts of the interim guidance that apply to this analysis or modeling activity are those pertaining to the characterization of the Yucca Mountain site (Subpart B, Section 15), the compilation of information regarding geology of the site in support of the License Application (Subpart B,

Table 4. Data Input

Data Description	Data Tracking Number (DTN)
Mineralogy, borehole UE-25 a#1	LADB831321AN98.002
Mineralogy, borehole UE-25 b#1	LADB831321AN98.002
Mineralogy, borehole UE-25 p#1	LADB831321AN98.002
Mineralogy, borehole UE-25 UZ#16	LA000000000086.002 LAJC831321AQ98.005
Mineralogy, borehole USW G-1	LADB831321AN98.002
Mineralogy, borehole USW G-2	LADB831321AN98.002
Mineralogy, borehole USW G-3/GU-3	LADB831321AN98.002
Mineralogy, borehole USW G-4	LADB831321AN98.002
Mineralogy, borehole USW H-3	LADB831321AN98.002 LADV831321AQ97.001
Mineralogy, borehole USW H-4	LADB831321AN98.002
Mineralogy, borehole USW H-5	LADB831321AN98.002 LADV831321AQ97.007
Mineralogy, borehole USW H-6	LADB831321AN98.002
Mineralogy, borehole USW NRG-6	LADV831321AQ97.001 LASC831321AQ96.002
Mineralogy, borehole USW NRG-7a	LADV831321AQ97.001
Mineralogy, borehole USW SD-6	LASC831321AQ98.003 LADV831321AQ99.001
Mineralogy, borehole USW SD-7	LADV831321AQ97.001 LAJC831321AQ98.005
Mineralogy, borehole USW SD-9	LADV831321AQ97.001 LAJC831321AQ98.005
Mineralogy, borehole USW SD-12	LADV831321AQ97.001 LAJC831321AQ98.005
Mineralogy, borehole USW UZ-14	LADV831321AQ97.001 LASC831321AQ96.002
Mineralogy, borehole USW UZN-31	LASL831322AQ97.001
Mineralogy, borehole USW UZN-32	LASL831322AQ97.001
Mineralogy, borehole USW WT-1	LADB831321AN98.002
Mineralogy, borehole USW WT-2	LADB831321AN98.002
Mineralogy, borehole USW WT-24	LASC831321AQ98.001 LADV831321AQ99.001
Stratigraphic surfaces, ASCII export files, GFM3.1	MO9901MWDGFM31.000
Water table from GFM3.0	MO9804MWDGFM03.001
Supplementary mineralogic data for MM3.0	LA9910JC831321.001

NOTES: For simplification, a shortened version of the borehole identifier is used when referring to boreholes in the text, figures, and tables (e.g., "UE-25 a#1" is simplified to "a#1").
See the DIRS database for the qualification status of data packages.

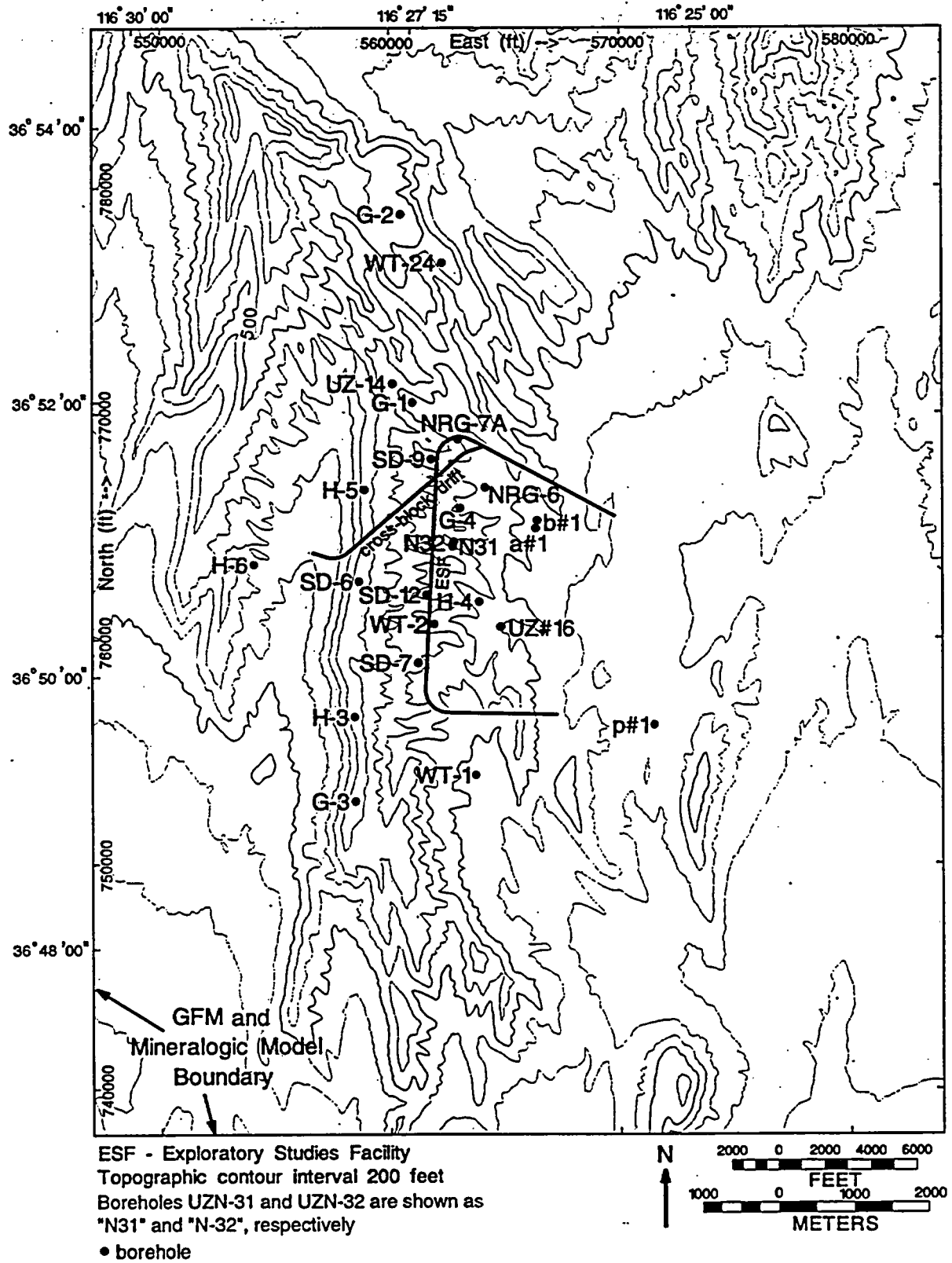


Figure 3. Locations of Boreholes Used in MM3.0

Section 21(c)(1)(ii)), and the definition of geologic parameters and conceptual models used in performance assessment (Subpart E, Section 114(a)).

4.3 CODES AND STANDARDS

No codes and standards are applicable to the MM.

5. ASSUMPTIONS

The assumptions used to build the MM are methodological and geological; therefore, they are an inherent part of the discussion in Section 6. Two key assumptions for model development are presented below.

5.1 SPATIAL CORRELATION OF MINERALOGY

It is assumed that mineral abundances at one location within a model stratigraphic unit have a value that is correlated with a spatially nearby value. The rationale for this assumption is that mineral assemblages are the products of geochemical processes that vary gradually in space. No additional confirmation of this assumption is required.

This assumption is the basis for the following methodological approaches:

- Modeling in stratigraphic coordinates (Section 6.2.3)
- Calculation of mineral distributions using an inverse distance weighting method (Section 6.2.4)

5.2 USE OF DRILL CUTTINGS DATA

An assumption is made that sample-collection methods for drill cuttings did not severely affect mineral-abundance data or MM predictions based on those data. The rationale for this assumption is that mineral-abundance data from cutting samples are similar to core-derived data for the same model sequences in a borehole (Levy 1984, Table 1). Based on this assumption, mineral-abundance data from drill-cuttings samples are acceptable input data for the MM. This assumption does not require additional confirmation.

INTENTIONALLY LEFT BLANK

6. MINERALOGIC MODEL

6.1 CHANGES FROM PREVIOUS VERSIONS TO MM3.0

MM3.0 incorporates stratigraphy from GFM3.1 and is constructed on a 200-foot (61-meter) north-south and east-west grid. MM3.0 represents a complete revision of earlier versions and the resulting model supercedes all previous versions. MM3.0 provides values for the entire region of GFM3.1: 547,000 to 584,000 feet (166,726 to 178,003 meters) easting and 738,000 to 787,000 feet (224,942 to 239,878 meters) northing, Nevada State Plane coordinates.

A synopsis of changes between versions of the MM is as follows:

- Preliminary MM: The initial model was developed in a stratigraphic framework taken from ISM1.0.
- MM1.0: The stratigraphic framework was upgraded to ISM2.0. New mineralogic data from boreholes H-3, NRG-6, NRG-7a, SD-7, SD-9, SD-12, UZ-14, and UZN-32 were incorporated.
- MM1.1: New mineralogic data from borehole WT-24 were incorporated.
- MM2.0: The stratigraphic framework was upgraded to GFM3.0. The grid resolution was refined from 800 to 200 feet (244 to 61 meters). Borehole H-6 was incorporated. New data from boreholes SD-6, SD-7, SD-12, UZ#16, and WT-24 were included. The modeled mineral classes were expanded from 6 to 10. Mineralogic modeling was conducted in stratigraphic coordinates (see Section 6.2.3 for further explanation). The stratigraphic framework used for the mineralogic framework was simplified from 31 to 22 sequences.
- MM3.0: The stratigraphic framework was upgraded to GFM3.1. New data from boreholes SD-6 and WT-24 were included. Tptpv3-Tptpv2 sequence was subdivided into two layers. The area covered by the MM was expanded to include the entire area of GFM3.1. The procedure for mineralogic modeling in stratigraphic coordinates was significantly improved, resulting in a more internally consistent representation of mineralogy and stratigraphy.

An additional layer was created in MM3.0 by subdividing the Tptpv3-Tptpv2 sequence (sequence 13) into two layers of equal thickness, partly to better represent the zone of intense smectite and zeolite alteration at the boundary between Tptpln (sequence 14) and Tptpv3. In some places, samples from this altered zone occur at the base of Tptpln as defined in GFM3.1, and these samples were adjusted in elevation to fall in the upper part of Tptpv3.

The areal boundaries of MM3.0 were extended to cover the entire region covered by GFM3.1. Although this extension includes areas where borehole data are sparse, project personnel requested that the MM be available for the entire region. The region of better supported mineralogic values is identified within this larger region.

The mineralogic data for MM3.0 and the previous versions were obtained from quantitative XRD analyses of cores and cuttings from boreholes at Yucca Mountain. Inclusion of the new data from boreholes SD-6 and WT-24 has resulted in a significant improvement of the model because these boreholes provide information from the northern and western parts of the site, where boreholes are scarce or the samples available are largely cuttings.

6.2 METHODOLOGY

The basic components of the 3-D MM are a stratigraphic framework, mineralogic data from boreholes, and 3-D geologic modeling software. The stratigraphic framework was obtained from GFM3.1 (DTN: MO9901MWDGFM31.000). The sources of mineralogic data (listed in Table 4) contain quantitative XRD data from boreholes. The 3-D geologic modeling was conducted with the software STRATAMODEL (STRATAMODEL V4.1.1, STN: 10121-4.1.1-00). STRATAMODEL performs distance-weighted interpolations of borehole data within stratigraphic units specified by the framework to produce a volumetric distribution of the rock properties associated with each stratigraphic horizon.

The modeling process consists of four sequential steps:

1. Modification of ASCII-format export files from GFM3.1: Missing values in the vicinity of faults were supplied by interpolation.
2. Creation of the stratigraphic framework: Stratigraphic surfaces from GFM3.1 were joined in three dimensions to create a stratigraphic framework.
3. Incorporation of mineralogic data from specific boreholes: Quantitative XRD analyses of mineral abundance as a function of geographic position (borehole location) and sample elevation were placed within the 3-D stratigraphic framework.
4. Calculation of mineralogic distribution data for the entire 3-D model with the use of a deterministic, inverse-distance-weighting function: Measured mineralogic data at each borehole were used to predict mineral abundances at all locations in the model.

Each modeling step is documented in Scientific Notebook LA-EES-1-NBK-99-001 (Carey 1999) and is discussed in detail in the following subsections.

6.2.1 Modification of GFM3.1 Files

The GFM3.1 ASCII-format export files used to create the stratigraphic framework for the MM lack elevation values at some grid nodes and along fault traces. These omissions occur only in the ASCII-format export files, not in GFM3.1. Therefore, before the creation of the stratigraphic framework, the GFM3.1 ASCII-format files were modified to fill in values in the vicinity of major faults. (To create the stratigraphic framework, STRATAMODEL requires values for all grid nodes.) In order to provide the missing values at these points in a controlled and reasonable manner, elevations for undefined grid nodes were interpolated from adjacent grid points by means of the Stratamap function in STRATAMODEL. For example, if the values adjacent to an undefined grid node were 600 and 700 meters, the interpolated value would be 650 meters. Each GFM3.1 surface included several thousand extrapolated values per grid with a total of

45,756 grid nodes (186 by 246 nodes). The operation of the Stratamap function was checked to ensure that the elevations of the original data points had not been adjusted and that the interpolated values accurately represented the faulted regions. The checks were done numerically, by visual comparison of the grids, and by checking to see that contacts of GFM3.1 within boreholes, as represented within STRATAMODEL, were correct. The interpolated data are available in DTN: LA9908JC831321.001.

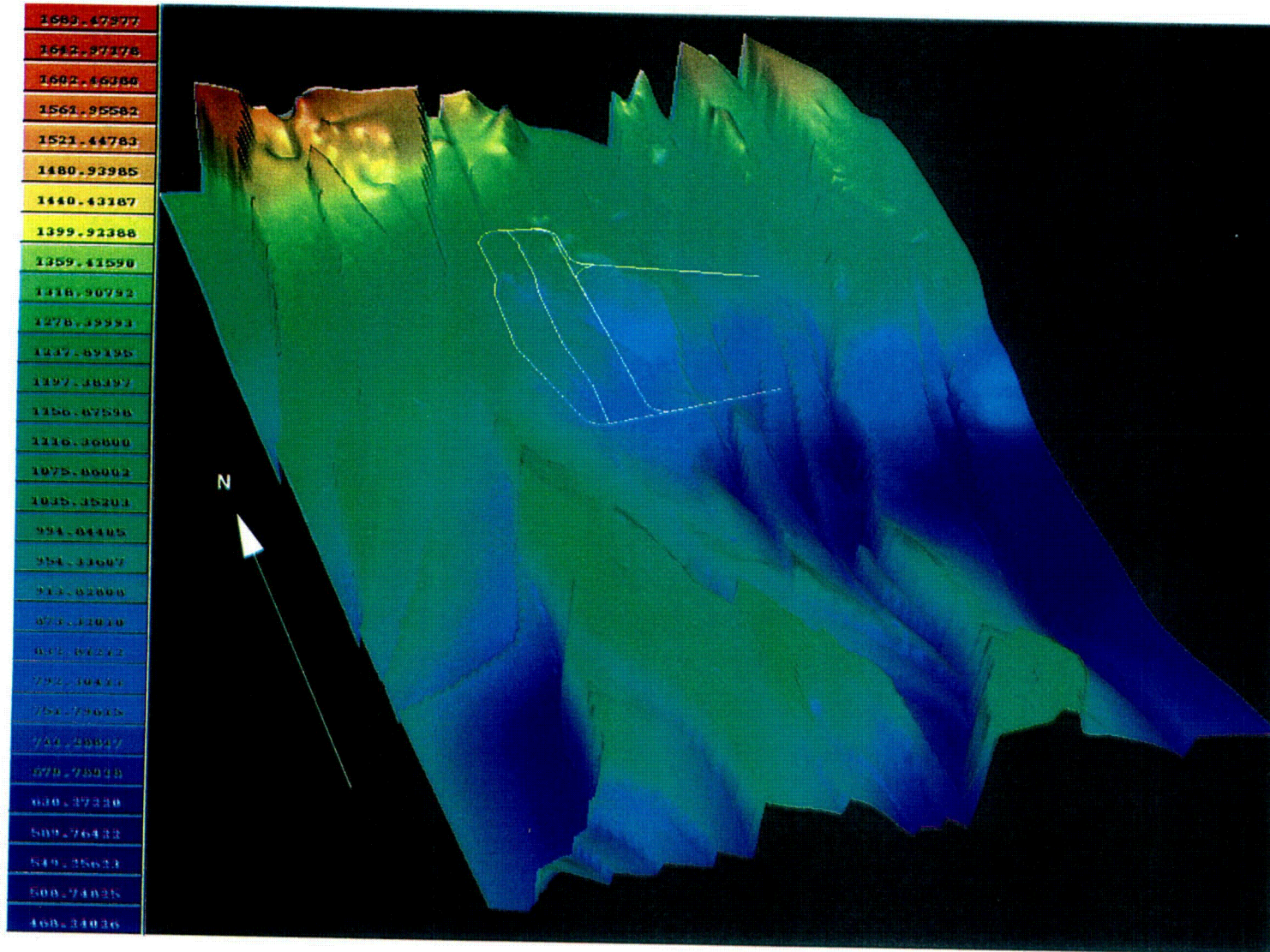
6.2.2 Creation of Stratigraphic Framework

The stratigraphic framework for the MM was created from the GFM3.1 stratigraphy Table 4. The GFM3.1 results were obtained as exported ASCII-format files with data listed at the 200-foot (61-meter) grid spacings. The grid used in the MM has the same 200-foot (61-meter) grid spacing as GFM3.1 and consists of 186 by 246 grid nodes. The areal extent is 65.7 square miles (170 square kilometers).

The stratigraphic framework for the MM was created with a subset of 22 of the 52 stratigraphic surfaces in GFM3.1. An example of a GFM3.1 surface, that of the Tiva Canyon Tuff vitric zone nonwelded subzone (Tpcpv1), is illustrated in Figure 4. The surface is notable for the fine resolution of topography, including faults such as the Solitario Canyon fault to the west. The 22 stratigraphic surfaces were linked via STRATAMODEL into a stratigraphic framework to define 22 volumetric *sequences*, as shown in Table 1 and illustrated in Figures 5 and 6. (Note Figures 5 and 6 can be used as a guide for locating the position of sequences in other figures.) Many of the sequences in MM3.0 incorporate several stratigraphic units as shown in Table 1 and Figure 7 in which each sequence is labeled with the units forming its upper and lower surfaces.

The modeling in the MM was conducted in stratigraphic coordinates so that the mineralogic data were constrained to their proper stratigraphic units. As a result, mineralogic and stratigraphic data are consistent and all mineral data are located in the correct stratigraphic unit. A detailed comparison of GFM3.1 stratigraphic assignments versus mineralogy for each of the borehole samples was conducted for every observation used in the MM. In several places, this analysis resulted in reassignment of borehole samples to the mineralogically correct stratigraphic unit. As a result, this version of the MM is more consistent with the GFM than previous versions.

The 22 sequences listed in Table 1 were defined to keep the MM as simple as possible and to accurately define zeolitic, vitric, and repository host units at Yucca Mountain. Sequence 22, the uppermost sequence, includes all stratigraphic units above Tpcpv because these units share a common devitrification mineralogy dominated by feldspar plus silica minerals. The next sequence (sequence 21) consists of a Tiva Canyon vitrophyre unit composed of two subzones (Tpcpv3 and Tpcpv2), combined in the MM because they share a similar abundance of welded glass. The hydrogeologic Paintbrush nonwelded unit (PTn) is represented by sequence 20, which extends from the nonwelded subzone of the lower vitric zone of the Tiva Canyon Tuff to the upper vitric zone of the Topopah Spring Tuff. It includes six stratigraphic units occurring between the top of Tpcpv1 and the base of Tptrv2. These six units are similar in having variable proportions of glass plus smectite that can not be captured within the larger scale of the MM; therefore these six units were combined into sequence 20. The remaining Topopah Spring Tuff below sequence 20 is represented as eight sequences in the MM, representing the upper



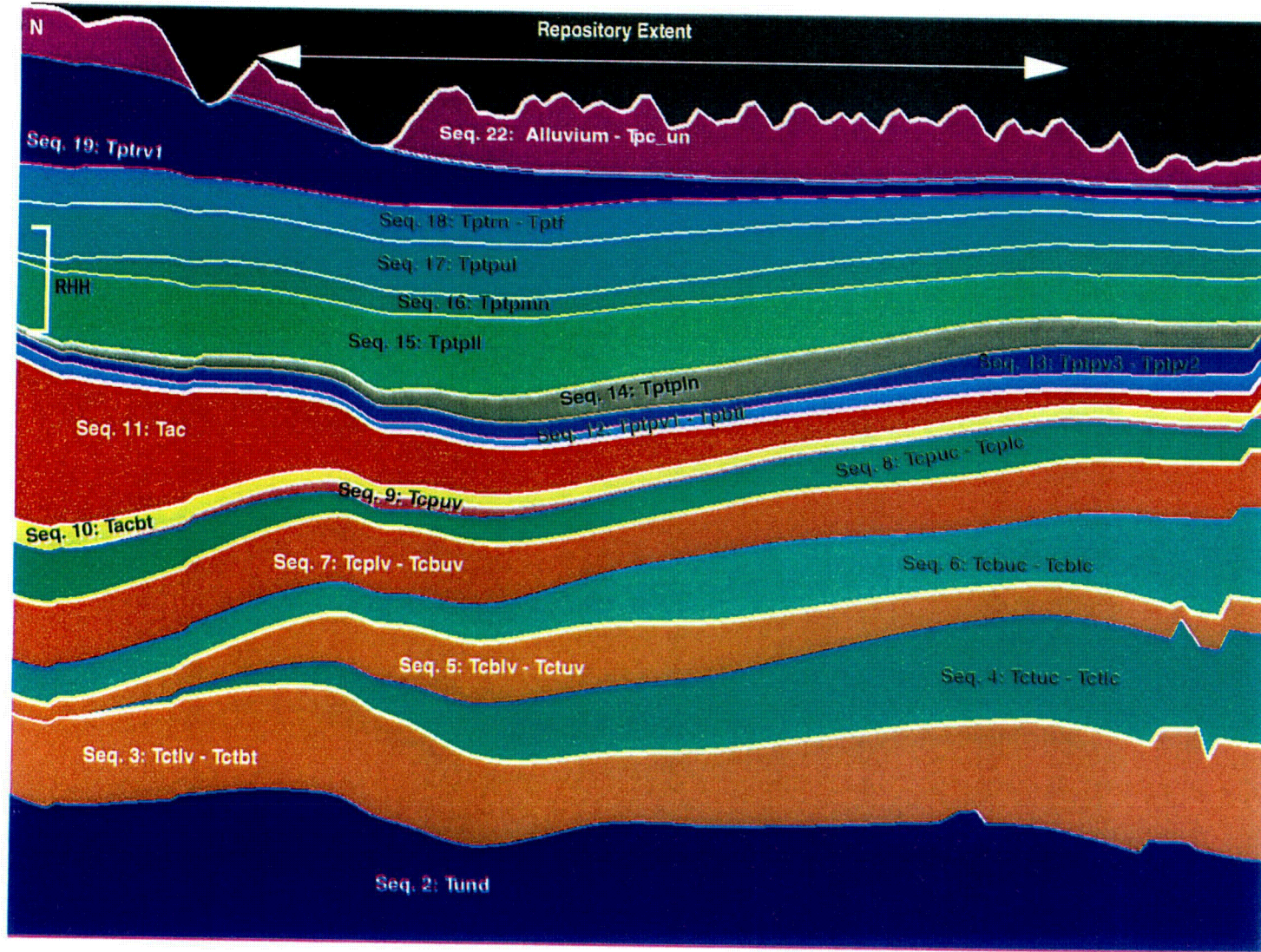
NOTES:

Color key indicates surface elevation in meters above mean sea level.

Exploratory Studies Facility and potential repository are outlined in white.

Figure 4. Shaded Relief View of Tpcpv1, Nonwelded Subzone of Vitric Zone of Tiva Canyon Tuff

C01



NOTES:

This figure serves as a guide for identifying sequences in other north-south cross sections.

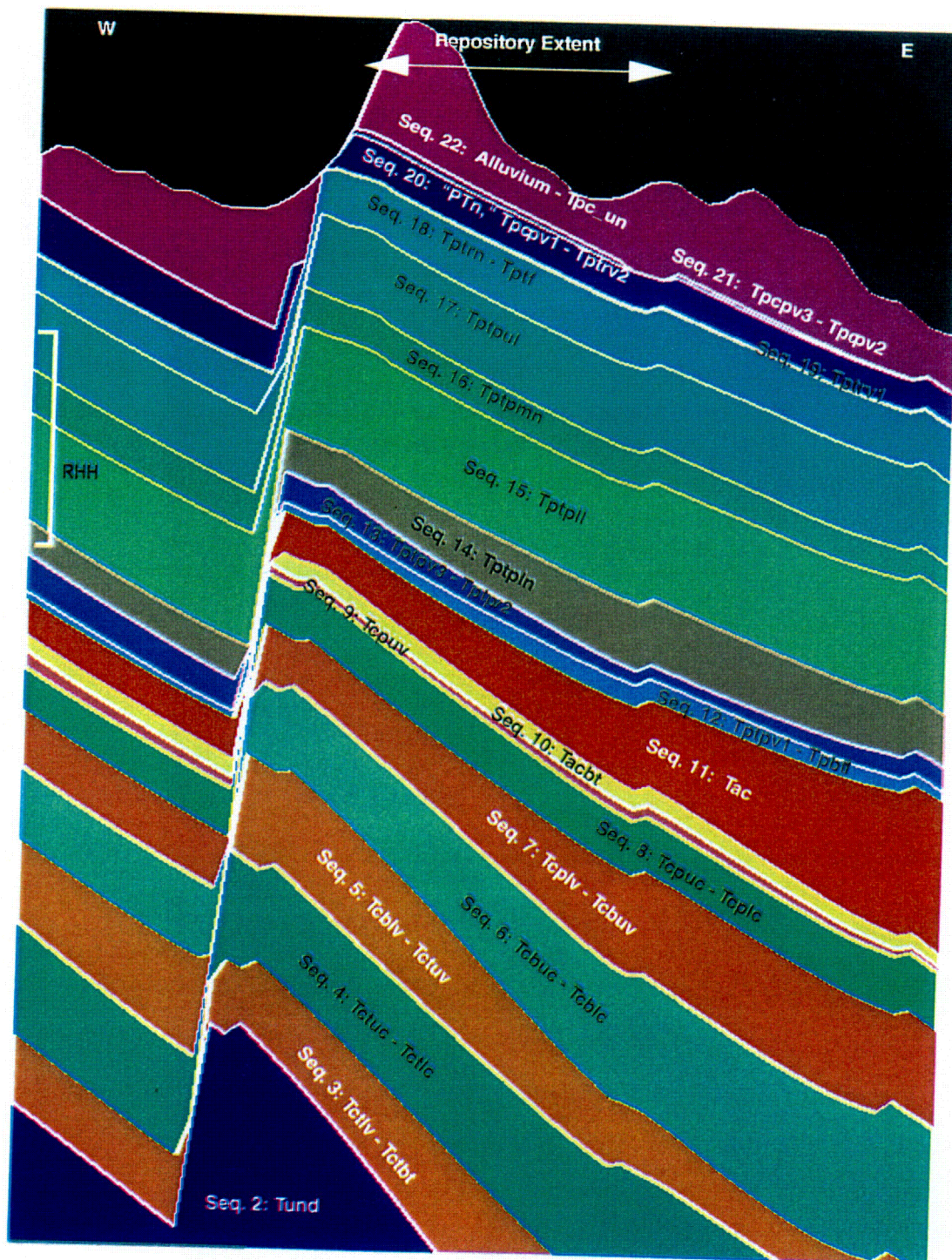
Sequences are defined in Table 1.

Delineation of cross section is shown in Figure 8.

Dimensions of north-south cross section are 26,200 feet (7,986 meters) long and 4,430 feet (1,350 meters) deep.

Figure 5. North-South Cross Section Through Potential Repository, Illustrating Sequences Used in MM3.0, Excluding Paleozoic

C02



NOTES:

This figure serves as a guide for identifying sequences in other east-west cross sections.

Sequences are defined in Table 1.

Delineation of cross section is shown in Figure 8.

Dimensions of east-west cross section are 12,398 feet (3,779 meters) long and 4,510 feet (1,375 meters) deep.

Figure 6. East-West Cross Section Through Potential Repository, Illustrating Sequences Used in MM3.0, Excluding Paleozoic

e03

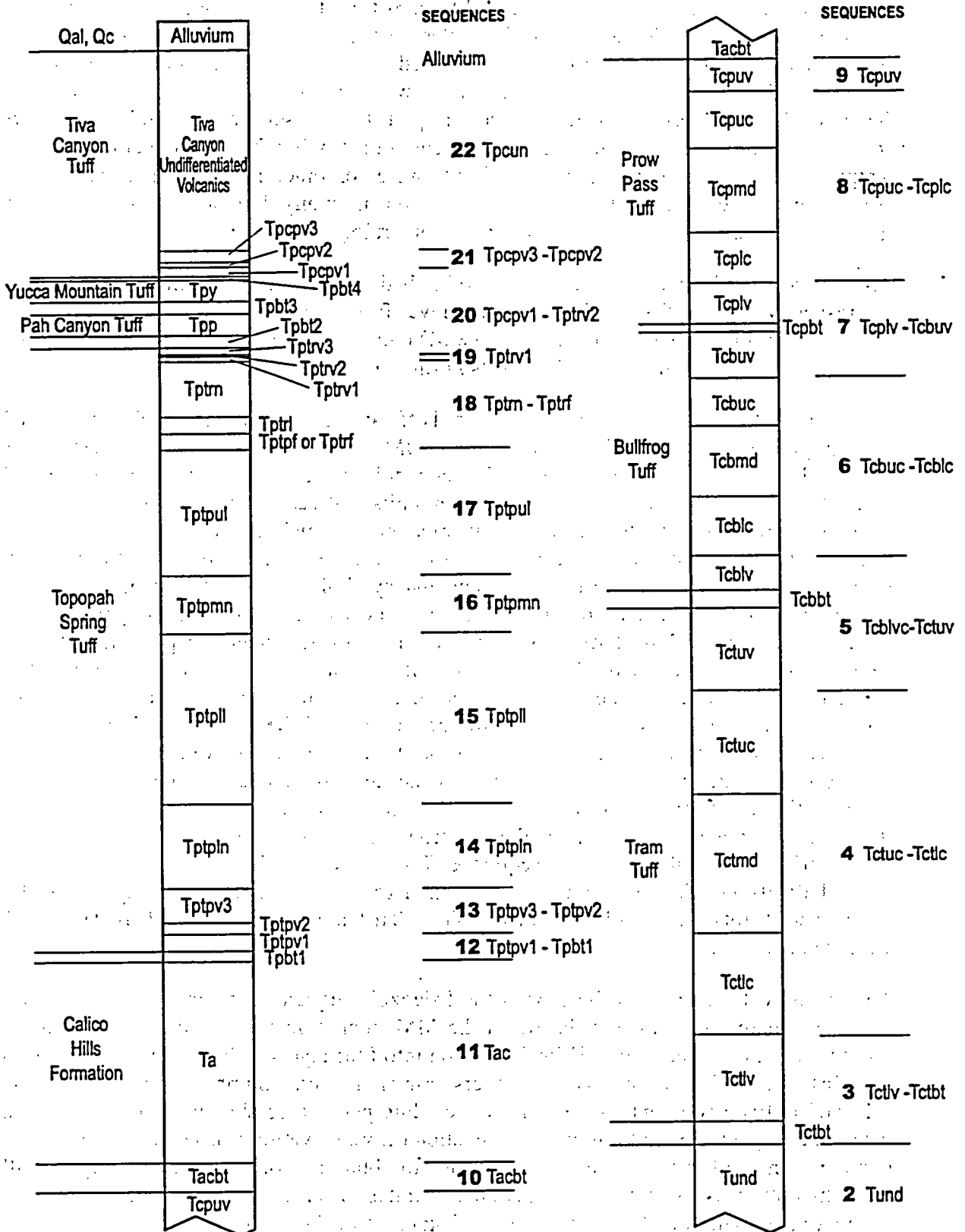


Figure 7. Schematic Stratigraphic Column Showing Approximate Thicknesses of Units Listed in Table 1 (excluding units between Qal or Qc and Tpc, and Paleozoic units)

vitrophyre, the upper quartz-latitude to rhyolite transition, the four lithophysal and nonlithophysal units, and units of welded and nonwelded glass at the base. The welded glass unit at the base, which includes Tptpv3 and Tptpv2, is represented as a single sequence in the MM (sequence 13). However, the sequence is subdivided into two equal-thickness layers. As described in Section 6.1, the uppermost layer was used, in part, to represent the "altered zone," or region of intense smectite and zeolite alteration that occurs in many boreholes at the contact of Tptpln and Tptpv3. Stratigraphic units Tptpv1 and Tpbt1 were combined into a single sequence in the MM (sequence 12) because of their similar character in many boreholes and because Tpbt1 is generally thin and not well represented in the mineralogic data.

The Calico Hills Formation and the underlying bedded tuff are represented by sequences 11 and 10, respectively. The Calico Hills Formation was further subdivided into four layers. The layers have distinct mineralogic abundances in the MM and were created to allow modeling of variable zeolitization with depth in the Calico Hills Formation.

In GFM3.1, the Prow Pass Tuff, Bullfrog Tuff, and Tram Tuff are each represented by six stratigraphic units (a total of 18 units). In the MM, these 18 units were combined into a total of four zeolitic or vitric and three devitrified nonzeolitic sequences. These sequences reflect the characteristic alternation at this depth between units that can be readily zeolitized and those that have devitrified to feldspar plus silica minerals and in which zeolitization does not occur. The uppermost, first zeolitic sequence is defined by the upper vitric subunit of the Prow Pass Tuff (Tcpv). (Note that the word "vitric" and the symbol "v" are used in GFM3.1 to describe originally vitric units, even when these units may now be zeolitic.) The upper vitric or zeolitic sequence in the Prow Pass Tuff is followed by a nonzeolitic sequence representing the devitrified center of the Prow Pass Tuff (Tcpc-Tcplc). It includes the upper crystalline, middle densely welded, and lower crystalline subunits. The second zeolitic sequence includes the lower vitric portion of the Prow Pass Tuff (Tcplv), the bedded tuff of the Prow Pass Tuff (Tcpcb), and the upper vitric subunit of the Bullfrog Tuff (Tcbuv). This sequence is identified as Tcplv-Tcbuv. The second nonzeolitic sequence consists of the devitrified Bullfrog Tuff and combines three subunits (Tcbuc, Tcbmd, and Tcblc). The third zeolitic sequence, labeled Tcblv-Tctuv, includes the lower vitric and bedded tuff of the Bullfrog Tuff in addition to the upper vitric unit of the Tram Tuff. The final nonzeolitic sequence, Tctuc-Tctlc, includes the devitrified center of the Tram Tuff (Tctuc, Tctmd, and Tctlc). The final zeolitic sequence is the base of the Tram Tuff (Tctlv and Tctbt). Units older than the Tram Tuff are undifferentiated as Tund and have a variable zeolitic character.

The lowermost sequence in the MM is the Paleozoic sequence, making a total of 22 sequences. However, there are 26 distinct layers in the MM, including the subdivision of Tptpv3-Tptpv2 into two layers and the Calico Hills Formation into four layers. The model contains 45,756 (186 by 246) grid nodes, which with 26 layers brings the total number of cells in the model to 1,189,656. Each cell contains 16 values, including percentage abundance for 10 mineral groups listed in Section 6.2.3, cell volume, cell location (x, y), elevation (z), sequence number, and layer number. Any cell in the model can be queried to obtain any of these values. Figure 5 illustrates a north-south cross section and Figure 6 illustrates an east-west cross section through Yucca Mountain, showing the distributions and thicknesses of the sequences used as the framework of the MM (Table 1).

The stratigraphic framework of MM3.0 was compared with that of GFM3.1 at all of the boreholes from which mineralogic data were obtained for the MM. Because the boreholes are not located precisely at grid nodes, some differences between the predicted and actual elevations of contacts were expected. Nonetheless, the elevations of the contacts between stratigraphic units were found to be within 3.3 feet (1 meter) to 49 feet (15 meters) of the GFM3.1 values (detailed in Scientific Notebook LA-EES-1-NBK-99-001 (Carey 1999, pp. 10–12, 199–221)).

6.2.3 Incorporation of Mineralogic Data from Boreholes

Mineralogic data, including core samples and cuttings, are available for 24 boreholes in the form of data files providing the mineralogy as a function of sample depth or elevation. The cuttings were used in the MM based on the assumption presented in Section 5.2. Elevations assigned to cutting samples were the midpoints of the depth ranges from which the cuttings were collected. The borehole locations are shown on the map in Figure 8. Ten mineral groups or classes were incorporated in MM3.0:

- Smectite + illite
- Sorptive zeolites (the sum of clinoptilolite, heulandite, mordenite, chabazite, erionite, and stellerite)
- Tridymite
- Cristobalite + opal-CT
- Quartz
- Feldspars
- Volcanic glass
- Nonsorptive zeolite (analcime)
- Mica
- Calcite.

The mineralogy (weight percent present for each of the 10 mineral groups), stratigraphy, and elevations of the samples collected from each of the 24 boreholes included in the MM is provided in a data input file in DTN: LA9908JC831321.001. Because boreholes UZN-31 and UZN-32 are separated by only 74 feet (23 meters), the mineralogical data from these boreholes were combined into a single borehole file (Scientific Notebook LA-EES-1-NBK-99-001 (Carey 1999, pp. 187–188)). Thus, a total of 23 boreholes was used in MM3.0.

The borehole data files were imported into STRATAMODEL in a process that involved mapping the elevations of the mineralogic samples onto the stratigraphic elevations obtained from GFM3.1. The MM was constructed with the use of the numeric mean of all of the mineralogic data within a given sequence at each borehole. Inevitably, there were some discrepancies

between elevations in the mineralogic data and the elevations predicted by STRATAMODEL and GFM3.1. These discrepancies included mineralogic data from a given stratigraphic unit being assigned to the incorrect sequence in STRATAMODEL. There were three causes of these discrepancies:

1. The boreholes are not located at grid nodes. The elevations calculated by STRATAMODEL for the stratigraphic contacts at the boreholes are based on an average of the nearest four grid nodes. The calculated value was in error where the average value differed from the true value because of uneven topography in the vicinity of the borehole. These occurrences are identified in Attachment II as "too close to boundary."
2. There are regions of some stratigraphic units where GFM3.1 does not precisely reproduce observed borehole contacts. In addition, three boreholes that were used in the MM were not used in the construction of GFM3.1 (a#1, UZN-31, and UZN-32) and one borehole in which only part of the stratigraphy was used (UZ-14). The GFM stratigraphy provides contact information only for units below Tptpv2 in UZ-14. These discrepancies are similar in character to discrepancies described in No. 1, and are also identified in Attachment II as "too close to boundary."
3. There were a few places in which STRATAMODEL predicted the absence of a sequence at a particular borehole. This occurred where the surface defining the sequence was absent. For example, at borehole H-4, Tpcpv3 is absent; therefore, the entire sequence Tpcpv3-Tpcpv2 was not present in the MM at H-4. There was also one location (WT-1) in which faulting caused the apparent removal of sequences in the MM. These discrepancies are identified in Attachment II as "removed; unit X not present in MM," in which case the mineralogic sample was removed from the model.

In correcting for these discrepancies there are two possible approaches: (1) assume the correct elevations but possibly incorrect assignments of mineralogy to stratigraphy or (2) assume the correct mineralogy associated with a mineral-stratigraphic unit but possibly incorrect elevations for the mineralogic data. The latter approach is known as modeling in stratigraphic coordinates and is based on the concept presented in Section 5.1. This approach was used in the construction of MM3.0. The advantages of the stratigraphic coordinate system are that all mineralogic data are correctly associated with a sequence and that the stratigraphic relationship of data from differing boreholes is preserved. Therefore, mineralogic data were assigned to the correct sequence by small adjustments to apparent elevations, where needed.

In addition, a detailed comparison of mineralogy and stratigraphy revealed some inconsistencies between stratigraphic and mineralogic assignments. For example, a sample near a contact, with mineralogy characteristic of a devitrified tuff, may have been placed in a vitric/zeolitic tuff when the data files were imported into STRATAMODEL. In this case, the sample elevation was adjusted to assign the mineralogy to the adjacent devitrified stratigraphic sequence.

The details of the adjustments for each borehole are provided in Attachment II, Table II-1.

6.2.4 Calculation of Mineral Distributions

The final stage of the MM construction in STRATAMODEL is the distribution of the mineralogic data in three dimensions using the concept presented in Section 5.1. This estimation can be accomplished by a number of methods, including geometric, distance-weighting, and geostatistical methods. In MM3.0, a distance-weighting method was used to estimate mineral distributions. Geostatistical calculations were not conducted in this version of the model, but the data in MM3.0 could be used for such calculations to provide a statistical framework for transport calculations.

The 3-D mineral distributions were calculated using an inverse-distance-weighting function that operates solely within sequences (i.e., mineral abundances in a given sequence were calculated solely from mineralogic data within that sequence):

$$W(r,R) = (1-r/R)^2(R/r)^X \quad (\text{Eq. 1})$$

Where:

W = weighting function

r = distance between the interpolated point and a known value

R = search radius

X = power factor.

This weighting function is provided by the STRATAMODEL software and yields, essentially, a $1/r^X$ weighting of the mineralogic data. At small values of r, the weighting function is approximately equal to $(R/r)^X$, which is the same as a simple inverse weighting function, $(1/r)^X$ multiplied by a normalization factor, R^X . The advantage of the STRATAMODEL function is apparent at values of r that approach R: the STRATAMODEL weighting function goes to 0, while a simple inverse weighting function retains non-zero weighting at R. In other words, the STRATAMODEL weighting function provides a smooth transition in weighting between values of r less than R to values greater than R, but the simple inverse weighting function yields an abrupt transition from non-zero weights ($r < R$) to zero weights ($r > R$). In calculating the mineral abundance at a specified location, the weights are normalized so that the sum of the weight is equal to 1.

In MM3.0, a power factor of $X=4$ was used. The choice of $X=4$ was made based on an analysis of the mineralogic data as documented in Scientific Notebook (LA-EES-1-NBK-99-001 (Carey 1999, pp. 222-246)). Three possible choices were investigated in detail: $X=2$, $X=4$, and $X=6$. The advantage of $X=4$ was most apparent in the analysis of the predicted zeolite distribution in the Calico Hills Formation (sequence 11; see Figures 14 through 18). A choice of $X=2$ allowed too much influence from distant boreholes such that substantial non-zero values of zeolite were predicted in the southwest region of the model. Such predictions differed from a basic mineralogic-data analysis, which indicated that there should be consistently low values of zeolite in the southwest. A choice of $X=6$ did yield low predicted values of zeolite in the southwest, but also predicted very localized control of mineralogy. For example, the transition zone between zeolitic and non-zeolitic Calico Hills Formation was very narrow. This high degree of local control was not consistent with the mineralogic analysis. The choice of $X=4$

allowed for sufficient local control to yield low abundances of zeolite in the southwest, while avoiding severe localization of predicted values.

The search radius, R, is also an important parameter and was set at 26,247 feet (8,000 meters) to allow the mineralogic data to fill all of the GFM3.1 model space.

6.3 RESULTS AND DISCUSSION

The results for MM3.0 are illustrated in cross sections and in map views of individual surfaces. The location and extent of the north-south and east-west cross sections are shown in Figure 8 in relation to the potential repository. The mineralogic stratigraphy is labeled on cross sections provided in Figures 5 and 6.

6.3.1 Model Limits and Illustration of Results

Figure 8 shows the distribution of boreholes on which the MM is based. Colors in the background to this figure are keyed to the abundance of volcanic glass in sequence 20 (PTn unit). The sources of the mineralogic data are confined to the central portion of the model area; the MM results are poorly constrained outside of the subregion indicated by the black box in Figure 8. Also shown in Figure 8 are regions in which sequence 20 is absent. These regions occur in linear zones in the vicinity of faults, where the MM resolution of fault geometry is poor. Accurate mineralogic results should not be expected adjacent to faults. Sequence 20 is also absent in broad areas where it has been removed by erosion. Figure 8 illustrates the relatively small, central area in which mineralogic data are abundant, relative to the broader extent of the GFM. This limitation should be kept in mind in considering the visualizations generated from the MM.

6.3.2 Sorptive Zeolite Distribution

Zeolite abundance is shown in Figure 9 as a range of colors from dark blue (0 percent) to red (20 percent or greater). Sorptive zeolites at Yucca Mountain play an important role in models of radionuclide retardation and thermohydrology and in repository design. Sorptive zeolites occur in variable amounts below the potential Repository Host Horizon (RHH) in four distinct stratigraphic groups separated by nonzeolitic intervals. (The RHH, as shown in Table 1, includes part of sequence 17 and all of sequences 14, 15, and 16.) Zeolite distributions are displayed in Figures 10 and 11. Cross-sectional keys to sequence names and numbers are provided on Figures 5 and 6. The distribution of sorptive zeolites is closely related to the internal stratigraphy of the tuffs (see also Section 6.2.2). Sorptive zeolites occur within the upper vitric, basal vitric, and basal bedded tuff units of each formation of the Crater Flat Group (Tram Tuff, Bullfrog Tuff, and Prow Pass Tuff). The devitrified center of each formation in the Crater Flat Group lacks zeolites. The net result is a sequence of alternating zeolitic and nonzeolitic rocks. The highest stratigraphic level at which extensive zeolitization of vitric units occurs varies across the geographic extent of the MM. In the south and west, the first occurrence of abundant zeolites below the RHH is in the lower vitric unit of the Prow Pass Tuff (sequence 7). Toward the north and east, the first occurrence of abundant zeolites extends into the bedded tuff below the Calico

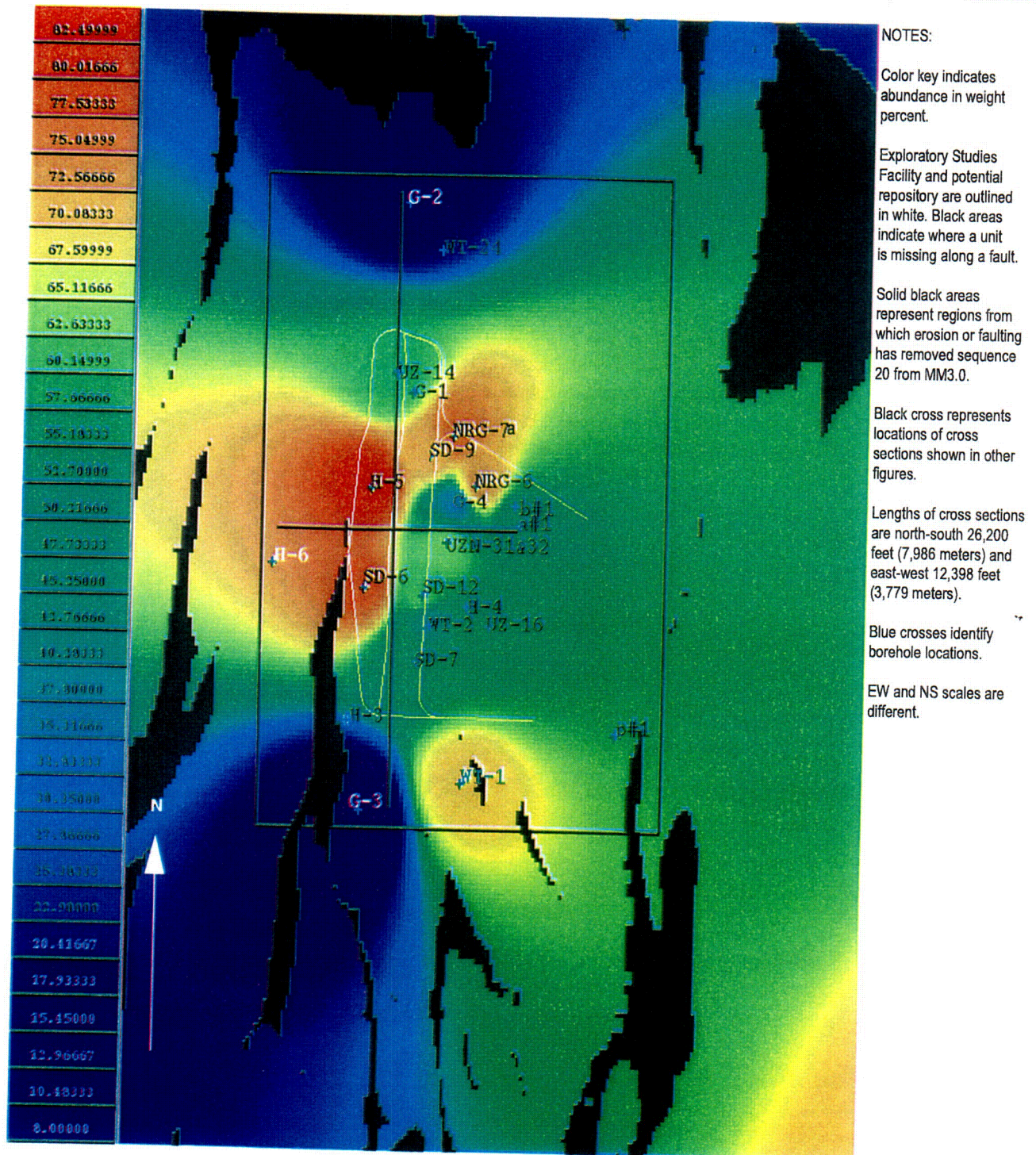


Figure 8. Map View of Volcanic Glass Distribution in "PTn" Unit, Tpcpv1 - Tptrv2 (Sequence 20) for Entire MM3.0

Hills Formation (sequence 10), into the Calico Hills Formation (sequence 11), and ultimately to the lower vitric units of the Topopah Spring Tuff (Ttpv1, Ttpv2, and Ttpv3; sequences 12 and 13) (Figure 10). The position of the water table relative to zeolitized rocks is shown in Figures 12 and 13. These cross sections were truncated at the water table, which rises in elevation toward the north and the west. In the north-south cross section, zeolite-rich rocks separate the proposed RHH (sequences 14, 15, 16 and part of 17) from the water table at all locations (Figure 12). Note the common occurrence of moderate-abundance zeolite units at the tops of the zeolite-rich units. In the east-west cross section, zeolites also occur between the RHH and the water table, except in several down-dropped blocks to the east of the repository. These zeolite-free regions develop where faulting drops the Topopah Spring Tuff below the water table.

The progressive development of zeolitization from northeast to southwest is illustrated in a series of map views through the Calico Hills Formation (Tac; Sequence 11) and into the upper vitric Prox Pass Tuff (Tcupv; Sequence 9); see Figures 14 through 19. The transition zone between regions of high (greater than 5%) and low (0 to 5%) zeolite abundance is an important feature to model accurately because it may be a zone of enhanced radionuclide sorption below the potential repository. The presence of the zeolites clinoptilolite and mordenite is associated with increased radionuclide sorptive capacity (Vaniman and Bish 1995, pp. 537-538). However, the decreased permeability associated with zeolitization of moderately welded to nonwelded vitric tuff (Loeven 1993, Table 6) may inhibit interaction between fluid-borne radionuclides and zeolites in the rock matrix. Within the transition zone, zeolites are present but the rock should be more permeable than completely zeolitized rock would be. This higher permeability may therefore allow the radionuclides better access to sorptive minerals.

The transition zone is not easily characterized. There is a striking reduction in zeolite abundance from east to west in the upper half of the Calico Hills Formation, across a north-south boundary that is well defined in the region of boreholes WT-2 and UZ#16 (Figures 14 and 15). The location and abruptness of this transition are very poorly constrained to the north and west of H-5 and moderately constrained to the south between WT-1 and G-3. In the lower half of the Calico Hills Formation (sequence 11), extensive zeolitization occurs in borehole SD-7 and moderate zeolitization occurs in SD-12 and H-6 (Figures 16 and 17). This leads to a complex transition zone, in which a high-zeolite "peninsula" extends westward from SD-7. The detailed sampling of SD-7 and SD-12 suggests a transition zone that may be quite heterogeneous both vertically and horizontally. In SD-7, sills of more than 25 percent zeolite alternate with largely vitric samples in the lower half of the Calico Hills Formation, suggesting an interfingered transition zone. In contrast, SD-12 shows a rather uniform development of increasing zeolitization with depth. These data indicate that the general reduction in zeolitization to the southwest may be strongly overprinted by patchy intervals of highly zeolitized Calico Hills Formation.

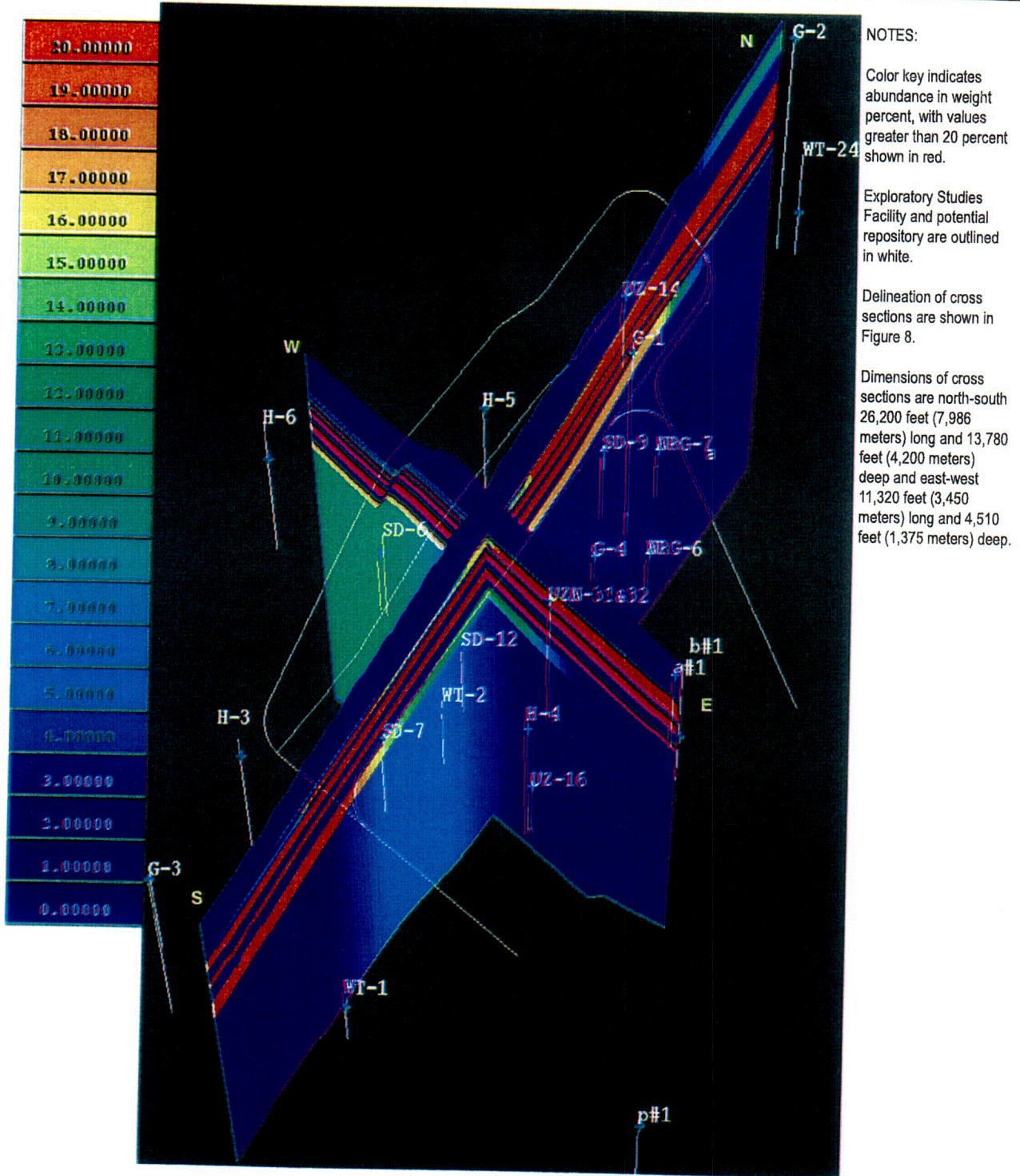
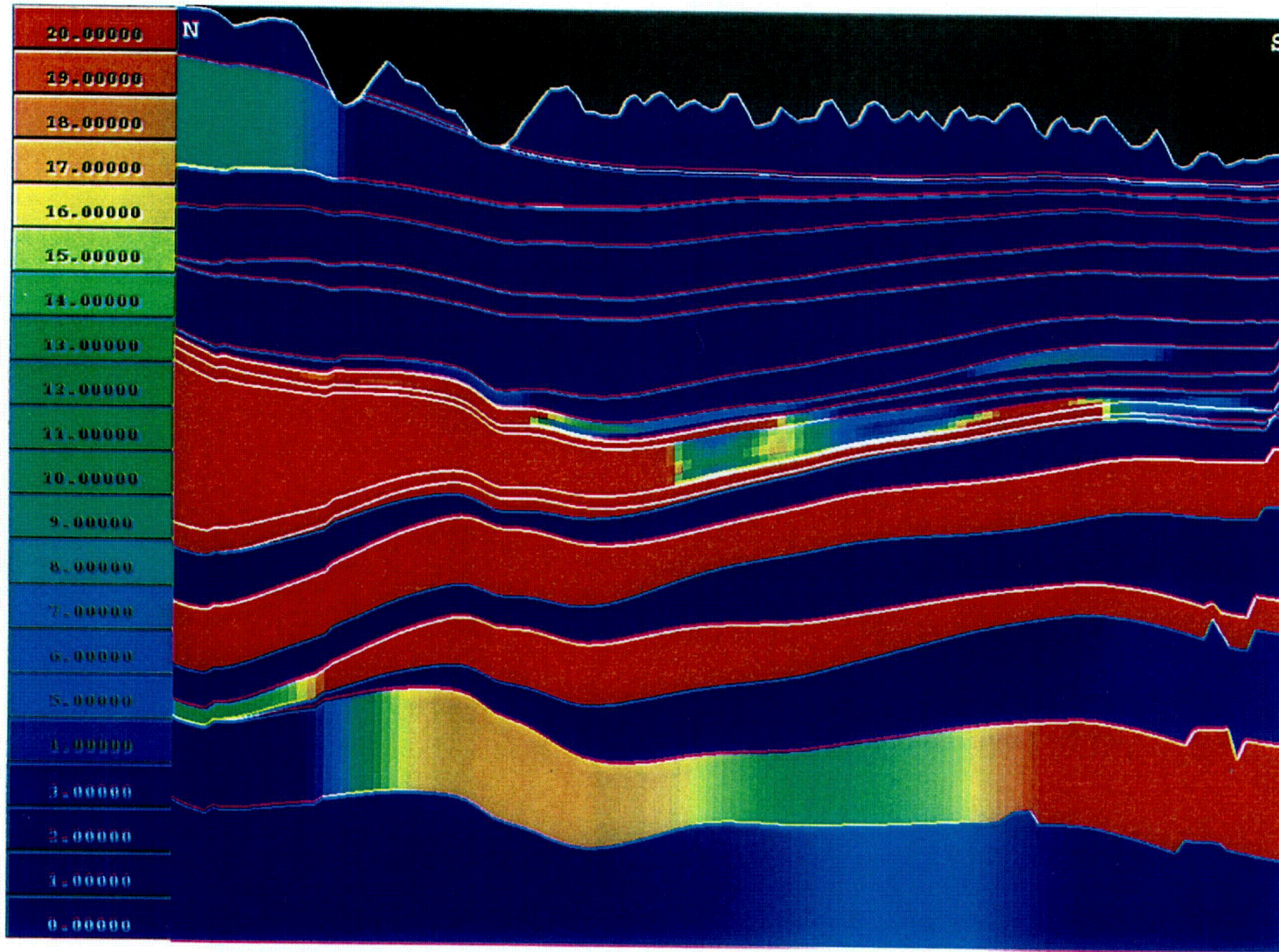


Figure 9. Zeolite Distribution in North-South and East-West Cross Sections Through Center of Potential Repository Block



NOTES:

Color key indicates abundance in weight percent, with values greater than 20 percent shown in red.

Delineation of cross section is shown in Figure 8.

Dimensions of cross section are 26,200 feet (7,986 meters) long and 4,430 feet (1,350 meters) deep.

Sequence definition and repository extent are shown in Figure 5.

Figure 10. Zeolite Distribution in North-South Cross Section Through Potential Repository Block

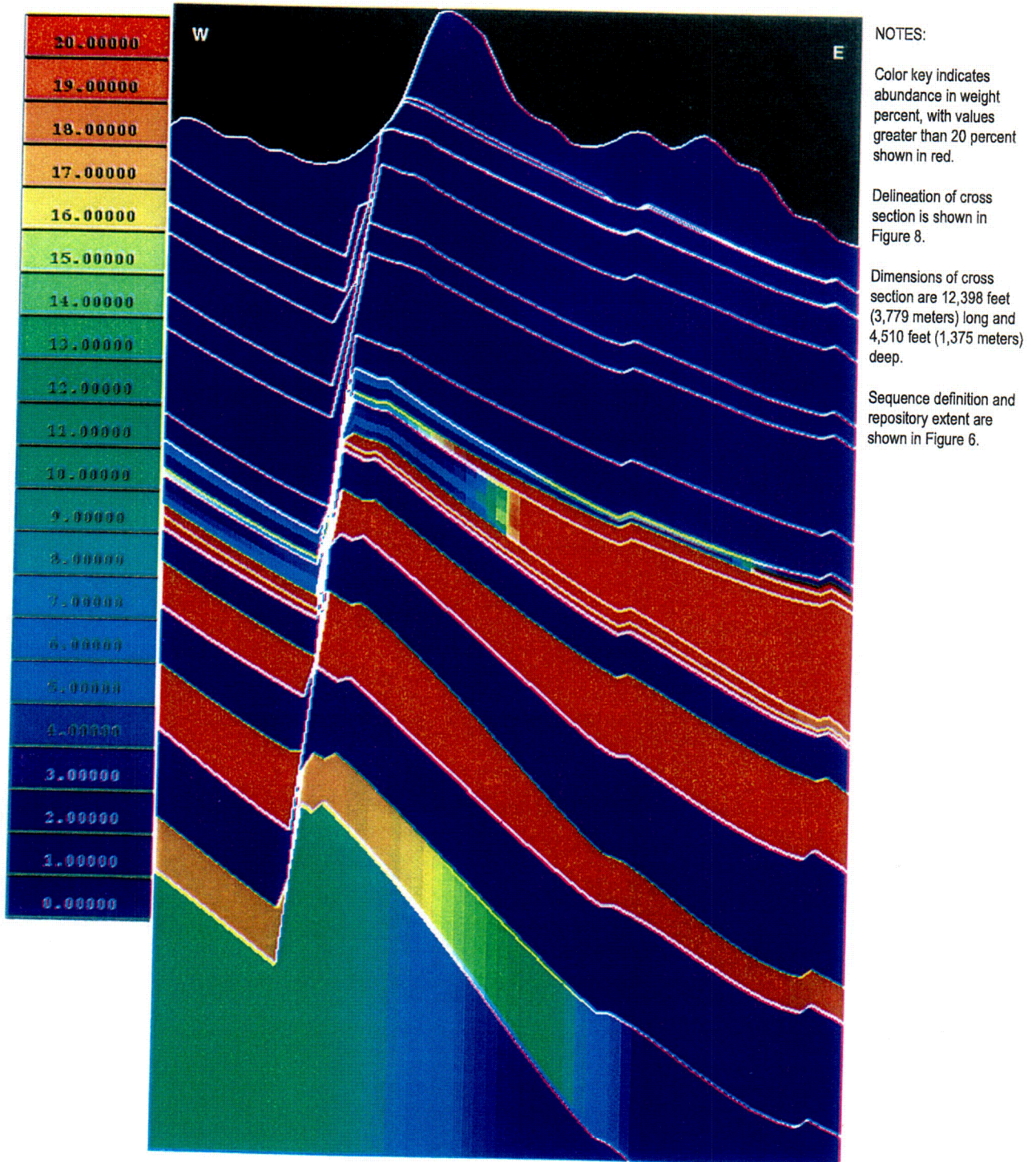
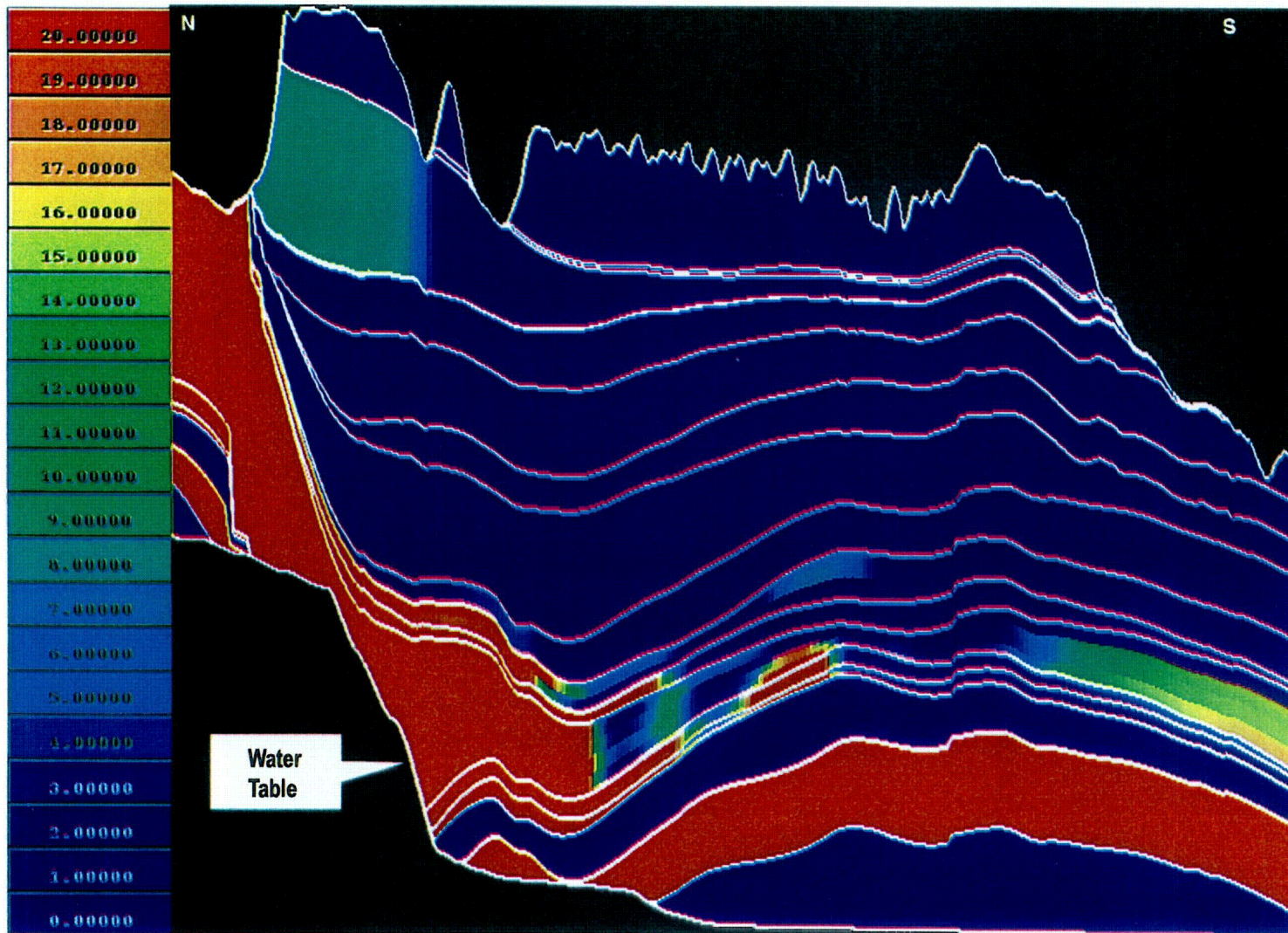


Figure 11. Zeolite Distribution in East-West Cross Section Through Potential Repository Block

C07



NOTES:

Color key indicates abundance in weight percent, with values greater than 20 percent shown in red.

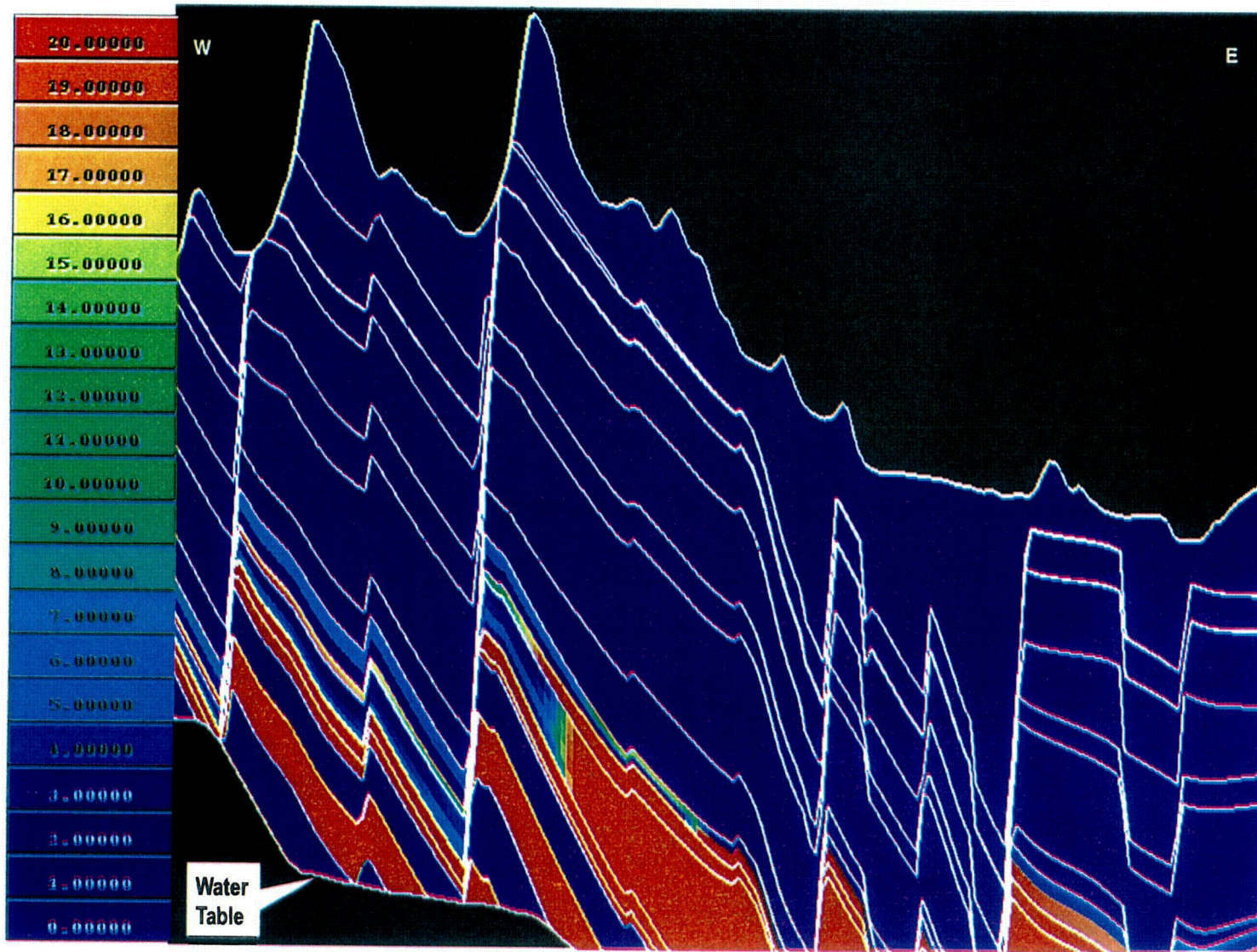
Line of section is as shown in Figure 8, with section endpoints extended to the north and south.

Dimensions of cross section are 49,000 feet (14,935 meters) long and 2,770 feet (845 meters) deep.

Sequence definitions and repository extent are shown in Figure 5.

Figure 12. Zeolite Distribution in North-South Cross Section Through Potential Repository Block and Above the Water Table

C08



NOTES:

Color key indicates abundance in weight percent, with values greater than 20 percent shown in red.

Line of section is as shown in Figure 8, but section endpoints are extended farther to the east and west.

Dimensions of cross section are 37,000 feet (11,278 meters) long and 2,445 feet (745 meters) deep.

Water table to the east is flat and coincides with the bottom of the figure.

Sequence definitions and repository extent are shown in Figure 6.

Figure 13. Zeolite Distribution in East-West Cross Section Through Potential Repository Block and Above Water Table

09

The bedded tuff below the Calico Hills Formation (sequence 10, Tacbt) is zeolitized in boreholes SD-7, WT-2, SD-12, and H-5 (Figure 18). The transition zone to low zeolite abundance is confined to the southwest, around SD-6, H-3, and G-3. However, SD-6 contains about 15 percent smectite and perhaps should be viewed as a part of the zone of abundant sorptive mineralogy. There are no data for this unit at H-6.

The upper vitric Prow Pass Tuff (sequence 9, Tcpu) has a zeolite distribution similar to that of Tacbt, except that there are data at H-6 with abundant zeolites (Figure 19). In addition, SD-6 lacks both smectite and zeolites in sequence 9.

Zeolitization is complete throughout the MM in sequence 7, which includes the lower vitric and bedded tuffs of the Prow Pass Tuff and the upper vitric unit of the Bullfrog Tuff.

In general, the MM represents the transition zone as a rather sharp boundary modified by the local effects of particular boreholes. The southwest region as a whole is characterized by low zeolite abundances (less than 10 percent). Values near 0 percent in the Calico Hills Formation (sequence 11) are restricted to regions adjacent to nonzeolite-bearing boreholes such as G-3, H-3, and H-5. There is little control on the extrapolation of zeolite data in the northeast, northwest, and southeast regions of the MM. The predicted values of extensive zeolitization in the north are strongly influenced by boreholes such as G-2 and G-1. It is possible that either of the regions distant from these boreholes may be characterized by more moderate values of zeolitization.

The most abundant zeolites at Yucca Mountain are clinoptilolite and mordenite (Bish and Chipera 1989, Appendix A). Major, stratigraphically continuous intervals of clinoptilolite occur in all boreholes, from about 330 to 500 feet (100 to 150 meters) above the water table to about 1,600 feet (500 meters) below the water table. Heulandite is fairly common at Yucca Mountain but is combined with clinoptilolite in the XRD analyses because the two minerals have the same crystal structure. Mordenite often occurs along with clinoptilolite but is less abundant in boreholes to the south; for example, it is virtually absent in bulk-rock samples from borehole G-3. The nonsorptive zeolite analcime occurs as a higher temperature alteration product at greater depths, and its occurrence deepens stratigraphically from the Prow Pass Tuff in G-2 to the Tram Tuff in G-1 and older lavas in G-3. Except in the north, the depths of analcime occurrence are so great that little interaction with migrating radioactive waste is likely.

Until core samples from borehole SD-7 were analyzed, chabazite was known only as a rare zeolite at Yucca Mountain. However, samples from the Calico Hills Formation (sequence 11) in SD-7 contained significant amounts of chabazite (up to 9 percent) in an approximately 46-foot- (14-meter-) thick zeolitized interval consisting principally of clinoptilolite + chabazite, overlying a clinoptilolite + mordenite zone (DTN: LADV831321AQ97.001). This occurrence indicates that the sorptive zeolite assemblages may be more complex at the southern end of the exploratory block than previously predicted.

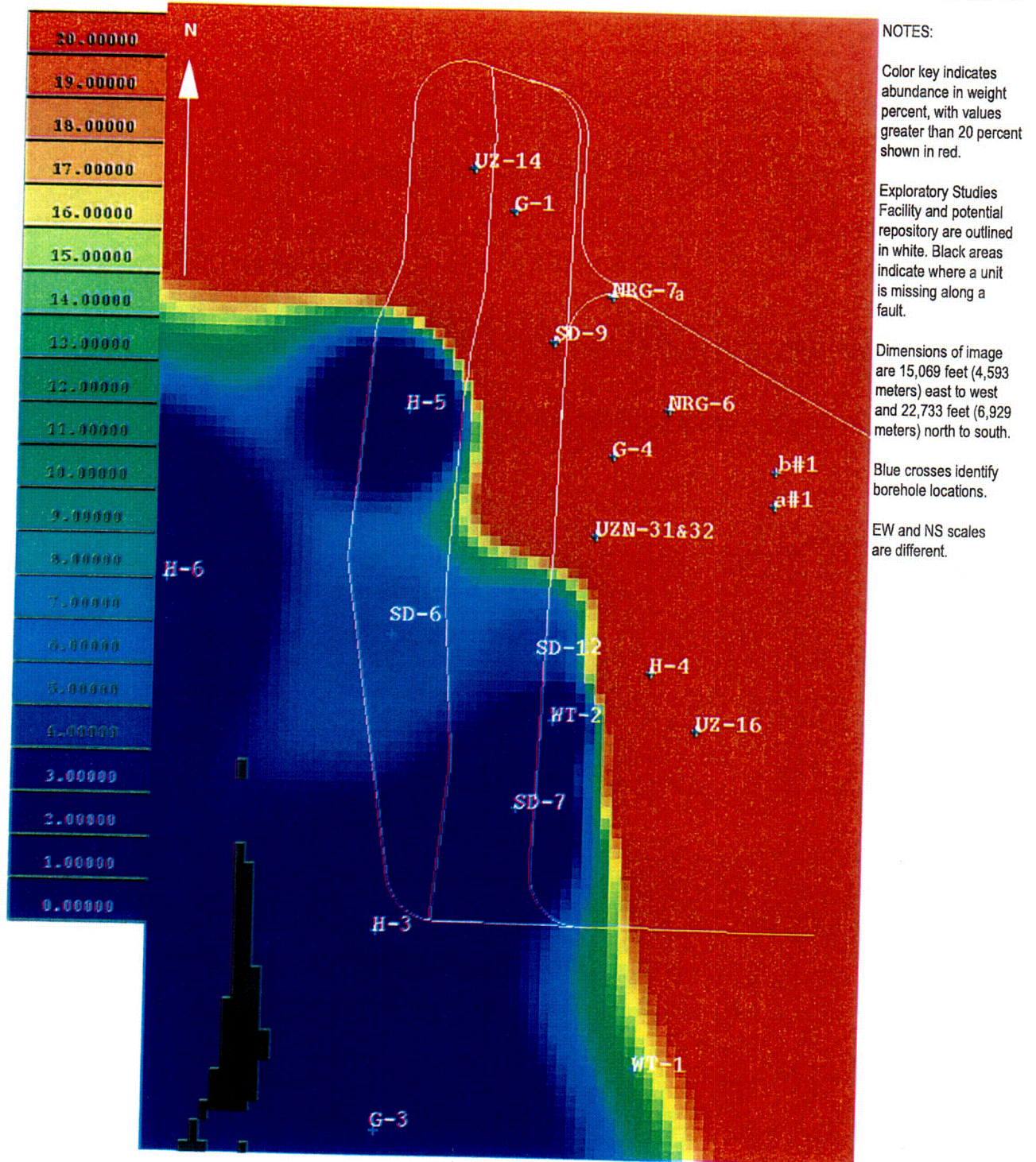


Figure 14. Zeolite Distribution in Map View of Upper Layer (Layer 14) of Calico Hills Formation (Tac, Sequence 11)

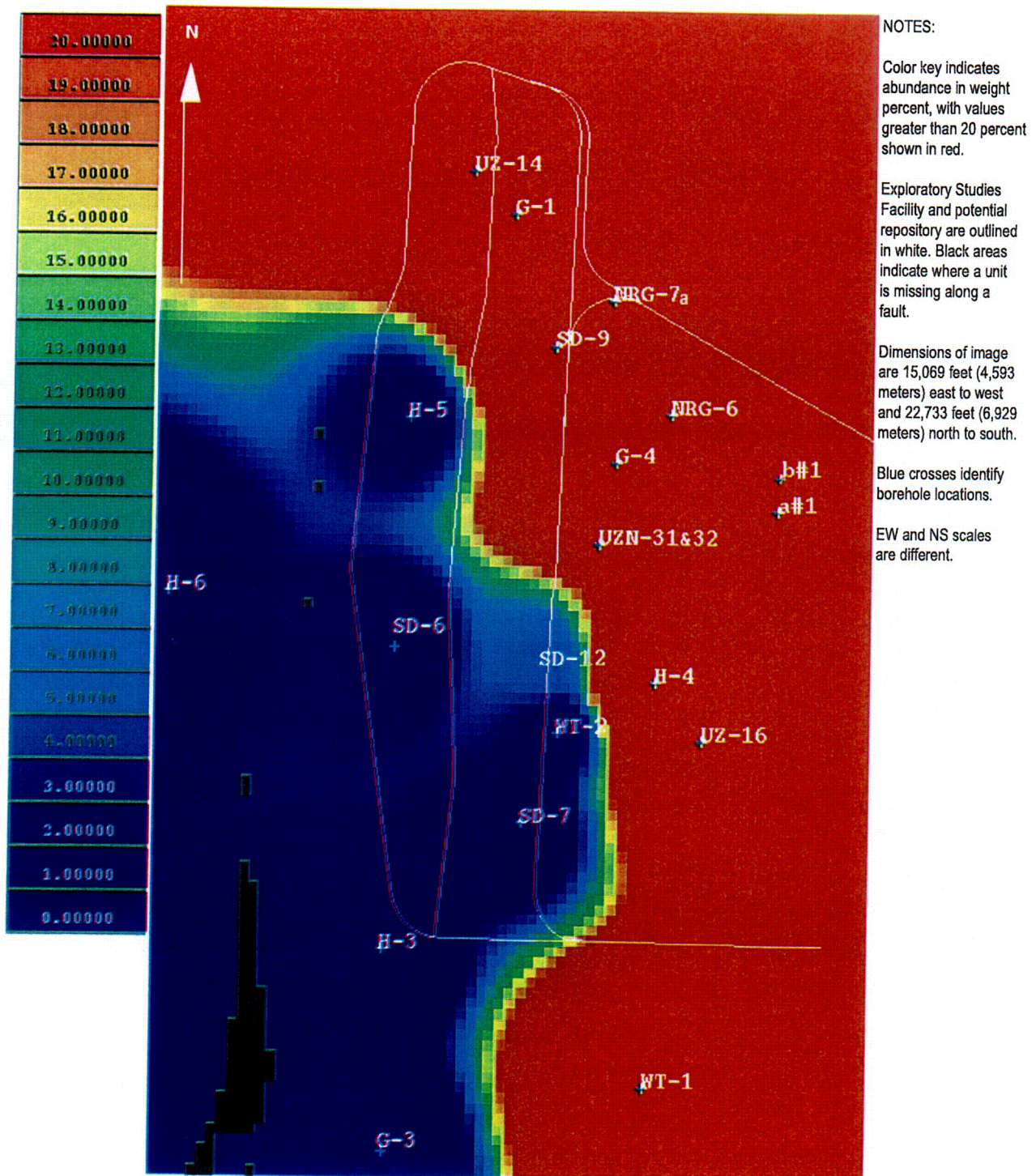


Figure 15. Zeolite Distribution in Map View of Middle-Upper Layer (Layer 13) of Calico Hills Formation (Tac, Sequence 11)

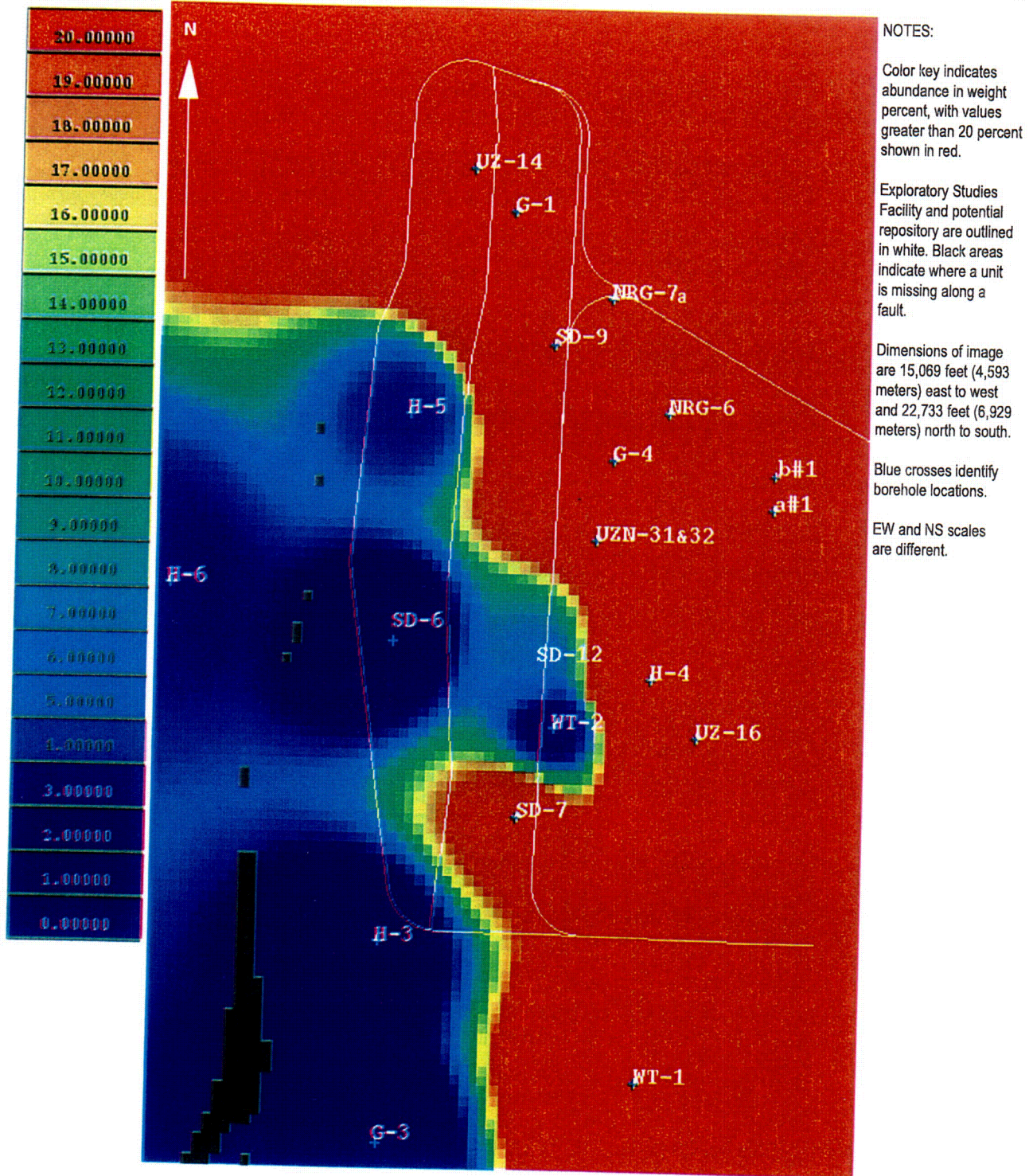


Figure 16. Zeolite Distribution in Map View of Middle-Lower Layer (Layer 12) of Calico Hills Formation (Tac, Sequence 11)

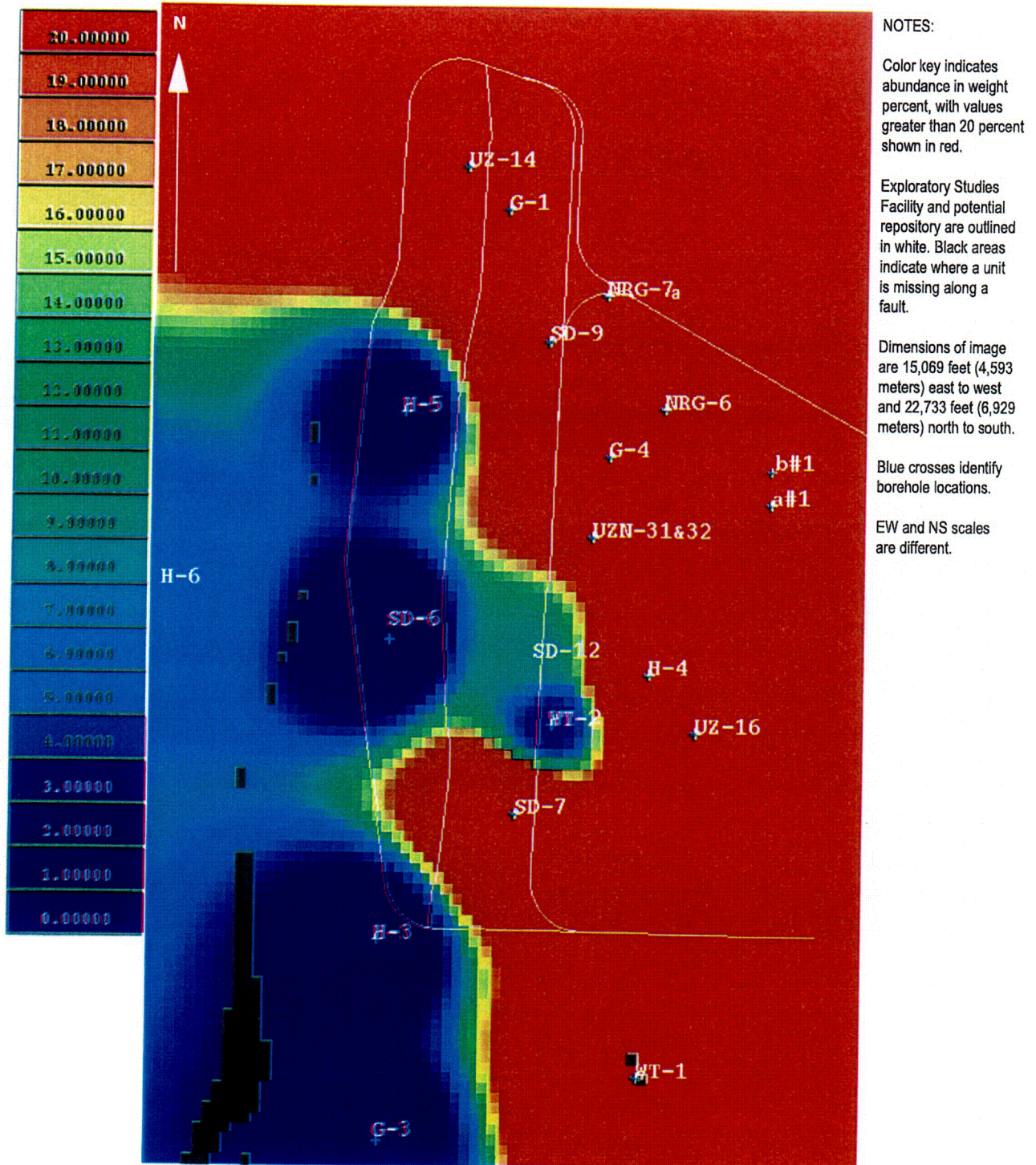


Figure 17. Zeolite Distribution in Map View of Lower Layer (Layer 11) of Calico Hills Formation (Tac, Sequence 11)

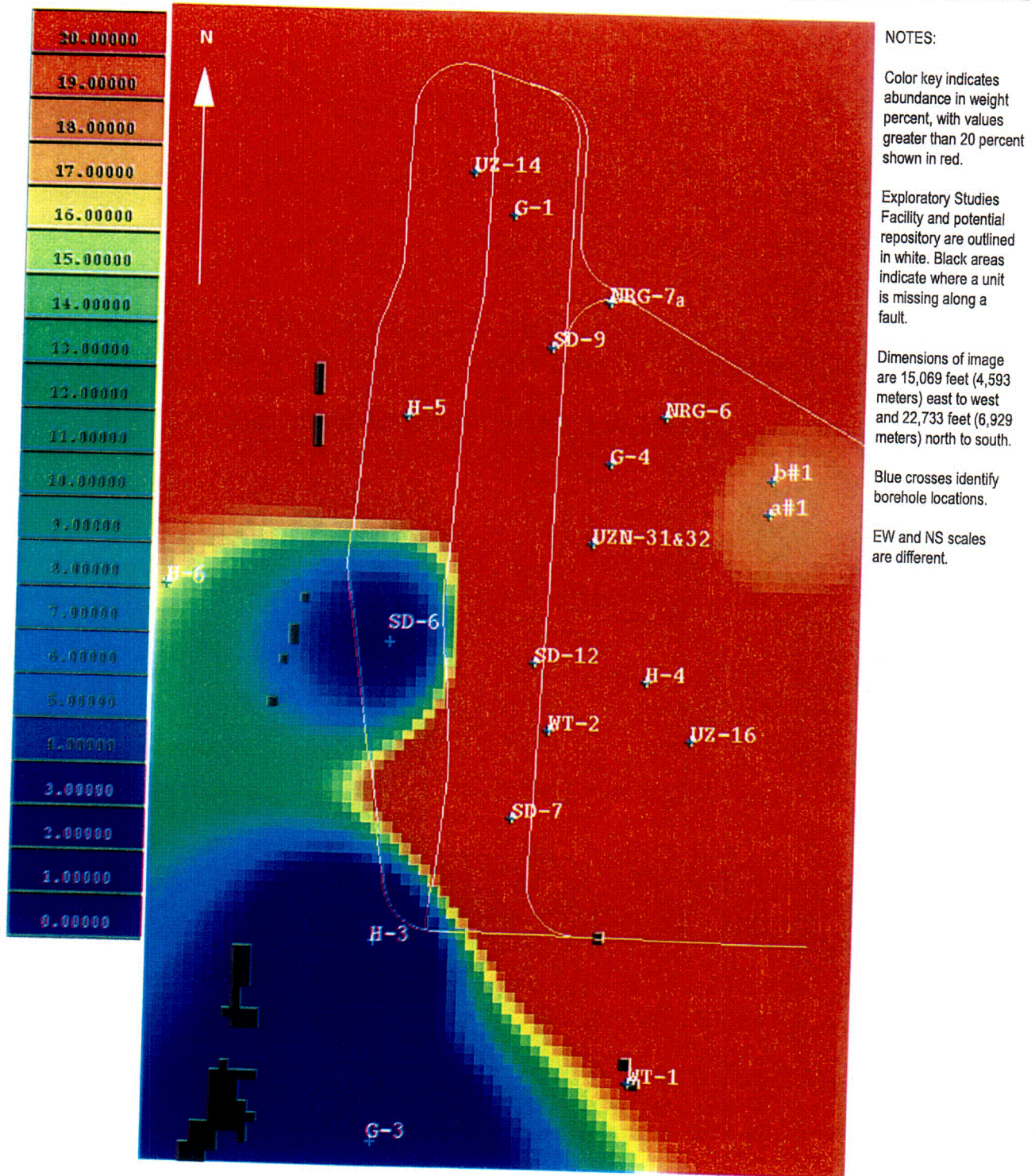


Figure 18. Zeolite Distribution in Map View of Bedded Tuff of Calico Hills Formation (Tactb, Sequence 10)

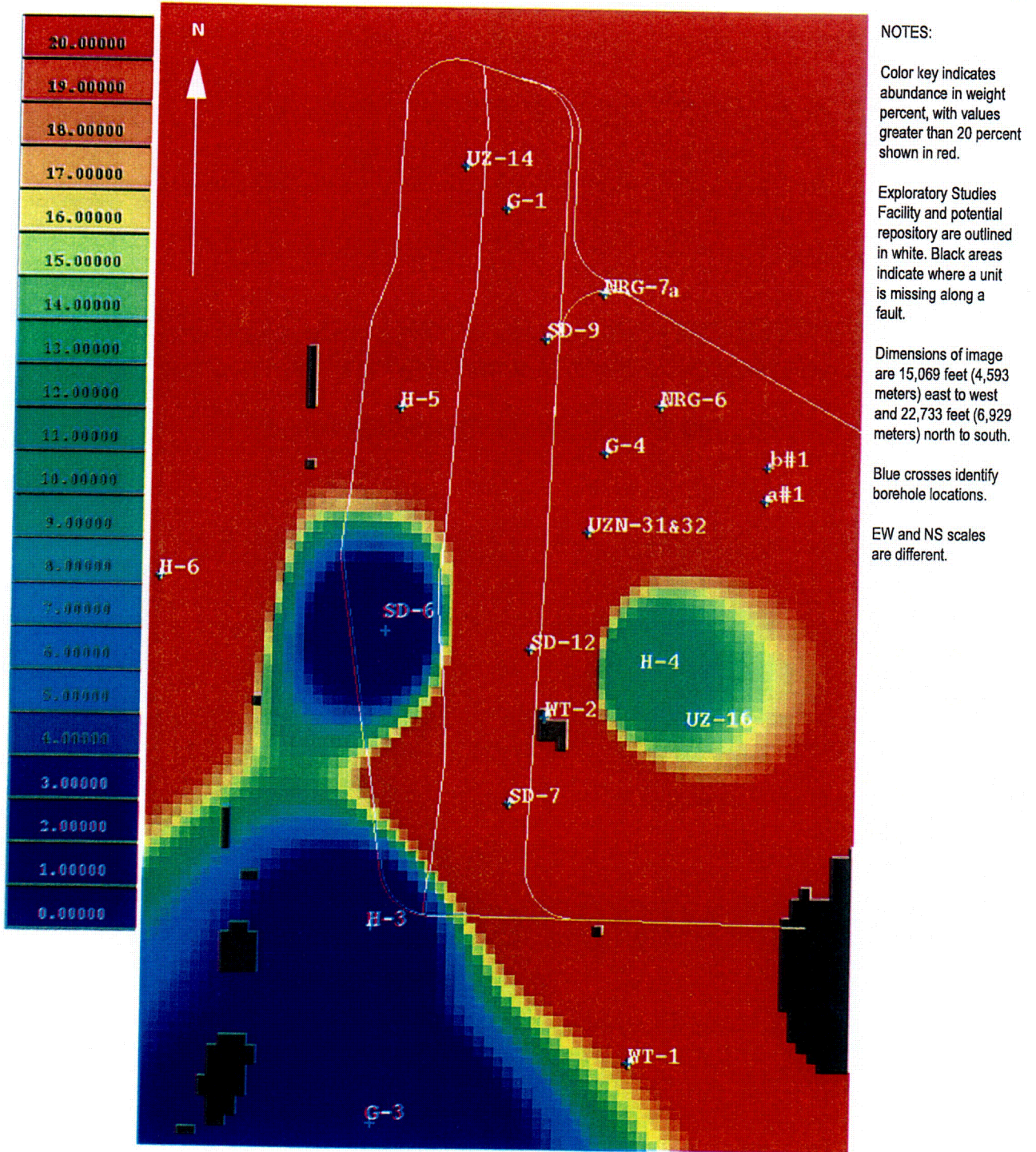


Figure 19. Zeolite Distribution in Map View of Upper Vitric Zone of Prow Pass Tuff (Tcpu, Sequence 9)

In addition to clinoptilolite, mordenite, analcime, and minor chabazite, localized occurrences of a few other zeolites were found at Yucca Mountain. Stellerite is common in fractures of the Topopah Spring Tuff and is particularly common in both the fractures and matrix of the Topopah Spring Tuff in borehole UZ#16. Stellerite extends into the lower devitrified portion of the Topopah Spring Tuff (sequences 14 and 15) in borehole UZ-14, spanning an interval in which perched water was observed during drilling. Phillipsite is a rare zeolite at Yucca Mountain that was found only in the altered zone above the water table at the top of the basal vitrophyre of the Topopah Spring Tuff (Carlos et al. 1995, pp. 39, 47). Laumontite occurs in very small amounts (less than 4 percent) in deep, altered tuffs in borehole p#1 and perhaps in G-1 (Bish and Chipera 1989). Phillipsite and laumontite are so rare that it was not necessary to consider them in the estimation of zeolite volume for the MM.

Erionite is another rare zeolite at Yucca Mountain and was at first observed only in the altered zone at the top of the Topopah Spring Tuff basal vitrophyre. However, it has since been found in significant quantities (up to 34 percent) in drill core from a 10-foot- (3-meter-) thick sequence in the bulk rock underlying the Topopah Spring Tuff basal vitrophyre in borehole UZ-14 and in trace amounts (1 percent) in a breccia zone in the south ramp of the ESF. Although the occurrence of erionite is rather sporadic and, where found, its abundance is typically low, it is a significant health concern due to its known carcinogenicity.

6.3.3 Smectite + Illite Distribution

Smectite is a swelling clay with a high cation-exchange capacity. Where present in significant amounts, it can act as a relatively impermeable barrier to fluid flow. It effectively sorbs many cationic species, such as Pu(V) in biocarbonate water, and is therefore an important factor in calculations of radionuclide retardation (Vaniman et al. 1996). Illites are clays with a higher layer charge than smectites, reducing their effective cation-exchange capacity and eliminating their impermeable character. At greater depths, illite develops as a prograde product of smectite alteration, particularly in the northern and central portions of the MM (Bish and Aronson 1993, pp. 151-155).

Smectite + illite are present in low abundance throughout Yucca Mountain except in some thin horizons and at depth in the region of boreholes G-1 and G-2 (Figures 20 and 21). XRD analyses indicate smectite in virtually all analyzed samples, although typically in amounts less than 5 percent. Volumes of smectite + illite increase at depth, particularly in the fossil geothermal system. Above the water table, there are two zones of up to 75 percent smectite in the Paintbrush Group, one within the vitric nonwelded section above the Topopah Spring Tuff (PTn, sequence 20) and one at the top of the basal vitrophyre of the Topopah Spring Tuff (upper layer of sequence 13). These smectites typically have nonexpandable illite contents of 10 to 20 percent (Bish and Aronson 1993, pp. 151-152). Well beneath the water table (depths greater than 3,300 feet (1,000 meters) below ground surface), the ancient (approximately 10.7 million years ago) geothermal system generated abundant smectite + illite but with a much higher illite content (up to about 80 to 90 percent) (Bish and Aronson 1993, Figures 3 and 4, pp. 152-153). However, the illitic clays occur at such great depths that they are of little importance for transport modeling at Yucca Mountain.

6.3.4 Volcanic Glass Distribution

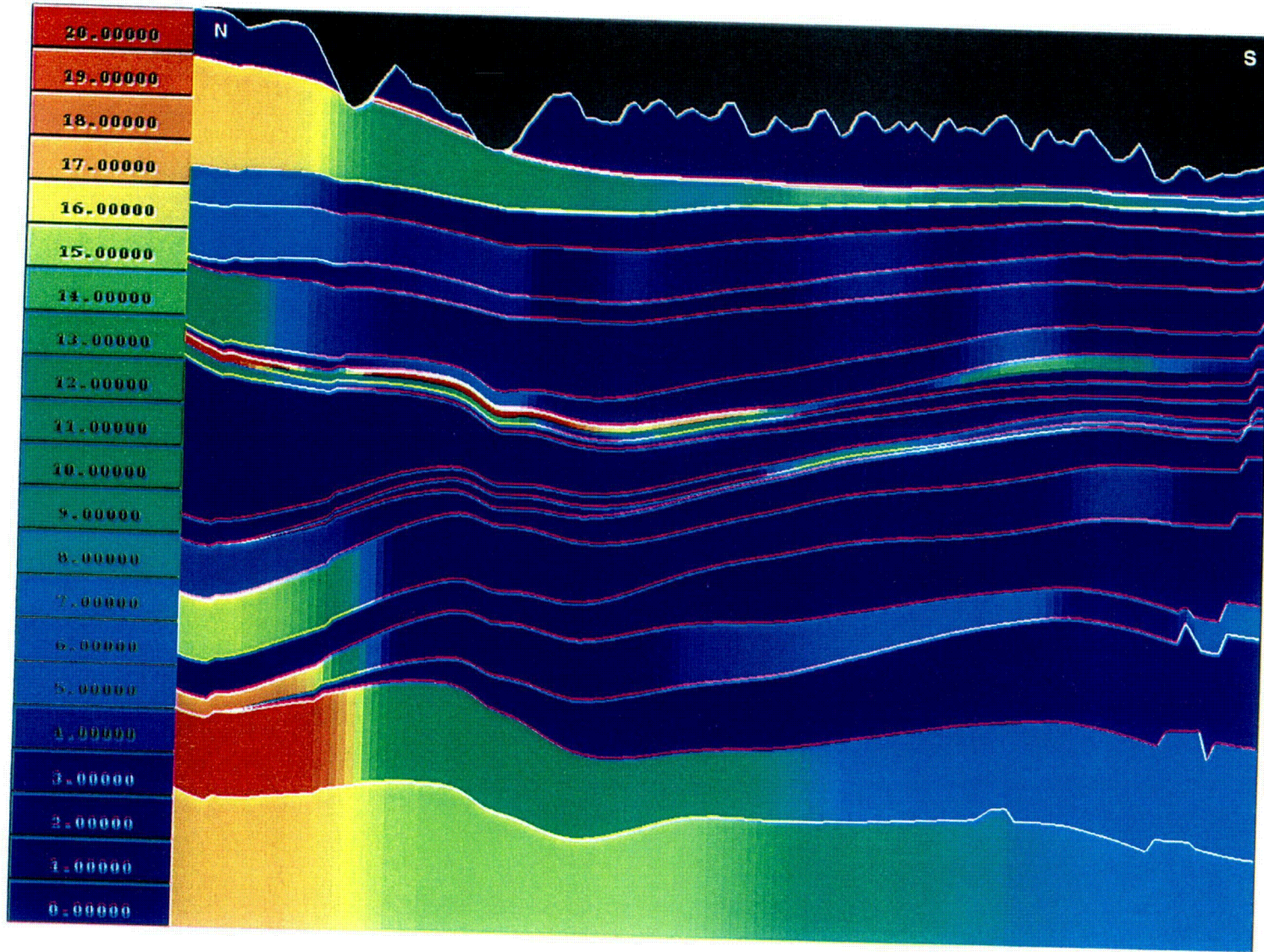
Volcanic glass is a highly reactive, metastable material that can react in the presence of water to form assemblages including zeolites and clays. The distribution of volcanic glass relative to the potential repository location is an important factor in evaluating possible repository-induced mineral reactions and assessing their impact on repository performance. Volcanic glass is almost entirely restricted to regions above the water table at Yucca Mountain (Figures 8, 22, and 23). The location of the water table is displayed in Figures 12 and 13. The most significant occurrences of volcanic glass are in the PTn unit (sequence 20), the lower vitrophyre of the Topopah Spring Tuff (top of sequence 13), and in vitric, zeolite-poor regions of the Calico Hills Formation (sequence 11) in the southwestern and western regions of the MM. The distribution of volcanic glass in the Calico Hills Formation is inversely correlated with zeolite abundance. In the transition zone between high- and low-abundance zeolite, volcanic glass and zeolite occur together.

6.3.5 Silica Polymorph Distribution

The common silica polymorphs at Yucca Mountain include quartz, cristobalite, opal-CT, and tridymite. These minerals could potentially affect repository performance because of their chemical reactivity, mechanical response to temperature, and potential impact on human health during mining operations. Repository-induced heating may accelerate the chemical reactions of cristobalite, opal-CT, and tridymite to quartz, which is the stable silica polymorph. In addition, all of the silica minerals are susceptible to dissolution/precipitation reactions. Therefore, the potential exists for substantial redistribution of silica with resulting changes in the permeability and porosity of the matrix and fractures in the repository environment. The results of the MM, showing ambient conditions, can be used to model in 3-D the effects of thermal and geochemical reactions of metastable silica polymorphs on repository performance. Tridymite and cristobalite also undergo phase transitions between 100 and 275°C (Thompson and Wennemer 1979, pp. 1018-1025), which may have an impact on the mechanical integrity of the repository. The α to β reaction in cristobalite is of particular concern in thermal-load designs because of effects on porosity, permeability, and mechanical strength. Finally, the crystalline silica polymorphs (quartz, cristobalite, and tridymite) are all regulated health hazards.

Cristobalite and tridymite are abundant in the potential RHH. Opal-CT is usually found in association with sorptive zeolites. Tridymite occurs above the water table and primarily above the potential RHH, particularly in those parts of the Topopah Spring and Tiva Canyon Tuffs where vapor-phase crystallization is common (Figures 24 and 25). Pseudomorphs of quartz replacing tridymite in deep fractures and cavities are evidence of the instability of tridymite under low-temperature aqueous conditions. Tridymite occurrences have been interpreted as a possible limit on past maximum rises in the water table at Yucca Mountain (Levy 1991, pp. 483-484). Volumes of exceptionally high tridymite content are restricted to the upper strata within the Tiva Canyon and Topopah Spring Tuffs but rarely exceed 20 percent.

Cristobalite is typically a devitrification product that is found in virtually every sample above the water table. Opal-CT, which is a typical byproduct of zeolitization, is found below the water table before disappearing at depths at or below the Tram Tuff. Cristobalite and opal-CT are



NOTES:

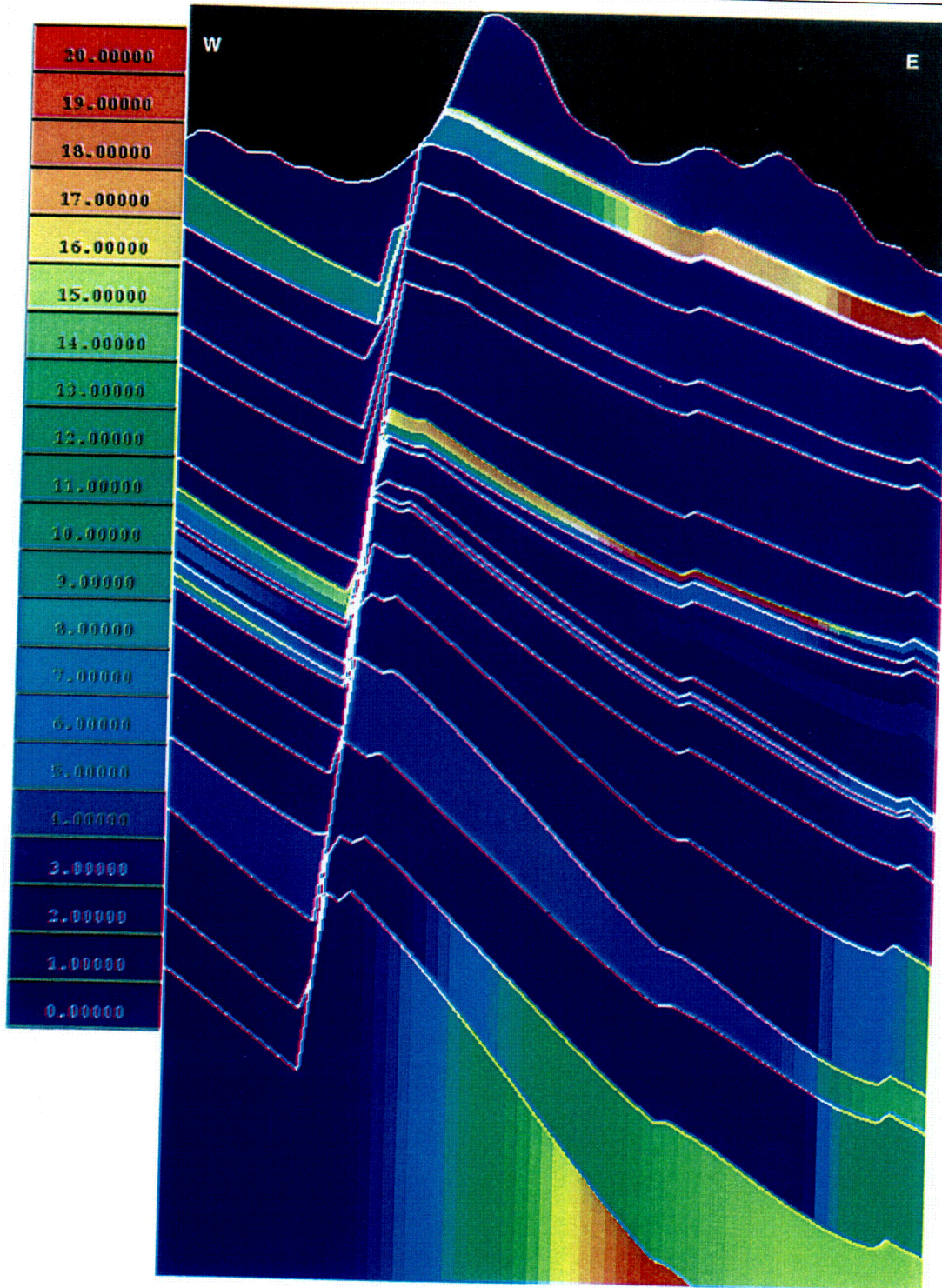
Color key indicates abundance in weight percent, with values greater than 20 percent shown in red.

Delineation of cross section is shown in Figure 8.

Dimensions of cross section are 26,200 feet (7,986 meters) long and 4,430 feet (1,350 meters) deep.

Sequence definitions and repository extent are shown in Figure 5.

Figure 20. Smectite + Illite Distribution in North-South Cross Section Through Potential Repository



NOTES:

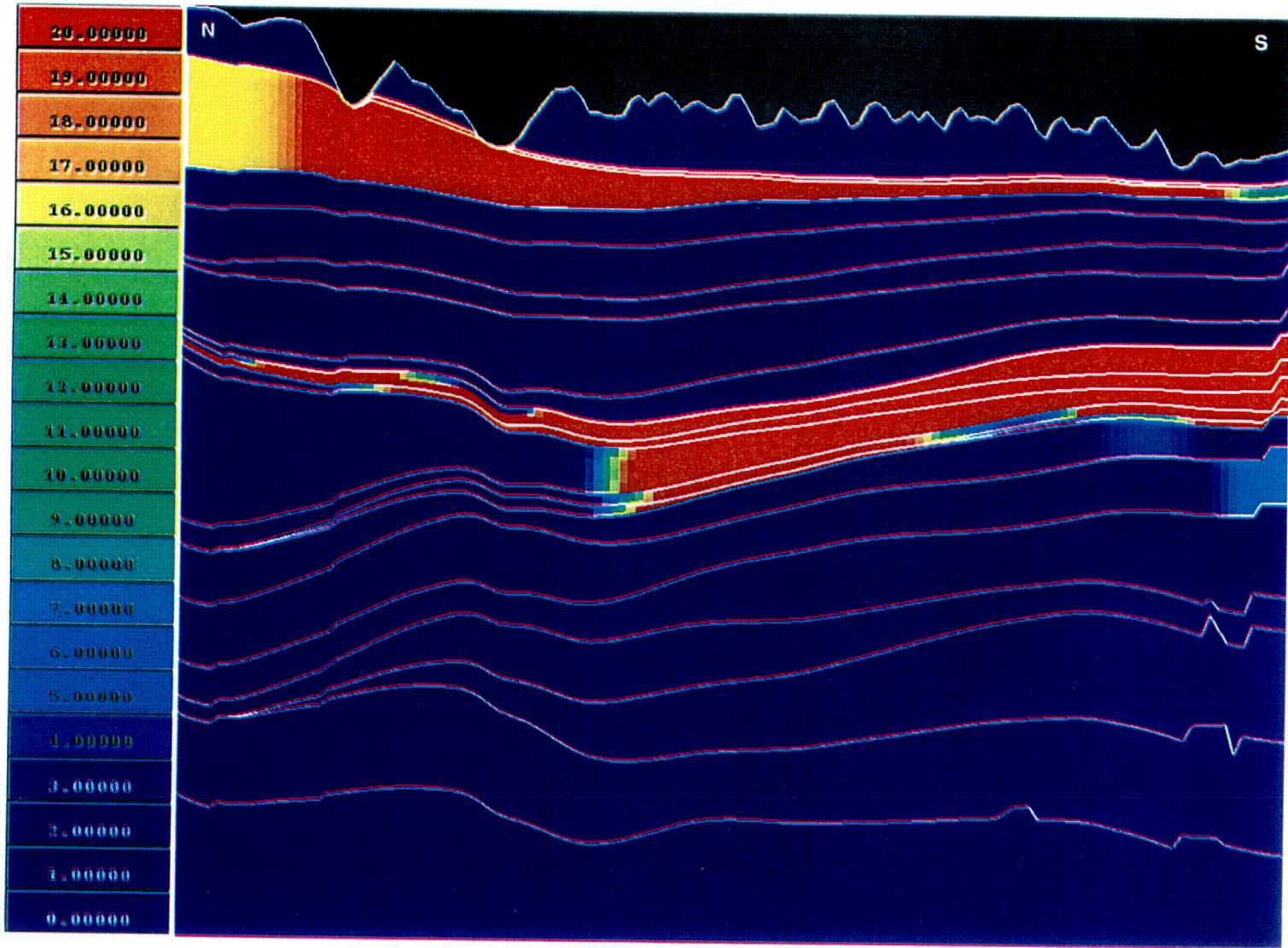
Color key indicates abundance in weight percent, with values greater than 20 percent shown in red.

Delineation of cross section is shown in Figure 8.

Dimensions of cross section are 12,398 feet (3,779 meters) long and 4,510 feet (1,375 meters) deep.

Sequence definitions and repository extent are shown in Figure 6.

Figure 21. Smectite + Illite Distribution in East-West Cross Section Through Potential Repository



NOTES:

Color key indicates abundance in weight percent, with values greater than 20 percent shown in red.

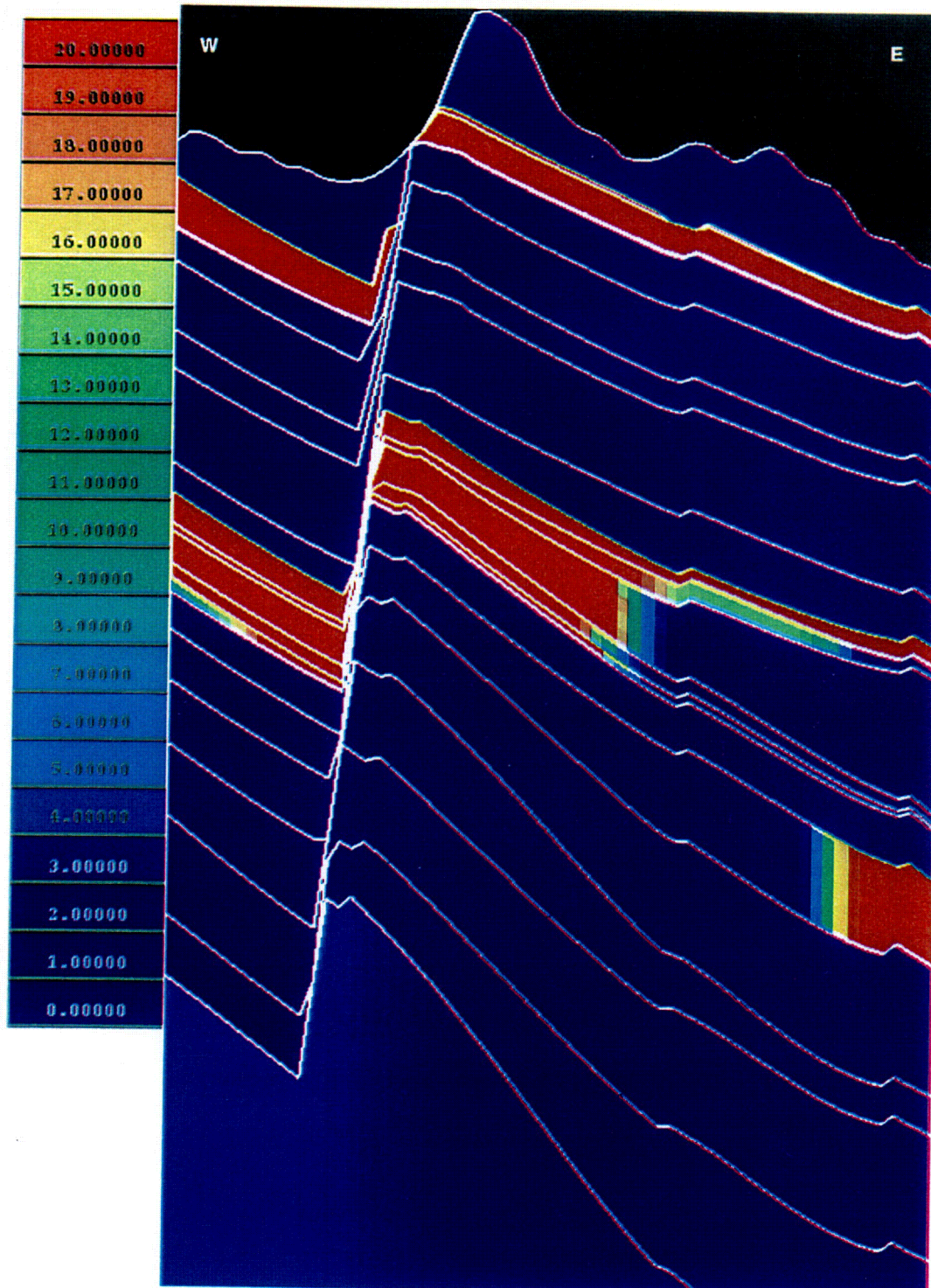
Delineation of cross section is shown in Figure 8.

Dimensions of cross section are 26,200 feet (7,986 meters) long and 4,430 feet (1,350 meters) deep.

Sequence definitions and repository extent are shown in Figure 5.

Figure 22. Volcanic Glass Distribution in North-South Cross Section Through Potential Repository

C18



NOTES:

Color key indicates abundance in weight percent, with values greater than 20 percent shown in red.

Delineation of cross section is shown in Figure 8.

Dimensions of cross section are 12,398 feet (3,779 meters) long and 4,510 feet (1,375 meters) deep.

Sequence definitions and repository extent are shown in Figure 6.

Figure 23. Volcanic Glass Distribution in East-West Cross Section Through Potential Repository

U combined in the MM, partly because the extra analytical procedures necessary to distinguish them were not commonly applied to the borehole data, but also because the two minerals dissolve to similar aqueous silica concentrations. As is evident in Figures 26 and 27, cristobalite and opal-CT are very abundant in the devitrified tuffs of the Paintbrush Group. Occurrences below the Paintbrush Group units are primarily opal-CT in tuffs containing abundant sorptive zeolites. Cristobalite and opal-CT disappear at depth and are replaced by quartz-bearing assemblages.

Quartz is common in the lower Topopah Spring Tuff and is abundant at depth in the Crater Flat Group (Figures 28 and 39).

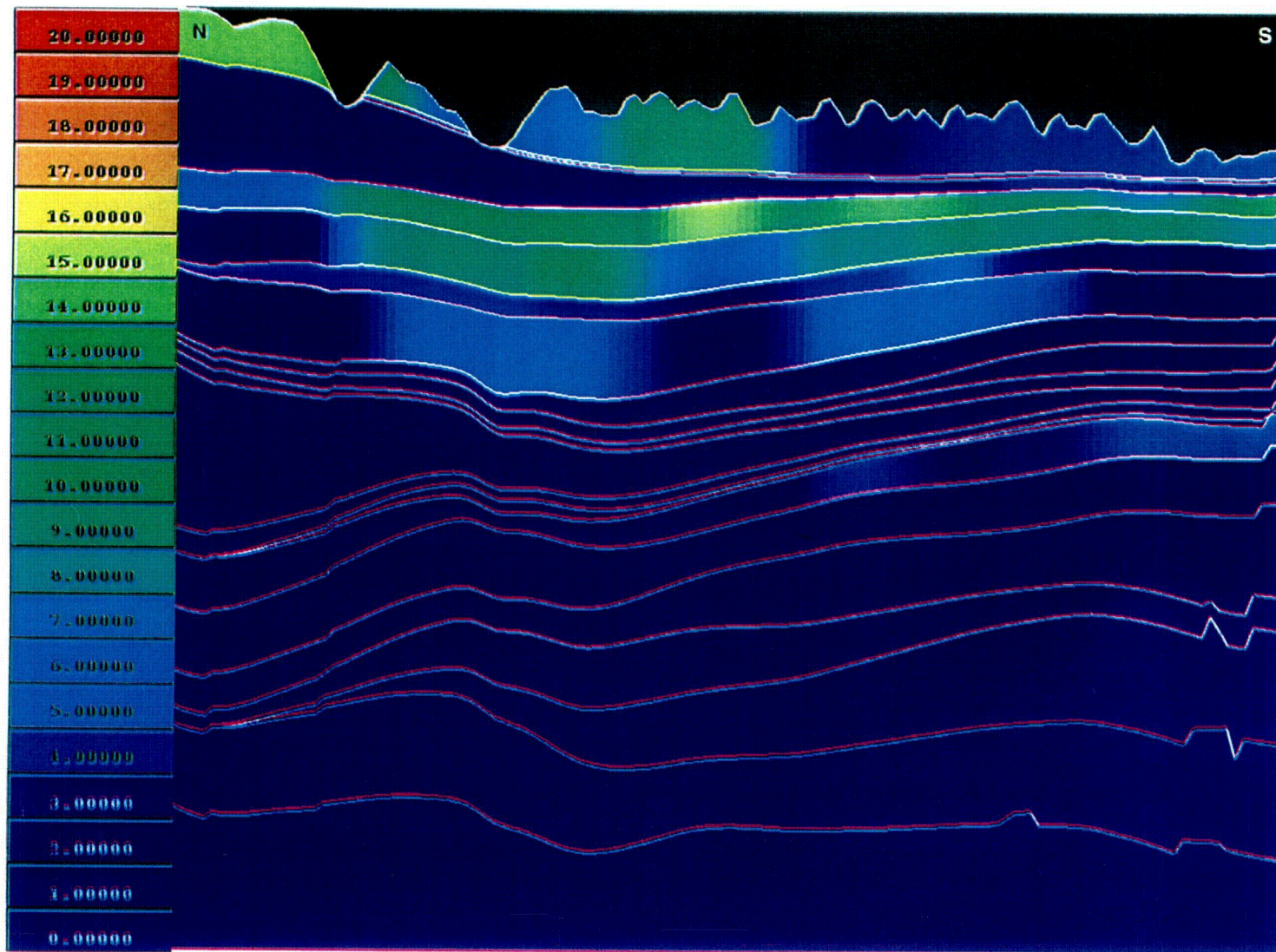
6.4 UNCERTAINTIES AND LIMITATIONS IN MINERALOGIC MODEL

Several uncertainties are associated with the MM in regions distant from the boreholes. In particular, there are striking geographic differences in mineral abundances that relate to past geologic processes. These are most obvious in the stratigraphic depth of zeolitization increasing to the southwest (from the Calico Hills Formation to the Prow Pass Tuff) across the MM (Figures 14 to 19). Currently, the borehole data are not adequate for determining the precise location of the transition from vitric to zeolitic Calico Hills Formation. There is considerable uncertainty associated with the trend of the transition to the north and west of borehole UZ-14 because of significant differences among UZ-14, G-2, and WT-24. There is also uncertainty related to the nature of the transition, that is, whether the depth to zeolitization decreases rapidly and smoothly along a well-defined front or whether zeolitized zones are interfingered with vitric zones along a highly irregular front.

With the exception of UZ-16, the input data have a to be verified (TBV) status, with some data unconfirmed and some unqualified (See the DIRS database). This report emphasizes that all data are essential to the development of an adequate 3-D model of mineral abundances. However, those TBV data on which the MM is based currently are being evaluated to verify their quality-assurance status. Data identified to be unqualified through this verification activity will be subject to an independent qualification process, in accordance with AP-SIII.2Q, to ensure that those data on which the MM is based are fully qualified. Because it is anticipated that all data on which the MM is based ultimately will be qualified, there is no need at this time to develop criteria, pursuant to AP-3.10Q, by which to assess the impact and appropriateness of the use of unqualified data on the applicability or validity of the MM. These issues are discussed in greater detail in the following subsections.

6.4.1 Model Limitations

The most significant limitation of MM3.0 is the scarce mineralogic data in the region beyond the western border of the potential repository. For example, an examination of Figure 3 demonstrates the importance of SD-6 in providing the only substantial quantity of mineralogic data along the western edge of Yucca Mountain. The uncertainty in the boundary regions of the MM is also elevated because of the limited number of sampling locations (see Figures 3 and 8).



NOTES:

Color key indicates abundance in weight percent, with values greater than 20 percent shown in red.

Location of cross section is shown in Figure 8.

Dimensions of cross section are 26,200 feet (7,986 meters) long and 4,430 feet (1,350 meters) deep.

Sequence definitions and repository extent are shown in Figure 5.

Figure 24. Tridymite Distribution in North-South Cross Section Through Potential Repository

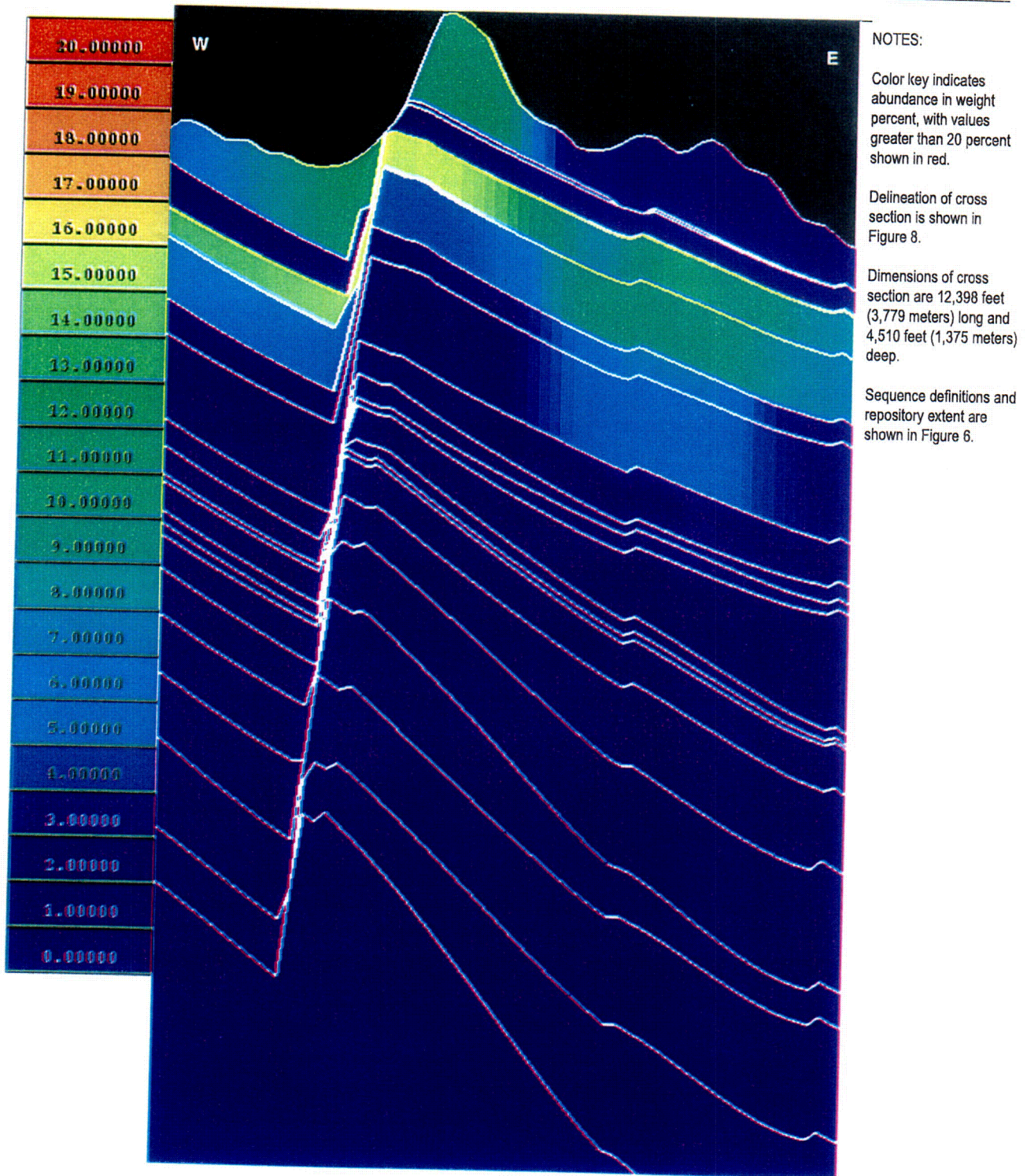
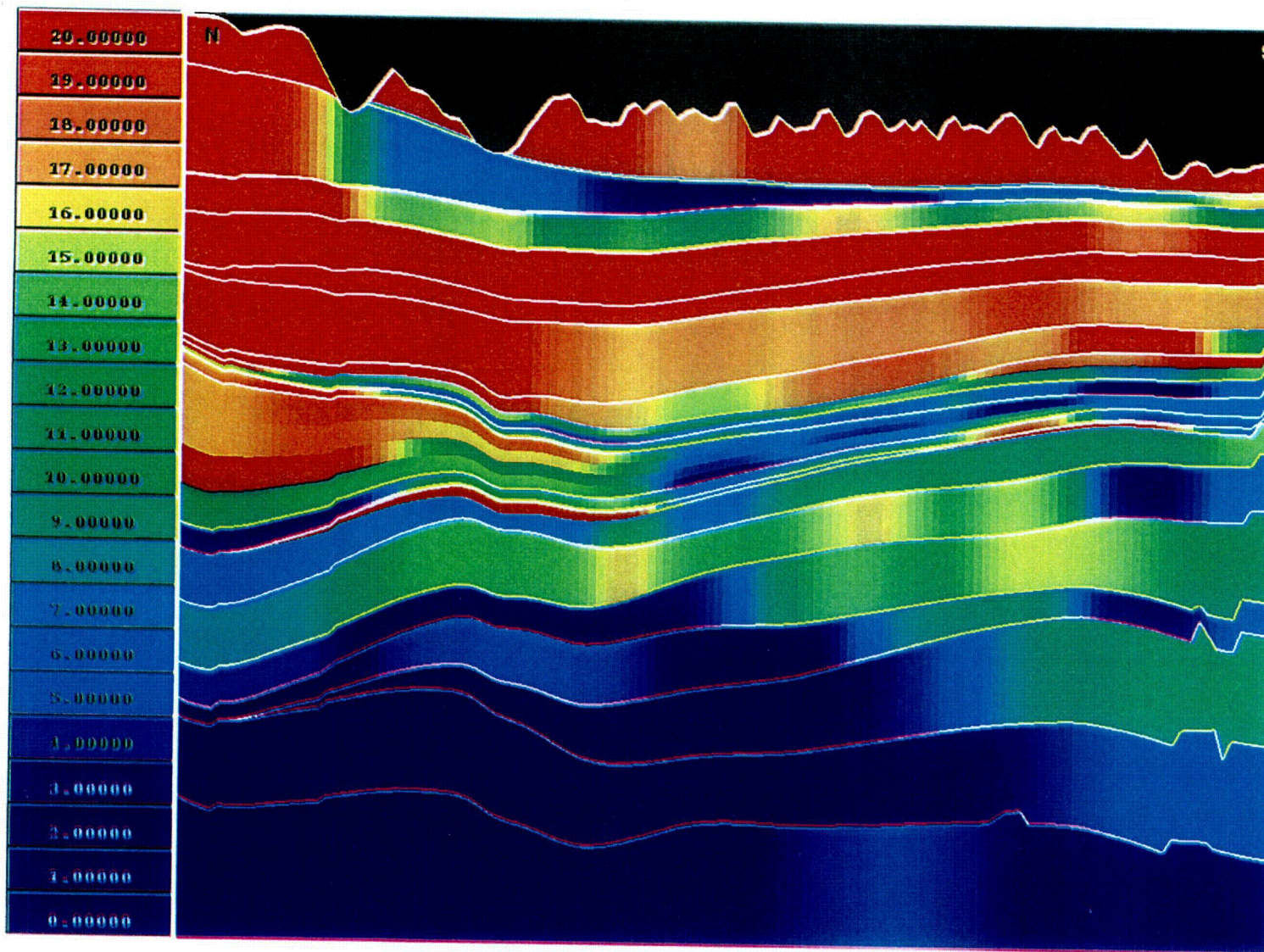


Figure 25. Tridymite Distribution in East-West Cross Section Through Potential Repository



NOTES:

Color key indicates abundance in weight percent, with values greater than 20 percent shown in red.

Delineation of cross section is shown in Figure 8.

Dimensions of cross section are 26,200 feet (7,986 meters) long and 4,430 feet (1,350 meters) deep.

Sequence definitions and repository extent are shown in Figure 5.

Figure 26. Cristobalite + Opal-CT Distribution in North-South Cross Section Through Potential Repository

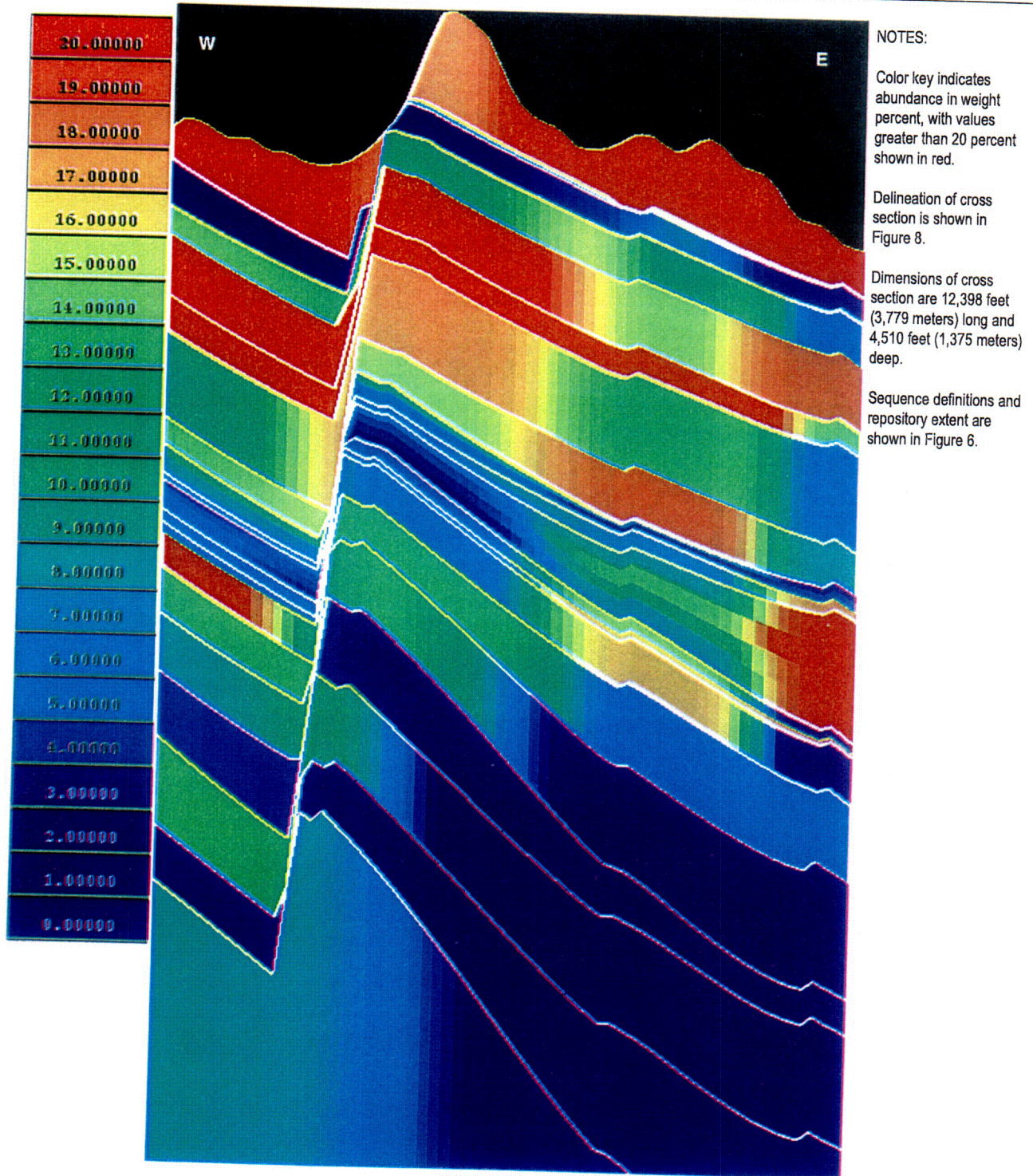
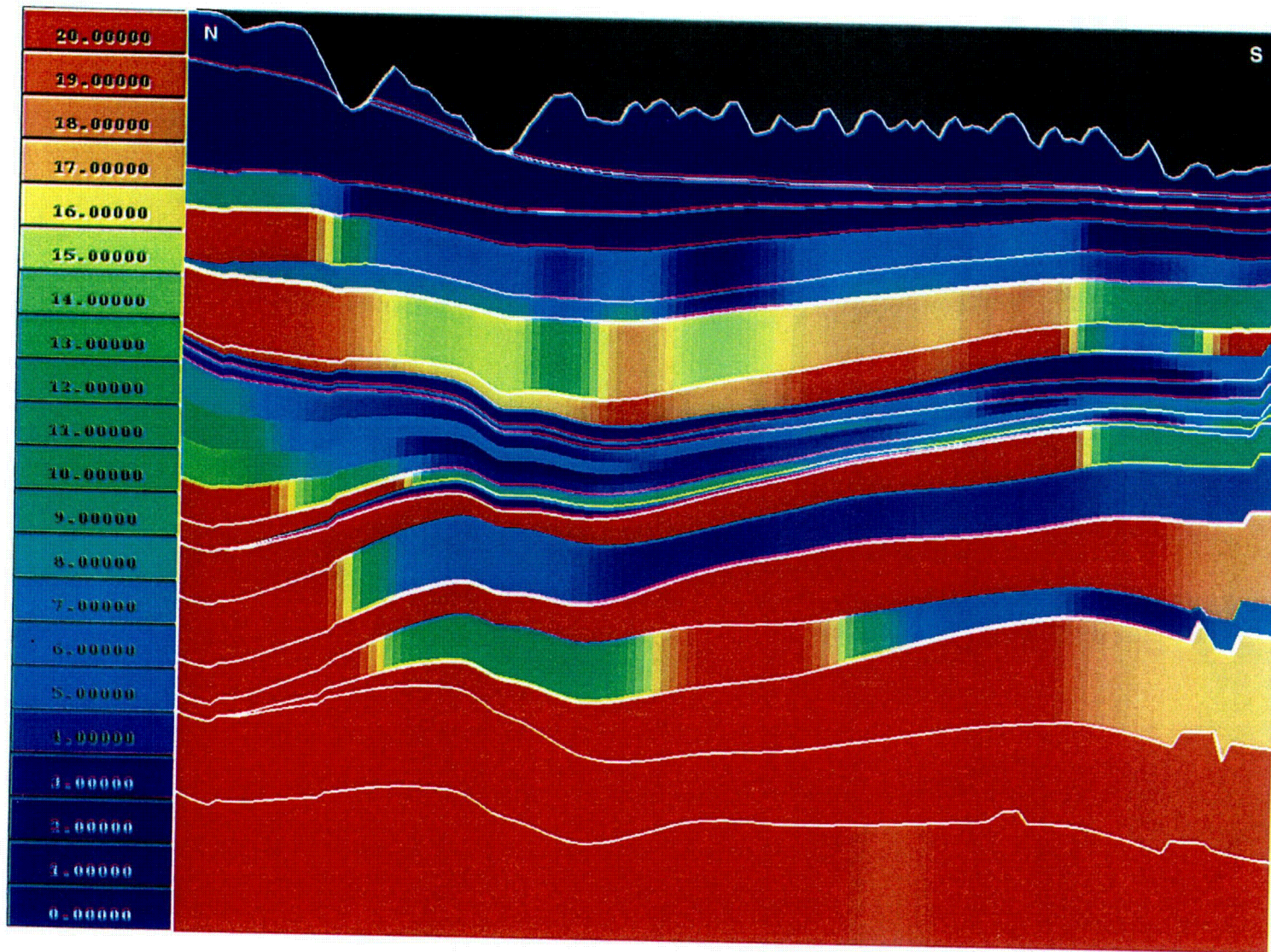


Figure 27. Cristobalite + Opal-CT Distribution in East-West Cross Section Through Potential Repository



NOTES:

Color key indicates abundance in weight percent, with values greater than 20 percent shown in red.

Delineation of cross section is shown in Figure 8.

Dimensions of cross section are 26,200 feet (7,986 meters) long and 4,430 feet (1,350 meters) deep.

Sequence definitions and repository extent are shown in Figure 5.

Figure 28. Quartz Distribution in North-South Cross Section Through Potential Repository

024

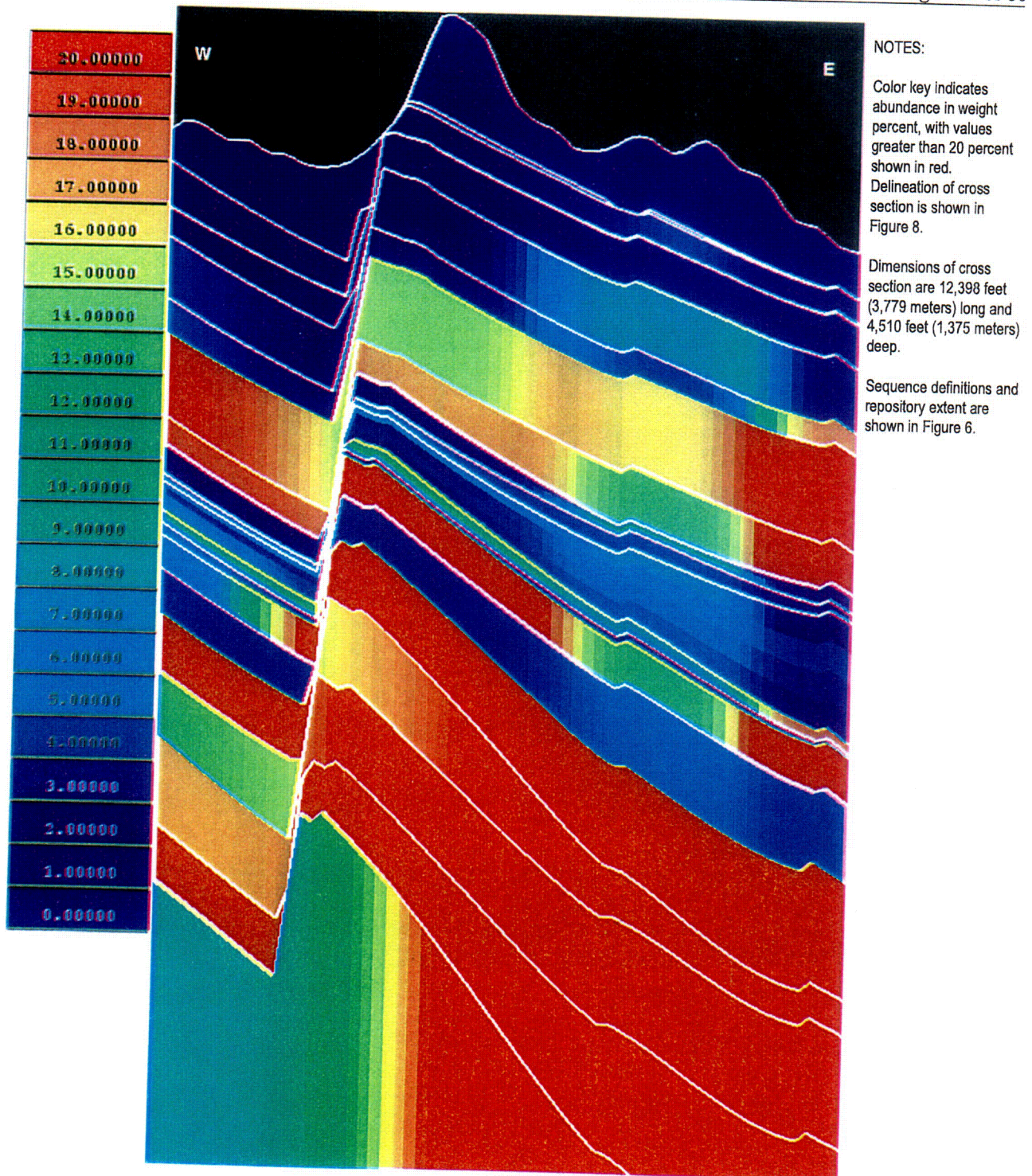


Figure 29. Quartz Distribution in East-West Cross Section Through Potential Repository

A geostatistical MM could be developed with the use of available borehole data and potentially with geophysical well-log data. The geophysical data are available for boreholes for which there are no mineralogic data and, in some cases, they offer finer resolution or greater depth range in boreholes for which mineralogic data exist. The development and refinement of a method of correlating geophysical and mineralogic data would provide a means of constraining and improving the accuracy of the zeolite modeling throughout the exploratory block.

Fault zones are represented as steeply dipping but continuous stratigraphic units. As a consequence, mineralogic predictions in the immediate vicinity of the major fault zones (Solitario Canyon and Ghost Dance) are less accurate. STRATAMODEL has the capability of incorporating faults; however the current level of effort has not permitted the development of this feature.

Quantitative mineralogic data from several boreholes were obtained primarily from cuttings rather than cores (all of WT-1 and WT-2, most of H-4, and significant portions of H-3, H-5, and p#1) (see assumption in Section 5.2). Drill cuttings have a tendency to average mineral abundance over a finite depth range, and more consolidated rock fragments may be over-represented with respect to the softer, more friable rock fragments. The practice of washing cuttings before collection can actually remove specific mineral fractions (especially clays). These limitations can result in inaccurate mineral analyses and in variations in mineral abundance, becoming less distinct and spread over a greater vertical range. Unfortunately, the possibility of nonrepresentative sampling increases the uncertainty in the data and the resultant model. It is difficult to predict the magnitude of the potential error without obtaining additional mineralogic data. However, the modeling process uses all of the available data, which tends to reduce the impact of any single data point.

The use of numeric means for the sequence at each borehole (Section 6.2.3) is a limitation with regard to the representativeness of the vertical variability within sequences. Some sequences, such as the PTn (sequence 21), will have more variability than others, but this is not captured in the MM.

6.4.2 Magnitude of Increased Uncertainty with Exclusion of TBV Data

With the exception of UZ-16, the mineralogic data from the boreholes used in MM3.0 have a TBV status. There are two different reasons for this TBV status: data from 11 of the boreholes are "unconfirmed" and data from 13 of the boreholes are "unqualified." Clearly, the MM cannot be constructed without the use of TBV data. Further, this report emphasizes that both "types of TBV data, unconfirmed and unqualified," are required to construct the MM.

If construction of the MM was restricted to data having a "TBV-unconfirmed" status, only 11 borehole locations would be available (NRG-6, NRG-7a, SD-6, SD-7, SD-9, SD-12, WT-24, UZ-14, UZN-31, UZN-32, and UZ#16). These boreholes are located primarily in or near the eastern half of the MM, providing little mineralogic information across the western portion of the MM. Furthermore, only partial data were collected from 4 of these 11 boreholes: SD-6, SD-7, WT-24, and UZ-14. In addition, NRG-6, NRG-7a, UZN-31, and UZN-32 are shallow holes and provide little mineralogic data below the Topopah Spring Tuff. To exclude data with a "TBV-unqualified" status would significantly limit the mineralogic information for the stratigraphic

units that make up Yucca Mountain. For example, the zeolite modeling of the upper-middle Calico Hills Formation (Layer 13) is based on 4 boreholes with "TBV-unconfirmed" data and on 13 boreholes with "TBV-unqualified" data.

A defensible MM of Yucca Mountain *cannot* currently be constructed with data from only 11 borehole locations having "TBV-unconfirmed" status; data from the 13 borehole locations having "TBV-unqualified" status are mandatory to exert adequate geological and statistical control.

6.5 MODEL VALIDATION

The model validation was based on two criteria. First, the model was required to reproduce the input data, including the adjustments described in Section 6.2.3. In this validation step, mineral abundance data (output) from the model were compared against the input values at borehole locations where these data were available (Scientific Notebook LA-EES-1-NBK-99-001 (Carey 1999, pp. 144-221)).

The second criterion checks that the model predictions are reasonable given the input mineralogy from the surrounding or adjacent borehole sources. In practice, this means that at a given location, the predicted mineral-abundance values for each of the ten mineral groups or classes in the model (as listed in Section 6.2.3) are similar to mineral-abundance values measured in the adjacent boreholes. To be acceptably similar, the predictions for the given test case should be within the range of the minimum and maximum measured values in adjacent boreholes; and should be within one standard deviation or within 1 weight percent of the average measured values for adjacent drill holes.

The model was tested for the second criterion using two basic cases. In the first case, the mineralogic predictions for a unit having relatively uniform mineralogy were compared to the average values of all borehole data for that unit. In the second case, the predictions for a unit having distinctly varying mineralogy were compared to average values of adjacent holes.

Case 1. The middle nonlithophysal zone of the Topopah Spring Tuff: Tptpmn

This unit is a devitrified tuff with a relatively constant feldspar content but highly variable ratios of tridymite:cristobalite:quartz. All of the borehole data were used to construct the average, standard deviation, minimum, and maximum of the input data. Values were predicted at a location near the center of the repository footprint, west of UZN-31 and UZN-32. As shown in Table 5, the predicted values are bounded by the minimum and maximum and are within one standard deviation of the average input values. The predicted value for feldspar is very similar to the average, consistent with the uniform feldspar content of the unit, but the values for the silica polymorphs are close to, but within, the one-standard-deviation limits, again consistent with the variability observed in the input values.

Case 2. The upper part (25 percent) of the Calico Hills Formation: Tac

This unit shows highly variable zeolite and volcanic glass content from the northeast to the southwest. Consequently, the model validation for this unit takes the geographic variation into account by testing at two locations within regions of different zeolite abundance. In this case,

the criterion is that the predicted values at the test location should be similar to the input values for the set of nearest boreholes. As for Case 1, acceptable similarity is defined as a predicted value within one standard deviation of the average.

Location 1 (zeolitic region) is within the repository footprint and lies within a triangle defined by G-1, SD-9, and NRG-7a. The predicted mineralogy of the test location should be similar to the values for the surrounding boreholes. As shown in Table 5, the predicted values meet the test criterion.

Location 2 (non-zeolitic region) is within the repository footprint and lies within a region defined by H-3, SD-6, SD-12, SD-7, and WT-2. The predicted values should be similar to the average mineralogy of the surrounding confining boreholes, and this criterion is satisfied as shown in Table 5.

Table 5. Mineralogy of the Topopah Spring Tuff and Upper Calico Hills Formation

Case 1: Middle Nonlithophysal Topopah Spring Tuff (Tptpmn)												
Prediction Location	Borehole	SMEC	ZEO	TRID	CR/CT	QRTZ	FELD	GLAS	ANAL	MICA	CALC	
Easting: 170657.9 meters	a#1	1	0	0	12	21	66	0	0	0.1	0	
	a#1	.3	0	2	13	18	60	0	0	0.1	0	
Northing: 233202.1 meters	a#1	2	0.1	0.1	16	13	67	0	0	0.1	0	
	G-1	2	0	0.1	22	3	72	0	0	0.1	0	
Elevation: 1140.8674 meters	G-1	1	0	6	27	4	67	0	0	0.1	0	
	G-3	1	0	0	17	6	70	0	0	1	0	
	G-3	1	0	6	22	1	65	0	0	1	0	
	G-4	3	0	4	23	4	66	0	0	0	0	
	G-4	3	0	17	13	4	62	0	0	0	0	
	G-4	1	0	0	28	3	68	0	0	0	0	
	H-3	1	0	0	26	4	68	0	0	1	0	
	H-3	2	0	0.1	27	2	69	0	0	1	0	
	H-4	3	0	12	14	1	68	0	0	1	0	
	H-4	1	0	0	20	11	67	0	0	0	0	
	H-4	1	0	0	21	7	71	0	0	0	0	
	H-5	3	0	3	28	1	59	0	0	0.1	0	
	H-5	0.1	0	0	40	2	55	0	0	1	0	
	NRG-6	2	0	4	31	4	54	0	0	0	0	
	NRG-6	3	0	1	29	10	54	0	0	0.1	0	
	NRG-6	2	0	5	17	17	55	0	0	0.1	0	
	NRG-6	3	0	2	33	3	57	0	0	0	0	
	NRG-6	3	0	3	27	10	55	0	0	0.1	0	
	NRG-6	2	0	3	32	4	54	0	0	0	0	
	NRG-7a	3	0	6	16	20	57	0	0	0.1	0	
	NRG-7a	3	0	3	21	16	55	0	0	0.1	0	
	NRG-7a	3	0	1	22	18	52	0	0	0.1	0	
	NRG-7a	4	0	2	26	13	57	0	0	0.1	0	
	NRG-7a	3	0	5	9	29	56	0	0	0.1	0	
	NRG-7a	3	0	0.1	24	17	53	0	0	0.1	0	
	p#1	2	0	0.1	3	30	67	0	0	0.1	0	
	SD-7	4	0	2	25	15	53	0	0	0.1	0	
	SD-7	3	0	2	35	4	53	0	0	0.1	0	
	SD-7	5	0	4	31	5	52	0	0	0.1	0	
	SD-7	3	0	4	35	2	52	0	0	0.1	0	
	SD-7	5	0	3	34	3	52	0	0	0.1	0	
	SD-7	3	0	2	35	3	54	0	0	0.1	0	
	SD-9	3	0	2	28	11	54	0	0	0.1	0	
	SD-9	3	0	3	28	8	55	0	0	0.1	0	
	SD-9	2	0	8	11	21	55	0	0	0.1	0	
	SD-9	3	0	4	26	9	53	0	0	0.1	0	
	SD-12	4	0	2	30	8	53	0	0	0.1	0	
	SD-12	5	0	4	26	11	52	0	0	0.1	0	
	SD-12	5	0	3	34	5	54	0	0	0.1	1	
	SD-12	4	0	4	28	9	54	0	0	0.1	0	
	SD-12	3	0	4	34	3	54	0	0	0.1	0	
	UZ-14	3	0	5	32	4	52	0	0	0	0	
	UZ-14	3	0	3	29	9	53	0	0	0.1	0	
	UZ-14	5	0	4	31	5	55	0	0	0.1	0	
	UZ-14	3	0	4	20	16	55	0	0	0	0	
	UZ-14	4	0	4	33	7	54	0	0	0.1	0	
	UZ-14	5	0	5	32	5	50	0	0	0.1	0	
	UZ-16	3	0	0.1	16	21	57	0	0	0.1	0	
	UZ-16	3	0	1	13	23	57	0	0	0.1	0	
	UZ-16	3	0	3	27	12	57	0	0	0.1	0	

Table 5. Mineralogy of the Topopah Spring Tuff and Upper Calico Hills Formation (Continued)

Case 1: Middle Nonlithophysal Topopah Spring Tuff (Ttpmnn) (Continued)											
	Borehole	SMEC	ZEO	TRID	CR/CT	QRTZ	FELD	GLAS	ANAL	MICA	CALC
	UZ-16	3	0.1	1	26	10	56	0	0	0.1	0
	UZ-16	4	1	4	27	6	54	0	0	0.1	0
	WT-1	1	0	3	9	25	61	0	0	1	1
	WT-1	1	0	6	16	20	56	0	0	1	0
	WT-2	2	0	10	22	6	58	0	0	1	0
	WT-2	1	0	10	19	8	61	0	0	1	0
	average	2.7	0.0	3.3	24.2	9.8	58.0	0.0	0.0	0.2	0.0
	stdev	1.2	0.1	3.2	8.0	7.4	6.0	0.0	0.0	0.3	0.2
	max	5	1	17	40	30	72	0	0	1	1
	min	0.1	0	0	3	1	50	0	0	0	0
	prediction	1.8	0.0	2.2	31.8	3.0	57.4	0.0	0.0	0.4	0.0
Case 2: Upper Calico Hills Formation (Tac)											
Zeolitic Region											
Prediction Location	Borehole	SMEC	ZEO	TRID	CR/CT	QRTZ	FELD	GLAS	ANAL	MICA	CALC
Easting: 171206.6 meters	G-1	0.1	74.0	0.0	19.0	3.0	5.0	0.0	0.0	0.0	0.0
	NRG-7a	1.0	80.0	0.0	13.0	2.0	8.0	0.0	0.0	0.0	0.0
Northing: 234543.2 meters	NRG-7a	0.1	84.0	0.0	7.0	4.0	7.0	0.0	0.0	0.1	0.0
	SD-9	0.1	74.0	0.0	20.0	3.0	6.0	0.0	0.0	0.1	0.0
Elevation: 838.8435 meters	SD-9	4.0	70.0	0.0	14.0	6.0	9.0	0.0	0.0	0.1	0.0
	SD-9	0.1	71.0	0.0	16.0	4.0	10.0	0.0	0.0	0.1	0.0
	SD-9	8.0	71.0	0.0	19.0	2.0	5.0	0.0	0.0	0.0	0.0
	SD-9	0.1	73.0	0.0	18.0	5.0	9.0	0.0	0.0	0.1	0.0
	average	1.7	74.6	0.0	15.8	3.6	7.4	0.0	0.0	0.1	0.0
	stdev	2.9	4.9	0.0	4.3	1.4	1.9	0.0	0.0	0.1	0.0
	max	8.0	84.0	0.0	20.0	6.0	10.0	0.0	0.0	0.1	0.0
	min	0.1	70.0	0.0	7.0	2.0	5.0	0.0	0.0	0.0	0.0
	prediction	0.7	75.4	0.0	16.1	3.2	6.4	0.3	0.0	0.0	0.0
Nonzeolitic Region											
Prediction Location	Borehole	SMEC	ZEO	TRID	CR/CT	QRTZ	FELD	GLAS	ANAL	MICA	CALC
Easting: 170901.8 meters	H-3	0.4	0.8	0.0	6.0	7.8	29.2	58.3	0.0	0.8	0.0
	SD-6	0.1	16.0	0.0	5.0	31.0	47.0	0.0	0.0	0.0	0.0
Northing: 231921.9 meters	SD-7	0.1	0.0	0.0	2.0	1.0	6.0	91.0	0.0	0.0	0.0
	SD-7	0.1	0.0	0.0	2.0	2.0	6.0	90.0	0.0	0.0	0.0
Elevation: 933.9188 meters	SD-12	0.0	1.0	0.0	2.0	2.0	6.0	89.0	0.0	0.1	0.0
	SD-12	1.0	4.0	0.0	7.0	2.0	8.0	78.0	0.0	0.1	0.0
	SD-12	1.0	2.0	0.0	1.0	2.0	6.0	88.0	0.0	0.1	0.0
	SD-12	0.1	6.0	0.0	2.0	2.0	5.0	85.0	0.0	0.1	0.0
	SD-12	1.0	4.0	0.0	3.0	2.0	8.0	82.0	0.0	0.1	0.0
	SD-12	1.0	6.0	0.0	3.0	3.0	6.0	81.0	0.0	0.1	0.0
	SD-12	1.0	7.0	0.0	3.0	2.0	5.0	82.0	0.0	0.1	0.0
	WT-2	1.0	1.0	0.0	8.0	11.0	40.0	40.0	0.0	1.0	0.0
	average	0.6	4.0	0.0	3.7	5.7	14.4	72.0	0.0	0.2	0.0
	stdev	0.5	4.5	0.0	2.3	8.5	15.2	27.2	0.0	0.3	0.0
	max	1.0	16.0	0.0	8.0	31.0	47.0	91.0	0.0	1.0	0.0
	min	0.0	0.0	0.0	1.0	1.0	5.0	0.0	0.0	0.0	0.0
	prediction	0.8	2.9	0.0	5.8	7.3	25.3	58.5	0.0	0.6	0.0

NOTE: Values shown are mineral abundances in weight percent.

7. CONCLUSIONS

The MM is one component of the ISM, which also includes the GFM and the RPM. The MM provides the abundance and distribution of 10 minerals and mineral groups within 22 stratigraphic sequences in the Yucca Mountain area for use in geoscientific modeling and repository design. The input data from the GFM provide stratigraphic controls, and quantitative analyses of mineral abundances by XRD at 24 boreholes provide controls for mineralogy; however, most of the modeled volume is unsampled. The MM is, therefore, an interpretation and a prediction tool rather than an absolute representation of reality. The model possesses an inherent level of uncertainty that is a function of data distribution and geologic complexity, and predictions or alternative interpretations that fall within the range of uncertainty are considered acceptable. Uncertainty in the model is mitigated by the application of sound geologic principles.

The MM shows the abundance and distribution of minerals that are of greatest interest to TSPA-related models and analyses, some of which are summarized here. There is a transition from high- to low-abundance zeolite in the Calico Hills Formation in the region directly underlying the potential repository. The MM of this region in combination with the RPM may identify regions of enhanced radionuclide sorption resulting from a combination of high permeability and moderate zeolite abundance. Smectite may also be important in transport, and moderate abundances of smectite are predicted throughout the MM. Reactive mineral phases in the MM include the silica polymorphs and volcanic glass. The 3-D distribution of these phases provided by the MM will allow thermohydrologic studies of the effects of dissolution and precipitation reactions on repository performance. Finally, the MM allows the prediction of the abundance and location of hazardous minerals (silica polymorphs and erionite) as a tool for repository design.

Limitations that may be of importance to users of the MM are: (1) scarcity of mineralogic data in the western margin of the potential repository block, as well as in the boundary regions of the MM; (2) the use of cuttings from several boreholes, leading to potential inaccuracies in mineral analyses because cuttings are washed prior to analysis; the mineralogic data is averaged over vertical intervals, or minerals from the more friable rock layers are potentially under represented; and (3) the use of numeric means to represent the mineral abundance for each sequence (or layer) at a borehole location.

The MM is an interactive 3-D database and volumetric representation of the mineralogy of Yucca Mountain. As such, it is a useful tool for geoscientific analyses of all types, including hydrologic modeling, thermohydrologic studies, reactive-transport modeling, confirmation test planning, site geotechnical analysis, uncertainty analysis, model integration, data analysis, and repository facilities design.

The MM is constructed using primarily TBV data. Because model inputs are TBV, the MM3.0 also has a TBV qualification status.

This document and its conclusions may be affected by technical product input information that requires confirmation. Any changes to the document or its conclusions that may occur as a result of completing the confirmation activities will be reflected in subsequent revisions. The status of the input information quality may be confirmed by review of the Document Input Reference System database.

8. INPUTS AND REFERENCES

8.1 DOCUMENTS CITED

Bish, D.L. and Aronson, J.L. 1993. "Paleogeothermal and Paleohydrologic Conditions in Silicic Tuff from Yucca Mountain, Nevada." *Clays and Clay Minerals*, 41, (2) 148-161. Long Island City, New York: Pergamon Press. TIC: 224613.

Bish, D.L. and Chipera, S.J. 1988. "Problems and Solutions in Quantitative Analysis of Complex Mixtures by X-Ray Powder Diffraction." *Advances in X-Ray Analysis*, 31, 295-308. New York, New York: Plenum Publishing Corporation. TIC: 224378.

Bish, D.L. and Chipera, S.J. 1989. *Revised Mineralogic Summary of Yucca Mountain, Nevada*. LA-11497-MS. Los Alamos, New Mexico: Los Alamos National Laboratory. ACC: NNA.19891019.0029.

Buesch, D.C.; Spengler, R.W.; Moyer, T.C.; and Geslin, J.K. 1996. *Proposed Stratigraphic Nomenclature and Macroscopic Identification of Lithostratigraphic Units of the Paintbrush Group Exposed at Yucca Mountain, Nevada*. Open File Report 94-469. Denver, Colorado: U.S. Geological Survey. ACC: MOL.19970205.0061.

Buesch, D.C. and Spengler, R.W. 1999. "Correlations of Lithostratigraphic Features with Hydrogeologic Properties, a Facies-Based Approach to Model Development in Volcanic Rocks at Yucca Mountain, Nevada." *Proceedings of Conference on Status of Geologic Research and Mapping in Death Valley National Park, Las Vegas, Nevada, April 9-11, 1999*. Open File Report 99-153, 62-64. Denver, Colorado: U.S. Geological Survey. TIC: 245245.

Buscheck, T.A. and Nitao, J.J. 1993. "The Analysis of Repository-Heat-Driven Hydrothermal Flow at Yucca Mountain." *High-Level Radioactive Waste Management, Proceedings of the Fourth Annual International Conference, Las Vegas, Nevada, April 26-30, 1993*, 1, 847-867. La Grange Park, Illinois: American Nuclear Society. TIC: 208542.

Carey, J.W. 1999. *Three-Dimensional Mineralogic Model of Yucca Mountain, Nevada*. Scientific Notebook LA-EES-1-NBK-99-001. ACC: MOL.19991028.0013.

Carlos, B.A.; Chipera, S.J.; and Bish, D.L. 1995. *Distribution and Chemistry of Fracture-Lining Minerals at Yucca Mountain, Nevada*. LA-12977-MS. Los Alamos, New Mexico: Los Alamos National Laboratory. ACC: MOL.19960306.0564.

Chipera, S.J. and Bish, D.L. 1995. "Multireflection RIR and Intensity Normalizations for Quantitative Analyses: Applications to Feldspars and Zeolites." *Powder Diffraction*, 10 (1), 47-55. Newton Square, Pennsylvania: Joint Committee on Powder Diffraction Standards. TIC: 222001.

CRWMS M&O 1997a. *Determination of Available Volume for Repository Siting*. BCA000000-01717-0200-00007 REV 00. Las Vegas, Nevada: CRWMS M&O. ACC: MOL.19971009.0699.

CRWMS M&O 1997b. *Abatement Plan: Respirable Silica Dust*. October 1, 1997 Update. Las Vegas, Nevada: CRWMS M&O. ACC: MOL.19971120.0179.

CRWMS M&O 1999a. Analysis and Modeling Report (AMR) *Development Plan (DP): Mineralogic Model (MM3.0) Version 3.0*, REV 00. Las Vegas, Nevada: CRWMS M&O. ACC: MOL.19990917.0185.

CRWMS M&O 1999b. *M&O Site Investigations*. Activity Evaluation. January 23, 1999. Las Vegas, Nevada: CRWMS M&O. ACC: MOL.19990317.0330.

CRWMS M&O 1999c. *M&O Site Investigations*. Activity Evaluation. September 28, 1999. Las Vegas, Nevada: CRWMS M&O. ACC: MOL.19990928.0224.

DOE (U.S. Department of Energy) 1998. *Quality Assurance Requirements and Description*. DOE/RW-0333P, Rev. 8. Washington, D.C.: U.S. Department of Energy, Office of Civilian Radioactive Waste Management. ACC: MOL.19980601.0022.

Dyer, J.R. 1999. "Revised Interim Guidance Pending Issuance of New U.S. Nuclear Regulatory Commission (NRC) Regulations (Revisions 01, July 22, 1999), for Yucca Mountain, Nevada." Letter from J.R. Dyer (DOE) to Dr. D.R. Wilkins (CRWMS M&O), September 3, 1999, OL&RC:SB-1714, with enclosure, "Interim Guidance Pending Issuance of New NRC Regulations for Yucca Mountain (Revision 01)." ACC: MOL.19990910.0079.

Johnstone, J.K. and Wolfsberg, K., eds. 1980. *Evaluation of Tuff as a Medium for a Nuclear Waste Repository: Interim Status Report on the Properties of Tuff*. SAND80-1464. Albuquerque, New Mexico: Sandia National Laboratories. ACC: NNA.19870406.0065.

Levy, S.S. 1984. *Petrology of Samples from Drill Holes USW H-3, H-4, and H-5, Yucca Mountain, Nevada*. LA-9706-MS. Los Alamos, New Mexico: Los Alamos National Laboratory. ACC: MOL.19970729.0322.

Levy, S.S. 1991. "Mineralogic Alteration History and Paleohydrology at Yucca Mountain, Nevada." *High-Level Radioactive Waste Management, Proceeding of the Second Annual International Conference, Las Vegas, Nevada, April 28-May 3, 1991*, 1, 477-485. La Grange Park, Illinois: American Nuclear Society. TIC: 204272.

Loeven, C. 1993. *A Summary and Discussion of Hydrologic Data from the Calico Hills Nonwelded Hydrogeologic Unit at Yucca Mountain, Nevada*. LA-12376-MS. Los Alamos, New Mexico: Los Alamos National Laboratory. ACC: NNA.19921116.0001.

Thompson, A.B. and Wennemer, M. 1979. "Heat Capacities and Inversions in Tridymite, Cristobalite, and Tridymite-Cristobalite Mixed Phases." *American Mineralogist*, 64, 1018-1026. Washington, D.C.: Mineralogical Society of America. TIC: 239133.

Vaniman, D.T. and Bish, D.L. 1995. "The Importance of Zeolites in the Potential High-Level Radioactive Waste Repository at Yucca Mountain, Nevada." *Natural Zeolites '93*, 533-546. Brockport, New York: International Committee on Natural Zeolites. TIC: 217194.

Vaniman, D.; Furlano, A.; Chipera, S.; Thompson, J. and Triay, I. 1996. "Microautoradiography in Studies of Pu (V) Sorption by Trace and Fracture Minerals in Tuff." *Scientific Basis for Nuclear Waste Management XIX, Symposium held November 27-December 1, 1995, Boston, Massachusetts*, Murphy, W.M. and Knecht, D.A., eds. 412. 639-646. Pittsburgh, Pennsylvania: Materials Research Society. TIC: 233877.

8.2 CODES, STANDARDS, REGULATIONS, AND PROCEDURES

AP-3.10Q, Rev. 1, ICN 0. *Analyses and Models*. Washington, D.C.: U.S. Department of Energy, Office of Civilian Radioactive Waste Management. ACC: MOL.19990702.0314.

AP-SI.1Q, Rev. 2, ICN 1. *Software Management*. Washington, D.C.: U.S. Department of Energy, Office of Civilian Radioactive Waste Management. ACC: MOL.19991101.0212.

AP-SIII.1Q, Rev 0, ICN 0. *Scientific Notebooks*. Washington, D.C.: U.S. Department of Energy, Office of Civilian Radioactive Waste Management. ACC: MOL.19990702.0311.

LANL-YMP-QP-03.5, Rev 8. *Documenting Scientific Investigations*. Notebook 99-01. Los Alamos, New Mexico: Los Alamos National Laboratory. ACC: 19990914.0135.

QAP-2-0, Rev 5. *Conduct of Activities*. Las Vegas, Nevada: CRWMS M&O. ACC: MOL.19980826.0209.

8.3 SOURCE DATA, LISTED BY DATA TRACKING NUMBER

LADB831321AN98.002. Revised Mineralogic Summary of Yucca Mountain, Nevada. Submittal date: 05/26/1998.

LA000000000086.002. Mineralogic Variation in Drill Core UE-25 UZ#16 Yucca Mountain, Nevada. Submittal date: 03/28/1995.

LAJC831321AQ98.005. Quantitative XRD Results for Drill Core USW SD-7, USW SD-9, USW SD-12 and UE-25 UZ#16. Submittal date: 10/27/1998.

LADV831321AQ97.001. Mineralogic Variation in Drill Holes. Submittal date: 05/28/1997.

LASC831321AQ96.002. QXRD Analyses of Drill Core USW NRG-6 and USW UZ-14 Samples. Submittal date: 08/02/1996.

LASC831321AQ98.003. Results of Real Time Analysis for Erionite in Drill Hole USW SD-6, Yucca Mountain, Nevada. Submittal date: 06/11/1998.

LADV831321AQ99.001. Quantitative XRD Results for the USW SD-6 and USW WT-24 Drill Core Samples. Submittal date: 04/16/1999.

LASL831322AQ97.001. Updated Mineralogic and Hydrologic Analysis of the PTN Hydrogeologic Unit, Yucca Mountain, Nevada, as a Barrier to Flow. Submittal date: 10/09/1997.

LASC831321AQ98.001. Results of Real-Time Analysis for Erionite in Drill Hole USW WT-24, Yucca Mountain, NV. Submittal date: 02/10/1998.

LA9908JC831321.001. Mineralogic Model "MM3.0" Version 3.0. Submittal date: 08/16/99

LA9910JC831321.001 Supplementary Mineralogical Data for Mineralogic Model 3.0. Submittal date: 10/29/1999.

LADV831321AQ97.007. Geotechnical Data Report: Hazardous Minerals. Submittal date: 01/27/1998.

MO9510RIB00002.004. RIB ITEM: Stratigraphic Characteristics: Geologic/Lithologic Stratigraphy. Submittal date: 06/26/1996.

MO9901MWDGFM31.000. Geologic Framework Model Version GFM3.1. Submittal date: 01/06/1999.

MO9804MWDGFM03.001. An Update to GFM 3.0; Corrected Horizon Grids for Four Fault Blocks. Submittal date: 04/14/1998.

8.4 SOFTWARE

STRATAMODEL Version 4.1.1. STN: 10121-4.1.1-00.

ATTACHMENT I

**DOCUMENT INPUT REFERENCE SYSTEM (DIRS)
REMOVED**

See electronic DIRS database.

Title: Mineralogic Model (MM3.0)

Attachment I

Document Identifier: MDL-NBS-GS-000003 REV 00 ICN 01

ATTACHMENT II

GENERAL OBSERVATIONS AND SUMMARY OF MINERALOGY

Title: Mineralogic Model (MM3.0)

Attachment II

Document Identifier: MDL-NBS-GS-000003 REV 00 ICN 01

ATTACHMENT II GENERAL OBSERVATIONS AND SUMMARY OF MINERALOGY

The stratigraphy of volcanic units at Yucca Mountain is complex, including both tuffs and lavas. However, within the areal extent of the MM, the only lavas of any significance occur within sequence 2 (Tund—undifferentiated older Tertiary rocks). In the MM, lavas, flow breccias, and tuffs within this sequence are grouped together because there are insufficient data for subdivision. The consequences of this grouping are minimal because (1) these units, below the Crater Flat Group, are far enough below the water table to be of little consequence in transport and (2) mineral alteration at these depths is so pervasive that the original lithology has only a limited effect on the alteration products. Above sequence 2, however, there are clear and definitive relationships between the nature of the tuffs and the occurrence of alteration minerals (principally clays and zeolites).

The tuffs above sequence 2 generally occur as ash-flow units with interspersed bedded tuffs. Within the area of the MM, the thicker ash flows generally have nonwelded to poorly welded exteriors at the margins of more welded interiors. Typically, where thicker than a few tens of meters, the welded ash-flow interiors have devitrified to a mineral assemblage consisting principally of feldspar plus anhydrous silica minerals. Above sequence 2 these devitrified zones rarely contain zeolites; where zeolites do occur in devitrified units, their abundance is low (generally less than 10 percent). In contrast, the nonwelded to poorly welded ash-flow margins and the bedded tuffs between ash flows are readily zeolitized, with typical zeolite abundances in the range of 25 to 80 percent below the water table and up to approximately 330 feet (100 meters) above the water table. The relationships between marginal zones of initially vitric tuff and zeolitization strongly indicate that zeolites cannot become abundant unless vitric tuff was originally present. The same relationships also lead to distinct transitions between zeolitized and devitrified sequences, particularly within the tuffs of the Crater Flat Group (MM sequences 3 through 9). In these sequences, the transition from abundant zeolitization of the flow margins to the devitrified flow interiors is typically definitive and abrupt (within about 3.3 feet (1 meter)). In places where this transition is definitive in the mineralogic data but inconsistent with the Stratamodel and GFM3.1 sequence, the elevations of the mineralogic data were adjusted. This prevented dispersion of zeolites into devitrified units and mixing of devitrification mineralogy into zeolitized sequences. Adjustments are listed in Table II-1.

From sequence 9 to sequence 13 in the MM (upper nonwelded Prow Pass Tuff to the moderately to densely welded lower vitric zone of the Topopah Spring Tuff), there is a highly variable transition between vitric and zeolitic lithologies. Because the initial tuff deposits in these sequences were all largely vitric, there are few stratigraphic controls over the extent of hydrous mineral alteration. However, the mineralogic data show that the bedded tuff below the Calico Hills Formation (sequence 10) is more readily altered to zeolite or smectite than the overlying ash flows (sequence 11). Conversely, sequence 11 is never significantly altered if the underlying bedded tuff is not significantly altered. At the top of this series of originally vitric sequences (sequence 13) is a common zone of smectite and zeolite alteration, with total hydrous mineral abundances ranging from a few percent to complete alteration of the upper few feet (decimeters) of the vitrophyre. In some places, this zone of alteration extends into the base of the overlying devitrified horizon (Tptpln, sequence 14). The elevations of mineralogic data corresponding to highly altered, basal Tptpln samples were adjusted to fall within the vitric horizon (sequence 13).

(Table II-1). This prevented dispersion of high zeolite and smectite abundances into the lower nonlithophysal zone (devitrification mineralogy) of the Topopah Spring Tuff (Table II-1).

Sequences 14 through 18 of the MM make up the thick devitrified interior of the Topopah Spring Tuff. The upper boundary of unit 18 is defined by a transition from devitrified to vitric composition. Therefore, mineralogic data near the contact of sequences 18 (upper devitrified Topopah Spring Tuff) and 19 (upper vitrophyre of the Topopah Spring Tuff) were adjusted in some boreholes to prevent unrealistic distribution of abundant glass into the devitrified tuff or extensive devitrification into the vitrophyre (Table II-1).

Sequence 20 in the MM incorporates all of the heterogeneous deposits from the zone of decreased welding at the top of the Topopah Spring Tuff (Tptrv2) through the nonwelded base of the Tiva Canyon Tuff (Tpcpv1). This interval is principally composed of initially vitric ash-flow and bedded deposits; however, it includes locally devitrified sequences in the Yucca Mountain Tuff and Pah Canyon Tuff in the north (e.g., in borehole G-2). In sequence 20, glasses are predominantly altered to smectite, with only local occurrences of significant zeolitization (e.g., in borehole UZ#16). The transition to sequence 21, the moderately to densely welded vitric base of the Tiva Canyon Tuff, is gradational; sequence 21 is distinguished by an intermingling of vitric remnants, devitrification, and smectite alteration. The transition from sequence 21 to sequence 22, the devitrified interior of the Tiva Canyon Tuff, is distinguished by a sharp decrease in smectite and/or glass. Sequence 22 consists of devitrification minerals throughout the areal extent of the MM. The elevations of mineralogic data were adjusted where unrealistic glass abundances would have been introduced from sequence 21 and where alluvial or surface-alteration features would have been introduced from above (Table II-1). Alluvial and surface-weathering features are not currently included in the MM.

II.1 SUMMARY OF MINERALOGIC RELATIONS

This section describes the mineralogy typical of each MM sequence and the rationale for modifying the elevations of sample data where such adjustments were deemed necessary. Modifications to the mineralogic data (as available in the TDMS) for the purpose of MM3.0 are documented in Table II-1.

II.1.1 Sequence 22: Devitrified Tiva Canyon Tuff (Alluvium–Tpcplnc)

The devitrified Tiva Canyon Tuff consists principally of feldspar and the anhydrous silica polymorphs (cristobalite, tridymite, and quartz). The primary distinction between this sequence and the underlying sequence in the MM is the absence of glass in sequence 22. A minor exception to this distinction is seen in borehole SD-6 at an elevation of 4,494.4 feet (1,369.9 meters) above mean sea level (msl), where a sample from the base of sequence 22 contained 7 percent glass, apparently representing a transitional lithology between the typical mineral properties of sequence 22 and the properties of underlying sequence 21 (the sample collected at 2.6 feet (0.8 meters) below, in sequence 21, contained 54 percent glass; the elevation of this sample was adjusted downward in the MM (Table II-1)).

As a devitrified unit, sequence 22 generally contains no zeolites. In one instance, the uppermost core sample from sequence 22 (in borehole SD-9 at an elevation of 4,217.8 feet (1,285.6 meters)

above msl) contained 29 percent zeolite (clinoptilolite). This sample was collected from a surface breccia that is not representative of sequence 22; this zeolite-bearing sample was therefore excluded from the MM.

II.1.2 Sequence 21: Densely to Moderately Welded Vitric Base of Tiva Canyon Tuff (Tpcpv3–Tpcpv2)

The densely to moderately welded vitric base of the Tiva Canyon Tuff is glass rich, with variable amounts of alteration to smectite. The greater welding of sequence 21 is the principal distinction between this sequence and the top of the underlying sequence (sequence 20).

II.1.3 Sequence 20: PTn Unit (Tpcpv1–Tptrv2)

The PTn unit is the least homogeneous sequence of the MM. The PTn includes the nonwelded base of the Tiva Canyon Tuff, the Yucca Mountain and Pah Canyon Tuffs with intercalated bedded tuffs, and the upper nonwelded portion of the Topopah Spring Tuff. Most of these units contain glass and variable amounts of smectite alteration. Alteration to zeolite is less common, although significant zeolitization occurs in G-2 and UZ#16 and there are minor occurrences of zeolite in boreholes SD-12, UZ-14, UZN-31, and UZN-32. Remnants of glass are almost pervasive, with the exception of those areas where the Yucca Mountain and/or Pah Canyon Tuffs are devitrified (boreholes G-2 and UZ-14), where smectite alteration and devitrification occur at the base of the PTn (boreholes SD-7 and UZ#16), and where glass was completely altered to smectite (some bedded tuffs in boreholes UZN-31 and UZN-32).

II.1.4 Sequence 19: Upper Vitrophyre of Topopah Spring Tuff (Tptrv1)

High glass content (greater than 20 percent; generally greater than 75 percent) distinguishes sequence 19 (the upper vitrophyre of the Topopah Spring Tuff) from the underlying devitrified unit (Tptrn). This densely welded quartz-latic glass is generally only slightly altered to smectite and rare clinoptilolite. In some instances, the depth assignments from GFM3.1 placed samples that were largely devitrified and contained only small amounts of glass (in borehole SD-9 at an elevation of 4,001.3 feet (1,219.6 meters) above msl, 7 percent glass) or samples that were fully devitrified and contained no glass (UZ#16 at 3,763.7 feet (1,147.2 meters) above msl) into sequence 19. Because sequence 19 is defined as a vitrophyre, these samples were reassigned to sequence 18 in the MM. In another instance, a sample with 23 percent glass (in borehole SD-12 at 4,011.8 feet (1,222.8 meters) above msl) was assigned by GFM3.1 to sequence 18, which is a devitrified unit. In this instance, the sample was reassigned to sequence 19 in the MM.

II.1.5 Sequence 18: Quartz-Latitic to Rhyolitic Transition Zone and Lithic-Rich Zone of Topopah Spring Tuff (Tptrn–Tptf)

This sequence within the Topopah Spring Tuff includes the transition from quartz-latic composition (above) to rhyolitic composition (below). Mineralogically, this interval has a generally higher tridymite:quartz ratio than the underlying devitrified zones of the Topopah Spring Tuff. The upper part of the sequence contains small amounts of glass (less than 10 percent) in boreholes NRG-7a and SD-9. In one instance, the depth assignments from GFM3.1 placed a sample that was devitrified, had a high tridymite:quartz ratio, and was free of glass or

hydrous alteration minerals (in borehole SD-6 at an elevation of 4,388.1 feet (1,337.5 meters) above msl) in sequence 20. In this case, the sample was reassigned to sequence 18 in the MM. In another instance, a sample that was devitrified and contained no glass (in borehole G-2 at 4,327 feet (1,318.9 meters) above msl) was assigned to sequence 19; this sample was reassigned to devitrified sequence 18 in the MM (Table II-1).

II.1.6 Sequence 17: Upper Lithophysal Zone of Topopah Spring Tuff (Tptpul)

This sequence of devitrified rhyolitic tuff has a relatively constant feldspar content but highly variable ratios of tridymite:crystalite:quartz.

II.1.7 Sequence 16: Middle Nonlithophysal Zone of Topopah Spring Tuff (Tptpmn)

This sequence of devitrified rhyolitic tuff has a relatively constant feldspar content but highly variable ratios of tridymite:crystalite:quartz. Small amounts of zeolite (stellerite) occur in the rock matrix in borehole UZ#16.

II.1.8 Sequence 15: Lower Lithophysal Zone of Topopah Spring Tuff (Tptpll)

This sequence of devitrified rhyolitic tuff has a relatively constant feldspar content but highly variable ratios of tridymite:crystalite:quartz. In borehole UZ#16, amounts of zeolite (stellerite) up to 11 percent occur in dispersed fractures and in the rock matrix.

II.1.9 Sequence 14: Lower Nonlithophysal Zone of Topopah Spring Tuff (Tptpln)

This sequence of devitrified rhyolitic tuff has a relatively constant feldspar content but highly variable ratios of tridymite:crystalite:quartz. In UZ#16, amounts of zeolite (stellerite) up to 14 percent occur in dispersed fractures and in the rock matrix. The base of the sequence may contain low percentages of glass, smectite, and/or zeolite, transitional with the altered upper surface of sequence 13. In one instance, GFM3.1 placed a sample that was devitrified and contained less than 2 percent hydrous alteration minerals (in borehole SD-9 at 2,915.8 feet (886.8 meters) above msl) into the underlying vitrophyre sequence 13. In this case, the sample was reassigned to sequence 14 in the MM. In another instance, a devitrified sample with only 6 percent zeolite alteration (in borehole G-3 at an elevation of 3,666.3 feet (1,117.5 meters) above msl) was assigned by GFM3.1 to sequence 13; this sample was reassigned to sequence 14 in the MM. At borehole NRG-7a the basal sample from Tptpln was altered to smectite and transitional to sequence 13 and was assigned to sequence 13. The remaining 11 samples from Tptpln were averaged into a single sample value (located at 2,834.6 feet (864.0 meters) above msl) to preserve the stratigraphic relationships.

II.1.10 Sequence 13: Densely to Moderately Welded Vitric Base of Topopah Spring Tuff (Tptpv3–Tptpv2)

This sequence consists of the lower densely welded quenched-glass horizon (vitrrophyre) and the underlying moderately welded glass of the Topopah Spring Tuff. In many boreholes, the upper few inches to feet (centimeters to decimeters) of this sequence are extensively altered to smectite and zeolites. The division of sequence 13 into two equal-thickness layers captures this alteration, in part, with the upper layer (17) having greater alteration than the lower layer (16). Generally,

the glass contents in this sequence are high (70 to 100 percent), with the exception of smectite and zeolite alteration that can completely replace the glass at the sequence top or at depths throughout the sequence (in boreholes UZ-14 and WT-24). Zeolite alteration in sequence 13 includes most of the occurrences of the mineral erionite (a carcinogen that poses an inhalation hazard) at Yucca Mountain.

In some instances, the depth assignments from GFM3.1 placed samples with abundant smectite and zeolite into sequence 14 (Tptpln), which, as a devitrified sequence, should not be associated with large amounts of hydrous minerals. These instances are common and occur in G-1 at an elevation of 3,063.6 feet (933.8 meters) above msl, in borehole G-2 at 3,463.2 feet (1,055.6 meters) above msl, in borehole G-4 at 2,852 feet (869.3 meters) above msl, in borehole NRG-7a at 2,795.2 feet (852.0 meters) above msl, and in borehole UZ-14 at 3,147.3 feet (959.3 meters) above msl. These samples were reassigned to sequence 13 in the MM.

II.1.11 Sequence 12: Nonwelded to Bedded Zone at Base of Topopah Spring Tuff (Tptpv1-Tpbt1)

This sequence varies from highly zeolitized with no remnant glass in the northern and eastern parts of Yucca Mountain, to vitric and relatively unaltered in the west and south. Where the underlying Calico Hills Formation (sequence 11) is fully zeolitized, the transition from vitric to zeolitic properties usually occurs near the top of sequence 12 or in the lower part of sequence 13 (in borehole WT-24).

II.1.12 Sequence 11: Calico Hills Formation (Tac)

As with sequence 12, the Calico Hills Formation (sequence 11) varies from highly zeolitized with no remnant glass in the northern and eastern parts of Yucca Mountain, to vitric and relatively unaltered in the west and south. Transitions from vitric to zeolitized properties within sequence 11 are highly variable, ranging from dispersion of low zeolite abundances (less than 10 percent) across tens of meters (in borehole SD-12), to stacked sills of high zeolite abundance (up to 69 percent) between largely vitric layers (in borehole SD-7). Because the vitric:zeolitic ratios vary with depth in some parts of sequence 11, these variations are approximated by the subdivision of sequence 11 into four layers. One sample from borehole SD-12, collected at an elevation of 2,742.4 feet (835.9 meters) above msl, contained a very sharp (centimeter-scale) transition between Tac and Tacbt. In this instance, the two parts of the sample (upper poorly zeolitic and glassy, lower zeolitic and without glass) are on opposite sides of the contact between sequence 11 and sequence 10.

There are no data for sequence 11 at a particularly crucial borehole (H-3). There are data for sequence 10 and sequence 12 at H-3, both of which are nonzeolitic and vitric in nature. The observed mineralogic relations at other boreholes demonstrate that if the upper part of sequence 10 (the bedded tuff below the Calico Hills Formation) is vitric, sequence 11 is also vitric (in boreholes G-3, H-5, SD-6, and SD-12) (see also Section 6.3.1). In the absence of mineralogic data for sequence 11 at H-3, the MM would predict abundant zeolite at borehole H-3 (due in part to the influence of borehole SD-7). This prediction is viewed as unrealistic. Consequently, a synthetic datum was placed at borehole H-3 in sequence 11. Because the mineralogic values for

borehole H-3 are most similar to those of borehole G-3, the mineralogic values of sequence 11 at borehole H-3 were assigned to be equal to the average values for sequence 11 at borehole G-3.

II.1.13 Sequence 10: Bedded Tuff Below Calico Hills Formation (Tactb)

Sequence 10, consisting of the bedded tuffs below the Calico Hills Formation, is invariably zeolitized where the overlying ash flows (sequence 11) are zeolitized; however, sequence 10 may also be extensively zeolitized (10 to 68 percent zeolite) where the overlying ash flows are poorly zeolitized (0 to 12 percent zeolite at boreholes H-5 and SD-12). In borehole SD-6, however, the greater alteration of the bedded tuff in sequence 10 is expressed by a higher smectite abundance rather than a difference in zeolitization. Because it more readily alters to sorptive minerals, sequence 10 is treated separately from the overlying Calico Hills ash flows in the MM.

II.1.14 Sequence 9: Upper Nonwelded Zone of Prow Pass Tuff (Tcupv)

Sequence 9 is vitric in boreholes to the south and west (G-3, H-3, and SD-6), both vitric and zeolitic in some transitional areas (H-5 and H-6), and zeolitized in the other boreholes for which data are available. In general, the zeolitization of the overlying bedded tuffs (sequence 10) is an indication of zeolitization in sequence 9, although the data from SD-6 indicate that the extensive formation of smectite (14 to 17 percent) in sequence 10 is not associated with any alteration in sequence 9. In some instances, the depth assignments from GFM3.1 placed samples that were zeolitized or glassy and representative of sequence 9 (p#1 at an elevation of 2,184.7 feet (665.9 meters) above msl and H-5 at 2,855.9 feet (870.5 meters) above msl) into underlying devitrified sequence 8. In these cases, the samples were reassigned to sequence 9 in the MM.

II.1.15 Sequence 8: Central Crystalline (Nonzeolitic) Zones of Prow Pass Tuff (Tcupc-Tcplc)

The devitrified central crystalline portions of the Prow Pass Tuff contain feldspar, cristobalite, and quartz across most of Yucca Mountain. Tridymite also occurs in boreholes to the south (G-3, H-3, and SD-7), where the Prow Pass Tuff is well above the water table. Sequence 8 is generally distinguished from the overlying and underlying sequences by the absence of any glass or zeolites, although minimal zeolitization (8 percent) may occur in the uppermost part of sequence 8 (UZ#16) or dispersed throughout (1 to 2 percent at H-3, p#1, and WT-2). The latter effect may be a product of sample impurity where cuttings were analyzed. In some instances, the depth assignments from GFM3.1 placed samples (a#1 at an elevation of 1,883.8 feet (574.2 meters) above msl and H-5 at 2,706 feet (824.8 meters) above msl) that were devitrified (zeolite-free) and representative of sequence 8 into sequence 7 (zeolitic). In these cases, the samples were reassigned to sequence 8 in the MM.

II.1.16 Sequence 7: Lower Nonwelded Prow Pass Tuff to Upper Nonwelded Bullfrog Tuff (Tcupv-Tcbuv)

Sequence 7 is fully zeolitized in all boreholes except at the very top of the sequence in a#1 and G-3. In G-3 the remnant glass at the top of sequence 7 occurs well above the water table; in a#1 the remnant glass at the top of this sequence occurs below the water table. This is a rare instance of glass preservation in the saturated zone. The sorptive zeolites in sequence 7 are partially supplanted by analcime only in G-2. In some instances, the depth assignments from GFM3.1

placed samples that were zeolitized and representative of sequence 7 into devitrified sequence 8 (SD-7 at an elevation of 2,604 feet (793.7 meters) above msl and SD-9 at 2,258 feet [688.4 meters] above msl). In these cases, the samples were reassigned to sequence 7 in the MM. In SD-7, two devitrified samples representative of sequence 6 (see below) were assigned by GFM3.1 to sequence 7 (two samples from SD-7 at 2,292 feet (698.6 meters) above msl); these samples were reassigned to sequence 6 in the MM. In one instance, the depth assignments from GFM3.1 placed a devitrified sample (H-6 at 2,441.6 feet (744.2 meters) above msl) into sequence 7. Because this sequence should contain only zeolitic or glassy samples, this sample was excluded from the MM.

II.1.17 Sequence 6: Central Crystalline (Nonzeolitic) Zones of Bullfrog Tuff (Tcbuc-Tcblc)

The devitrified central crystalline portions of the Prow Pass Tuff contain abundant feldspar and quartz. Cristobalite occurs with quartz in G-1, G-2, G-3, G-4, H-6, SD-7, and WT-2. Tridymite occurs only at the top of sequence 6 in G-3 and at more than one depth in SD-6, in both instances well above the water table. Zeolites are absent. In some instances, the depth assignments from GFM3.1 placed in sequence 7 samples that were devitrified, contained no zeolites, and were representative of sequence 6 (SD-12 at an elevation of 2,193.9 feet (668.7 meters) and 2,179.4 feet (664.3 meters) above msl; and WT-2 at 2,217.8, 2,214.2, and 2,208.6 feet (676.0, 674.9, and 673.2 meters) above msl). These samples were reassigned to sequence 6 in the MM.

II.1.18 Sequence 5: Lower Nonwelded Bullfrog Tuff to Upper Nonwelded Tram Tuff (Tcblv-Tctuv)

Sequence 5 is completely zeolitized in all boreholes. The sorptive zeolites, however, are partially supplanted by analcime in G-2 and p#1. In some instances, the depth assignments from GFM3.1 placed zeolitic or smectite-rich samples that are typical of sequence 5 (G-2 at an elevation of 1,643 feet (500.8 meters) above msl; and G-3 at 2,307.4 feet (703.3 meters) above msl) into the adjacent devitrified sequence (sequence 6). In such cases, the samples were reassigned to sequence 5 in the MM. In another instance, the depth assignments from GFM3.1 placed samples that were zeolitized and representative of sequence 5 into the underlying devitrified sequence 4 (SD-7 at 1,850.4, 1,822.2, and 1,797.2 feet (564.0, 555.4, and 547.8 meters) above msl). In these cases, the samples were also reassigned to sequence 5.

II.1.19 Sequence 4: Central Crystalline (Nonzeolitic) Zones of Tram Tuff (Tctuc-Tctlc)

The devitrified central crystalline portions of the Tram Tuff contain abundant feldspar and quartz. Minor amounts of cristobalite occur in G-1; major amounts of cristobalite occur in G-3 and H-6; and zeolites occur along with the devitrification products in G-3.

II.1.20 Sequence 3: Lower Nonwelded Tram Tuff and Underlying Bedded Tuff (Tctlv-Tctbt)

Sequence 3 was sampled in G-3, H-6, and p#1 (smectite + sorptive zeolite alteration), in G-1 (smectite + sorptive zeolite + analcime alteration), and in b#1 and G-2 (smectite + analcime alteration). The clays represented by smectite + illite included a significant illite component in many of these occurrences.

II.1.21 Sequence 2: Undifferentiated Lavas, Flow Breccias, Bedded Tuffs, Lithic Ridge Tuff, Sediments, and Tuff of Yucca Flat (Tund)

Sequence 2 incorporates a highly varied sequence of lithologies. Sorptive zeolites occur in some portions of this sequence; however, they are largely supplanted by analcime and authigenic albite (authigenic albite is included among the other feldspars in the MM).

II.1.22 Sequence 1: Paleozoic Rocks

Paleozoic rocks were sampled only in p#1. These rocks contain no zeolites but do contain significant amounts of clay. Although the calcite abundances are low (3 to 4 percent), these rocks are rich in carbonates and contain up to 93 percent dolomite. The mineralogy of the Paleozoic sequence was not modeled in the MM.

Table II-1. Adjustments to Borehole Sample Elevations

Borehole	Original Elevation (meters above msl)	Modified Elevation (meters above msl)	Explanation	
a#1	1142.3	1147.0	Too close to boundary	
	1114.9	1116.0	Too close to boundary	
	860.4	854.0	Too close to boundary	
	809.5	806.0	Too close to boundary	
	785.4	783.0	Too close to boundary	
	778.1	773.0	Too close to boundary	
	643.3	637.0	Too close to boundary	
	634.8	621.0	Too close to boundary	
	574.2	Unchanged	Assigned to sequence 7 by GFM3.1	MM assigned to sequence 8
	479.7	474.0	Too close to boundary	
b#1	439.7	Unchanged	Basal duplicate	
	170.0	172.4	Too close to boundary	
	-7.2	-13.0	Too close to boundary	
G-1	-14.8	Unchanged	Basal duplicate	
	933.8	932.0	Assigned to sequence 14 by GFM3.1	MM assigned to sequence 13, Magic Zone
G-2	-496.7	Unchanged	Basal duplicate	
	1318.9	1317.0	Assigned to unit 19 by GFM3.1	MM assigned to sequence 18
	1055.6	1048.0	Assigned to sequence 14 by GFM3.1	MM assigned to sequence 13, Magic Zone
	500.8	490.0	Assigned to sequence 6 by GFM3.1	MM assigned to sequence 5
	-14.3	Removed	Spherulite sample not included	
G-3	-272.8	Unchanged	Basal duplicate	
	1420.3	Removed	Vein sample	
	1349.3	1347.0	Too close to boundary	
	1348.9	1346.0	Too close to boundary	
	1117.5	Unchanged	Assigned to sequence 13 by GFM3.1	MM assigned to sequence 14
	1048.7	1047.0	Too close to boundary	
	1019.6	1018.0	Too close to boundary	
	992.9	Unchanged	Assigned to sequence 10 by GFM3.1	MM assigned to sequence 9
	703.3	700.0	Assigned to sequence 6 by GFM3.1	MM assigned to sequence 5
G-4	-48.2	Unchanged	Basal duplicate	
	869.3	866.5	Assigned to sequence 14 by GFM3.1	MM assigned to sequence 13, Magic Zone
	452.6	448.0	Too close to boundary	
	404.2	400.0	Too close to boundary	
H-3	355.4	Unchanged	Basal duplicate	
	Addition	1054.0	Synthetic sample added to provide mineralogy for sequence 11	Sample mineralogy the same as average values for sequence 11 in G-3
H-4	724.2	Unchanged	Basal duplicate	
	759.3	770.0	Too close to boundary	
	743.8	741.0	Assigned to sequence 9 by GFM3.1	MM assigned to sequence 8
H-5	643.5	Unchanged	Basal duplicate	
	1350.6	1353.0	Too close to boundary	
	870.5	879.2	Assigned to sequence 8 by GFM3.1	MM assigned to sequence 9

Table II-1. Adjustments to Borehole Sample Elevations (Continued)

Borehole	Original Elevation (meters above msl)	Modified Elevation (meters above msl)	Explanation
	824.8	830.0	Assigned to sequence 7 by GFM3.1 MM assigned to sequence 8
	788.2	Unchanged	Basal duplicate
H-6	744.2	Removed	Sample mineralogy indicates problems with sample location
	141.7	Unchanged	Basal duplicate
NRG-6	1105.4	1110.0	Too close to boundary
	912.1	Unchanged	Basal duplicate
NRG-7a	1260.5	Removed	Sequence 21 does not exist in MM at this location
	1191.6	1192.0	Too close to boundary
	901.3	Combined	Sample at 864.0
	894.0	Combined	Sample at 864.0
	887.6	Combined	Sample at 864.0
	880.3	Combined	Sample at 864.0
	873.8	Combined	Sample at 864.0
	867.8	Combined	Sample at 864.0
	864.6	Combined	Sample at 864.0
	861.6	Combined	Sample at 864.0
	857.9	Combined	Sample at 864.0
	854.9	Combined	Sample at 864.0
	852.7	Combined	Sample at 864.0
	Addition	864.0	Average of 11 samples from 901.3 to 852.7
	852.7	851.0	Assigned to sequence 14 by GFM3.1 MM assigned to sequence 13, Magic Zone
	821.0	Unchanged	Basal duplicate
p#1	734.5	730.0	Too close to boundary
	665.9	668.0	Assigned to sequence 8 by GFM3.1 MM assigned to sequence 9
	-128.1	Unchanged	Basal duplicate
	-131.1	Removed	Sample of Paleozoic Not modeled in MM
	-158.5	Removed	Sample of Paleozoic Not modeled in MM
	-201.5	Removed	Sample of Paleozoic Not modeled in MM
SD-6	1369.1	1368.2	Too close to boundary
	1369.0	1368.1	Too close to boundary
	1365.2	1363.7	Too close to boundary
	1364.4	1363.6	Too close to boundary
	1364.1	1363.5	Too close to boundary
	1337.5	1335.0	Assigned to sequence 20 by GFM3.1 MM assigned to sequence 18
	1054.2	1055.5	Too close to boundary
	1054.0	1055.4	Too close to boundary
	1033.9	1035.0	Too close to boundary
	1020.5	1022.0	Too close to boundary
	974.6	985.0	Too close to boundary
	973.6	984.0	Too close to boundary
	966.3	969.0	Too close to boundary
	844.0	Unchanged	Basal duplicate
SD-7	1245.8	1248.0	Too close to boundary
	1002.8	1003.4	Too close to boundary
	885.4, #1	886.5	Too close to boundary Sample #1 at this elevation adjusted

Table II-1: Adjustments to Borehole Sample Elevations (Continued)

Borehole	Original Elevation (meters above msl)	Modified Elevation (meters above msl)	Explanation
	885.4, #2	Removed	Second sample at this depth removed
	793.7	788.0	Assigned to sequence 8 by GFM3.1
	698.6, both samples	693.0	Assigned to sequence 7 by GFM3.1
	564.0	570.0	Assigned to sequence 4 by GFM3.1
	555.4	569.5	Assigned to sequence 4 by GFM3.1
	547.8	569.0	Assigned to sequence 4 by GFM3.1; also basal duplicate
SD-9	1286.1	Removed	Breccia sample removed from MM
	1283.4	Removed	Sequence 21 not present in MM
	1281.0	Removed	Sequence 21 not present in MM
	1219.6	1218.2	Assigned to sequence 19 by GFM3.1
	886.8	890.0	Assigned to sequence 13 by GFM3.1
	688.4	685.0	Assigned to sequence 8 by GFM3.1
	625.3	Unchanged	Basal duplicate
SD-12	1222.8	1224.0	Assigned to sequence 18 by GFM3.1
	893.7, two samples	894.4	Too close to boundary
	835.9, #1	837.0	Assigned to sequence 10 by GFM3.1
	668.7	652.0	Assigned to sequence 7 by GFM3.1
	664.3	651.0	Assigned to sequence 7 by GFM3.1 and basal duplicate
UZ-14	1344.4	Removed	Sequence 22 not present in MM
	1338.9	Removed	Sequence 22 not present in MM
	1263.8	1268.0	Too close to boundary
	1263.1	1267.0	Too close to boundary
	1262.5	1264.0	Too close to boundary
	1206.8	1212.0	Too close to boundary
	996.6	978.6	Too close to boundary
	990.3	978.4	Too close to boundary
	984.4	978.2	Too close to boundary
	959.3	955.0	Assigned to sequence 14 by GFM3.1
	929.5	930.1	Too close to boundary
	917.4	922.2	Too close to boundary

Table.II-1. Adjustments to Borehole Sample Elevations (Continued)

Borehole	Original Elevation (meters above msl)	Modified Elevation (meters above msl)	Explanation
	916.6	922.0	Too close to boundary and basal duplicate
UZ#16	1147.2	1145.0	Assigned to sequence 19 by GFM3.1 MM assigned to sequence 18
	1106.1	1102.0	Too close to boundary
	834.7, #2	Removed	Lithic fragment not included in MM
	762.2	760.0	Too close to boundary
	705.8	Unchanged	Basal duplicate
UZN-31	1239.3	1266.0	Too close to boundary
	1238.6	1247.4	Too close to boundary
	1237.9	1247.4	Too close to boundary
	1237.1	1247.3	Too close to boundary
	1236.2	1247.1	Too close to boundary
	1235.5	1246.8	Too close to boundary
	1234.7	1241.6	Too close to boundary
	1217.2	1217.9	Too close to boundary
	1216.4	1217.9	Too close to boundary
	1215.7	1217.9	Too close to boundary
	1214.8	1217.9	Too close to boundary
	1214.2	1217.9	Too close to boundary
	1213.4	1217.9	Too close to boundary
	1212.7	1217.9	Too close to boundary
	1211.9	1217.9	Too close to boundary
	1211.2	1217.9	Too close to boundary
	1210.7	1217.9	Too close to boundary
	1209.8	1217.3	Too close to boundary
1209.2	1217.2	Too close to boundary	
1208.6	Unchanged	Basal duplicate	
UZN-32	1236.9	1247.2	Too close to boundary
	1236.1	1247.0	Too close to boundary
	1235.6	1246.9	Too close to boundary
	1234.9	1246.8	Too close to boundary
	1234.2	1246.5	Too close to boundary
	1217.2	1217.9	Too close to boundary
	1216.4	1217.9	Too close to boundary
	1215.7	1217.9	Too close to boundary
	1214.9	1217.9	Too close to boundary
	1214.2	1217.9	Too close to boundary
	1213.4	1217.9	Too close to boundary
	1212.8	1217.9	Too close to boundary
	1211.9	1217.9	Too close to boundary
	1211.1	1217.9	Too close to boundary
	1210.4	1217.9	Too close to boundary
	1209.5	1217.9	Too close to boundary
	1208.8	1217.9	Too close to boundary
	1208.0	1217.9	Too close to boundary
	1207.3	1217.9	Too close to boundary
	1206.5	1217.9	Too close to boundary
	1205.7	1217.1	Too close to boundary
WT-1	803.2	Removed	Sequence 13 not present in MM

Table II-1: Adjustments to Borehole Sample Elevations (Continued)

Borehole	Original Elevation (meters above msl)	Modified Elevation (meters above msl)	Explanation
	797.1	Removed	Sequence 13 not present in MM
	791.0	Removed	Sequence 13 not present in MM
	751.4	767.0	Too close to boundary
	739.2	766.0	Too close to boundary
	727.0	765.0	Too close to boundary and basal duplicate
	720.9	Removed	Sequence 10 not present in MM
WT-2	676.0	645.0	Assigned to sequence 7 by GFM3.1 MM assigned to sequence 6
	674.9	644.0	Assigned to sequence 7 by GFM3.1 MM assigned to sequence 6
	673.2	643.0	Assigned to sequence 7 by GFM3.1 and basal duplicate MM assigned to sequence 6
WT-24	735.0	Unchanged	Assigned to sequence 11 in GFM3.1 MM assigned to sequence 10
	730.2	Unchanged	Assigned to sequence 11 in GFM3.1 MM assigned to sequence 10
	726.5	Unchanged	Assigned to sequence 11 in GFM3.1 MM assigned to sequence 10
	725.5	Unchanged	Assigned to sequence 11 in GFM3.1 MM assigned to sequence 10
	724.7	Unchanged	Assigned to sequence 11 in GFM3.1 and basal duplicate MM assigned to sequence 10

NOTES: UZN-31 and UZN-32 were combined into a single borehole in the MM. The assignment of identical elevations to multiple samples (e.g., UZN-31 and UZN-32) causes no problems for the Stratamodel calculation of mineral abundances. There are several occurrences of two analyzed samples with the same elevation; they are referred to as #1 and #2, according to the order in which they are presented in the table.

Addition = A sample at H-3 in the Tac was added, with mineralogy derived from the results of Tac in G-3. A sample at NRG-7a in Tptpln was added; it was derived from the average of 11 samples within Tptpln in NRG-7a.

Assigned to sequence = Sample elevation adjusted (or in some cases not adjusted) to assign sample to a different mineralogic-stratigraphic sequence on the basis of sample mineralogy.

Basal duplicate = The basal sample in all boreholes is duplicated per Stratamodel requirements.

Combined = Eleven samples in NRG-7a, all from Tptpln, were averaged as a single sample located at 864.0 meters within Tptpln.

Magic Zone = Refers to highly altered, smectite-rich samples occurring near the contact of Tptpln and Tptpv3. Such samples were assigned to the Tptpv3 sequence in the MM.

msl = mean sea level

Removed = Some samples of fracture minerals, lithic fragments, etc. that are included in the technical database were not included in the MM.

Too close to boundary = Sample elevation adjusted to keep samples in the correct mineralogic-stratigraphic sequence.

Table II-1. Adjustments to Borehole Sample Elevations (Continued)

Sequence x not present in MM = In some places, a stratigraphic sequence pinches out in the vicinity of a borehole and is not present in the MM.